Supporting Information

for

Tri-coordinated zinc alkyl complexes with *N^S/Se* coordination of imino-phosphanamidinate chalcogenide ligands as precursors for efficient hydroboration of nitriles and esters

Himadri Karmakar,[a] Gobbilla Sai Kumar,[a] Kuntal Pal,[b] Vadapalli Chandrasekhar,*[c,d] and Tarun K. Panda*[a]

Table of Contents

1. X-ray crystallographic analyses
   1.1 Table TS1. Crystallographic data and refinement parameters of **3a** and **3b**.
   1.2 Table TS2. Crystallographic data and refinement parameters of **4a** and **4b**.
   1.3 Table TS3. Selected bond lengths [Å] and angles [°] for compounds **3a**, **3b**, **4a** and **4b**.
2. NMR spectra of metal complexes **3a**, **3b**, **4a** and **4b**.
3. Catalytic hydroboration of nitrile
   3.1 General procedure for the catalytic hydroboration of nitriles
   3.2 NMR data of *N*,*N*-diborylamines
   3.3 NMR spectra of *N*,*N*-diborylamines
   3.4 Hydrolysis of *N*,*N*-diborylamines
4. Catalytic hydroboration of esters
   4.1 General procedure for the catalytic hydroboration of esters
   4.2 NMR data of boryl esters
   4.3 NMR spectra of boryl esters
   4.4 Plausible mechanism of the catalytic hydroboration of esters with pinacolborane
5. NMR spectra of competitive experiments for chemoselective hydroboration.
6. NMR spectra of controlled reactions
7. References.

1. X-ray crystallographic analyses

Single crystals of complexes **3a**, **3b**, **4a**, and **4b** were obtained from a toluene/hexane mixture (1:2) solution in an argon-filled atmosphere at room temperature. In each case, a crystal of suitable dimensions was mounted on a CryoLoop (Hampton Research Corp) with a layer of light mineral oil. All measurements were made on a Bruker SCXRD D8 VENTURE or a Rigaku Supernova X-calibur Eos CCD detector with graphite monochromatic Mo-Kα (0.71073 Å) radiation. Crystal data and structure refinement parameters are summarized in Tables TS1 and TS2. The structures were solved by direct methods (SIR2004) and refined on F^2 by full-matrix least-squares methods, using SHELXL-97.[1] Non-hydrogen atoms were anisotropically refined. The ORTEP-*III* program drew the molecule with 30% probability displacement ellipsoids and H atoms omitted for clarity.[1] In the structure of 2341736 (**3b**) and 2341735 (**4a**), 'Et' group in Zn-Et moiety was disordered over two positions which were refined using standard protocol implemented in the OleX2 program.

In the crystal structure of 2341737 (**3a**), One Toluene molecule was disordered over two positions which were refined using standard protocol implemented in OleX2 program. In addition, half of the toluene molecule per asymmetric unit suffered from special position disordered over multiple positions which were squeezed using standard protocol implemented in OleX2 program where the solvent mask was calculated as 48 electrons in a volume of 240 A3 in 1 void per unit cell. This is consistent with the presence of 0.5[Toluene] per Asymmetric Unit which account for 50 electrons per unit cell.

Crystallographic data (excluding structure factors) for the structures reported in this paper have been deposited with the Cambridge Crystallographic Data Centre as supplementary publication no. CCDC 2341734 - 2341737. Copies of the data can be obtained free of charge by application to CCDC, 12 Union Road, Cambridge CB21EZ, UK (fax: + (44)1223-336-033; email: deposit@ccdc.cam.ac.uk).

1.1 Table TS1. Crystallographic data and refinement parameters of **3a** and **3b**.

Crystal parameters	**3a.Toluene**	**3b**
CCDC NO.	2341737	2341736
Empirical formula	$C_{54}H_{71}N_4PSZn$	$C_{47}H_{63}N_4PSeZn$
Formula weight	902.54	859.31
T (K)	100	100
λ (Å)	0.71073	0.71073
Crystal system	Triclinic	Monoclinic
Space group	P-1	$P2_1/c$
a (Å)	9.4591(2)	9.6029(4)
b (Å)	13.2462(3)	38.6821(18)
c (Å)	22.8703(6)	12.2040(5)
α (°)	94.294(2)	90
β (°)	97.700(2)	101.243(4)
γ (°)	109.859(2)	90
V (Å^3)	2648.49(11)	4446.3(3)
Z	2	4
D_{calc} (g cm^{-3})	1.134	1.284
μ (mm^{-1})	0.570	1.443
F(000)	968	1808
Theta range for data collection	2.428 to 30.584 deg.	2.692 to 28.946 deg.
Limiting indices	$-10 \le h \le 13$, $-18 \le k \le 17$, $-31 \le l \le 32$	$-11 \le h \le 13$, $-43 \le k \le 52$, $-16 \le l \le 16$
Reflections collected / unique	54508 / 14650 [R(int) = 0.0515	45472 / 10081 [R(int) = 0.0518]
Completeness of theta	100 %	99 %
Absorption correction	Multi-scan	Multi-scan

Max. and min. transmission	1.00000 and 0.90382	1.00000 and 0.27304
Refinement method	Full-matrix least-squares on F^2	Full-matrix least-squares on F^2
Data / restraints / parameters	14650 / 21 / 557	10081 / 2 / 493
Goodness-of-fit on F^2	1.056	1.020
Final R indices [$I \geq 2\sigma(I)$]	$R_1 = 0.0676$, $wR_2 = 0.1648$	$R_1 = 0.0471$, $wR_2 = 0.1004$
R indices (all data)	$R_1 = 0.0933$, $wR_2 = 0.1764$	$R_1 = 0.0798$, $wR_2 = 0.1076$

1.2 Table TS2. Crystallographic data and refinement parameters of **4a** and **4b**.

Crystal parameters	**4a**	**4b**
CCDC NO.	2341735	2341734
Empirical formula	$C_{31}H_{47}N_4PSZn$	$C_{31}H_{47}N_4PSeZn$
Formula weight	604.15	650.26
T (K)	273.15	100
λ (Å)	0.71073	0.71073
Crystal system	Monoclinic	Monoclinic
Space group	$P2_1/n$	$P2_1/n$
a (Å)	11.0220(16)	11.0079(4)
b (Å)	16.528(3)	16.5327(4)
c (Å)	18.701(3)	18.6878(6)
α (°)	90	90
β (°)	105.216(4)	105.609(4)
γ (°)	90	90
V (Å^3)	3287.3(8)	3275.57(19)
Z	4	4
D_{calc} (g cm^{-3})	1.221	1.319

μ (mm^{-1})	0.884	1.924
F(000)	1288.0	1358.7
Theta range for data collection	1.951 to 27.115 deg.	2.711 to 28.911 deg.
Limiting indices	$-14 \leq h \leq 14$, $-21 \leq k \leq 21$, $-23 \leq l \leq 23$	$-12 \leq h \leq 14$, $-20 \leq k \leq 21$, $-24 \leq l \leq 25$
Reflections collected / unique	32571 / 7092 [R(int) = 0.0853]	26776 / 7524 [R(int) = 0.0344]
Completeness of theta	98 %	100 %
Absorption correction	Multi-scan	Multi-scan
Max. and min. transmission	1.0000 and 0.851	1.00000 and 0.66280
Refinement method	Full-matrix least-squares on F^2	Full-matrix least-squares on F^2
Data / restraints / parameters	7092 / 3 / 355	7524 / 0 / 355
Goodness-of-fit on F^2	1.007	1.026
Final R indices [$I \geq 2\sigma$ (I)]	$R_1 = 0.0569$, $wR_2 = 0.1068$	$R_1 = 0.0421$, $wR_2 = 0.0893$
R indices (all data)	$R_1 = 0.1371$, $wR_2 = 0.1306$	$R_1 = 0.0690$, $wR_2 = 0.0967$

1.3 Table TS3. Selected bond lengths [Å] and angles [°] for compounds **3a**, **3b**, **4a** and **4b**.

Compounds	**3a**	**3b**	**4a**	**4b**
P1-S1/Se1	2.0228(10)	2.1723(8)	2.0488(14)	2.2110(7)
P1-N1	1.626(2)	1.623(2)	1.623(3)	1.630(2)
P1-N2	1.621(3)	1.606(2)	1.575(3)	1.576(2)
Zn1-N1	1.963(3)	1.972(2)	1.979(3)	1.975(2)
Zn1-S1/ Se1	2.399(1)	2.485(1)	2.353(1)	2.451(1)
Zn1-C1	1.945(4)	2.031(6)	1.945(4)	1.947(3)
N1-Zn1-S1/ Se1	80.64(7)	82.10(7)	80.80(9)	82.67(6)

N1-Zn1-C1	142.80(16)	136.2(3)	145.52(19)	146.12(12)
C1-Zn1-S1/Se1	136.52(14)	141.1(3)	133.67(17)	131.20(11)
N1-P1-S1/Se1	101.78(10)	101.15(9)	99.82(11)	98.99(8)
P1-N1-Zn1	100.54(12)	102.10(13)	101.02(15)	103.46(11)
P1-S1/Se1-Zn1	77.01(3)	73.70(2)	78.28(5)	74.80(2)

2. NMR spectra of metal complexes 3a, 3b, 4a and 4b

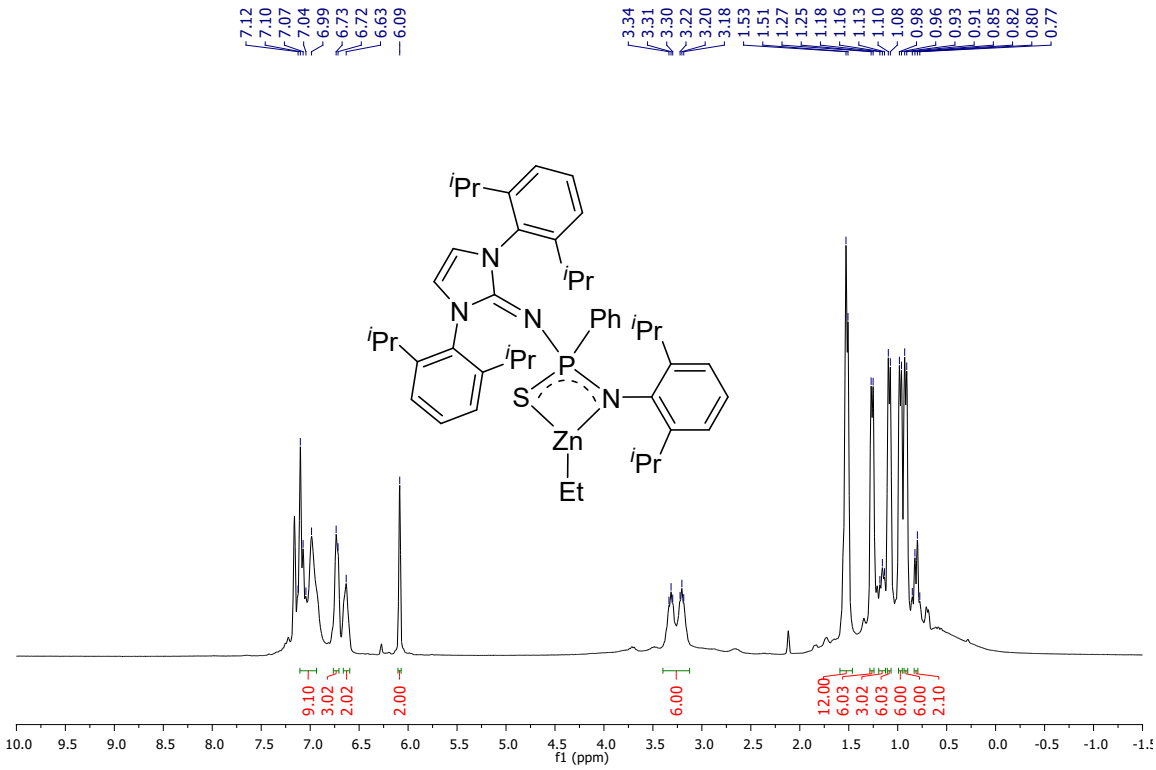

Figure FS1. ^{1}H NMR (300 MHz, C_6D_6, 298 K) spectrum of **3a**.

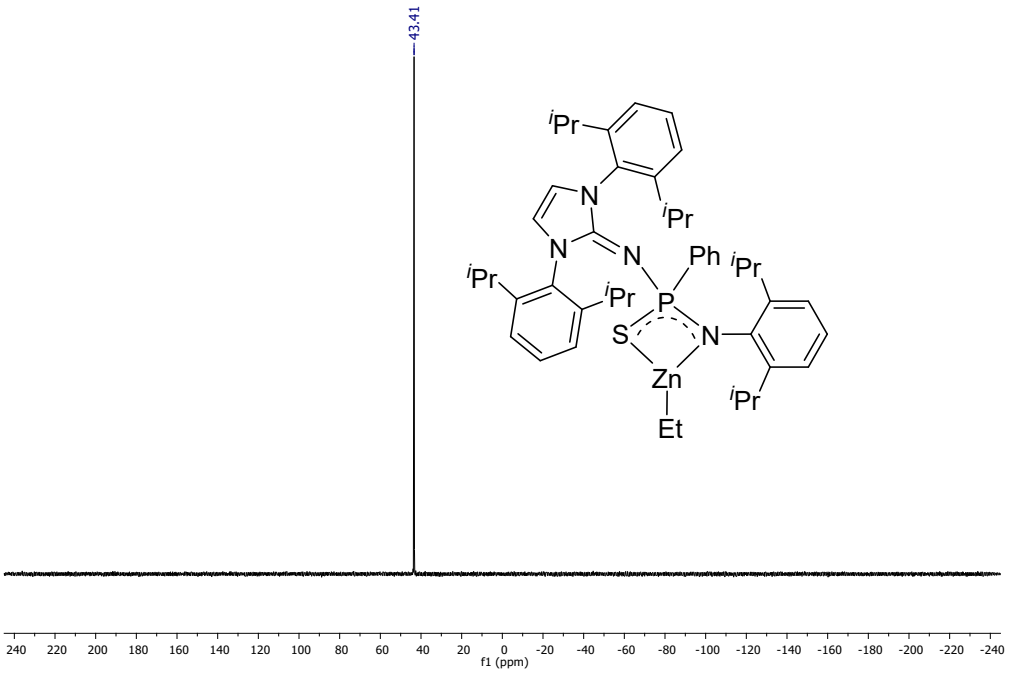

Figure FS2. $^{31}P\{^{1}H\}$ NMR (121.5 MHz, C_6D_6, 298 K) spectrum of **3a**.

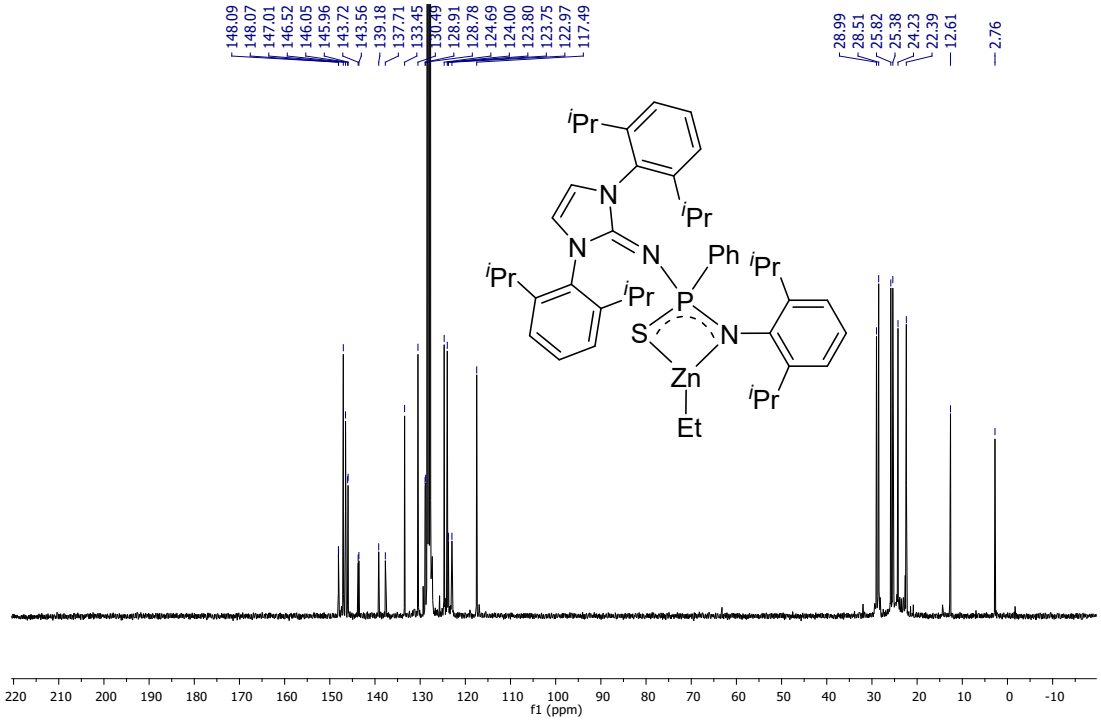

Figure FS3. $^{13}C\{^{1}H\}$ NMR (75 MHz, C_6D_6, 298 K) spectrum of **3a**.

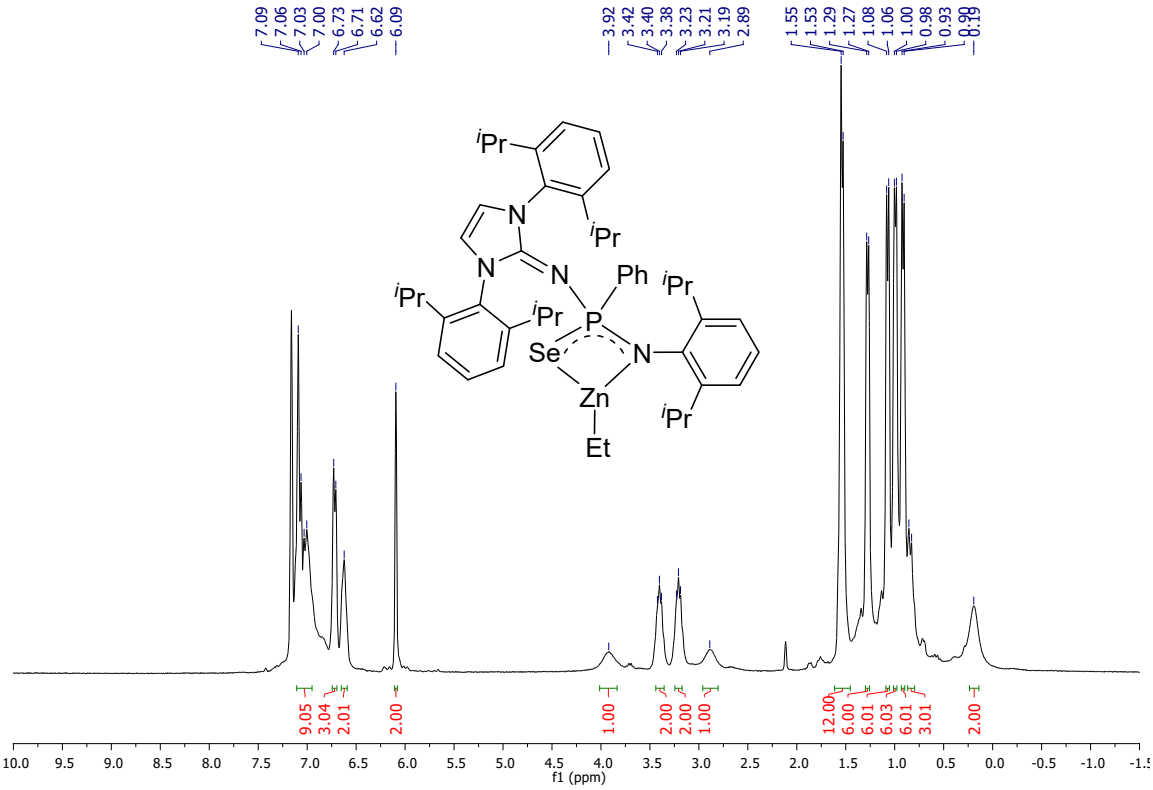

Figure FS4. ^{1}H NMR (300 MHz, C_6D_6, 298 K) spectrum of **3b**.

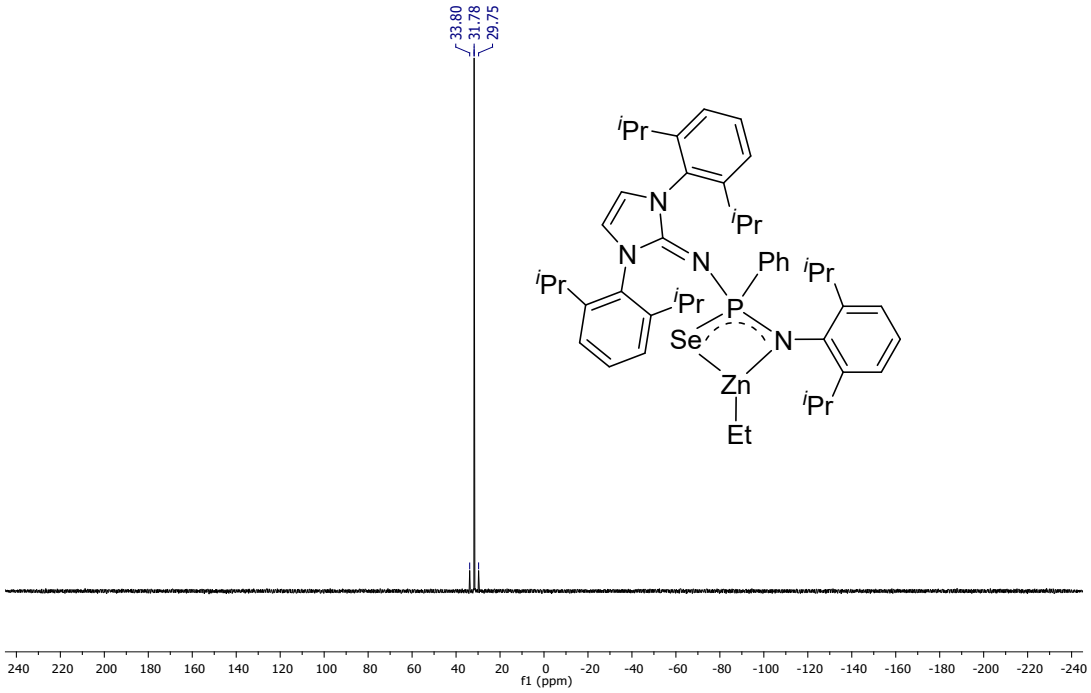

Figure FS5. ^{31}P{^{1}H} NMR (121.5 MHz, C_6D_6, 298 K) spectrum of **3b**.

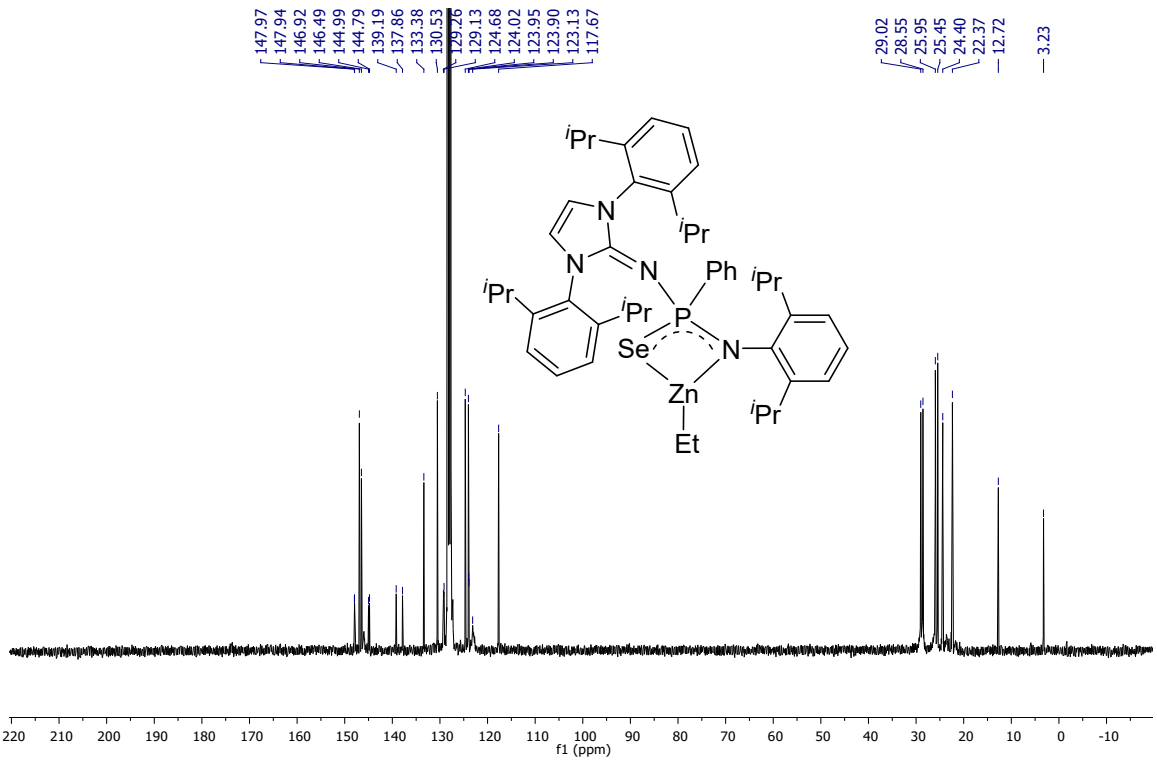

Figure FS6. $^{13}C\{^{1}H\}$ NMR (75 MHz, C_6D_6, 298 K) spectrum of **3b**.

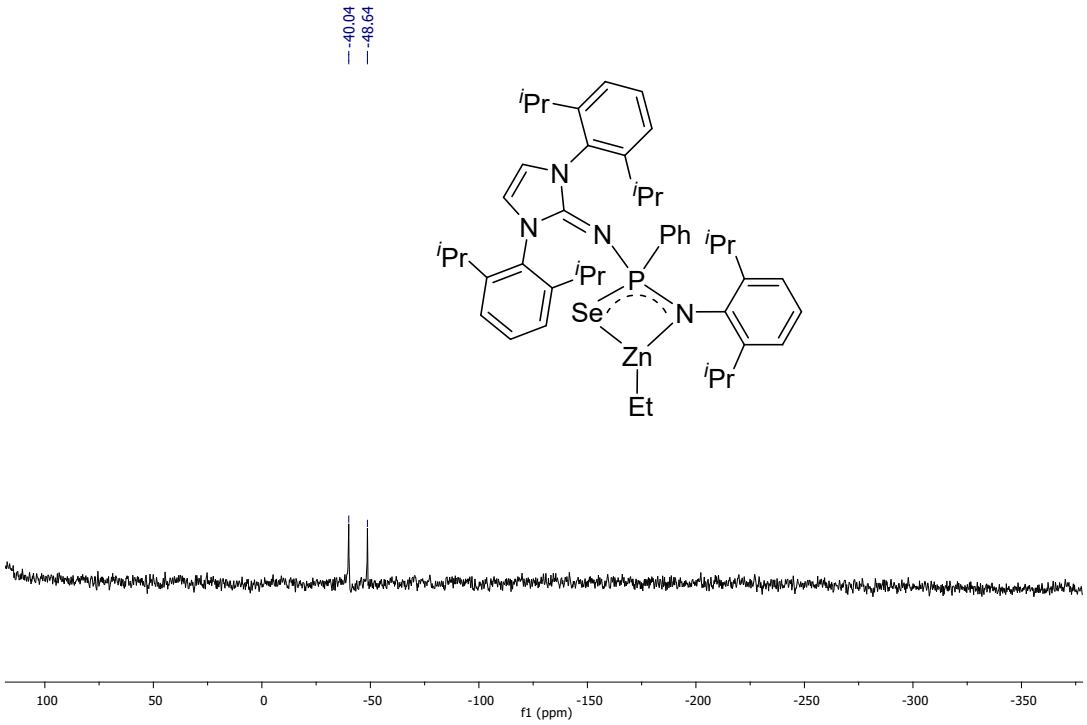

Figure FS7. $^{77}Se\{^{1}H\}$ NMR (57.4 MHz, C_6D_6, 298 K) spectrum of **3b**.

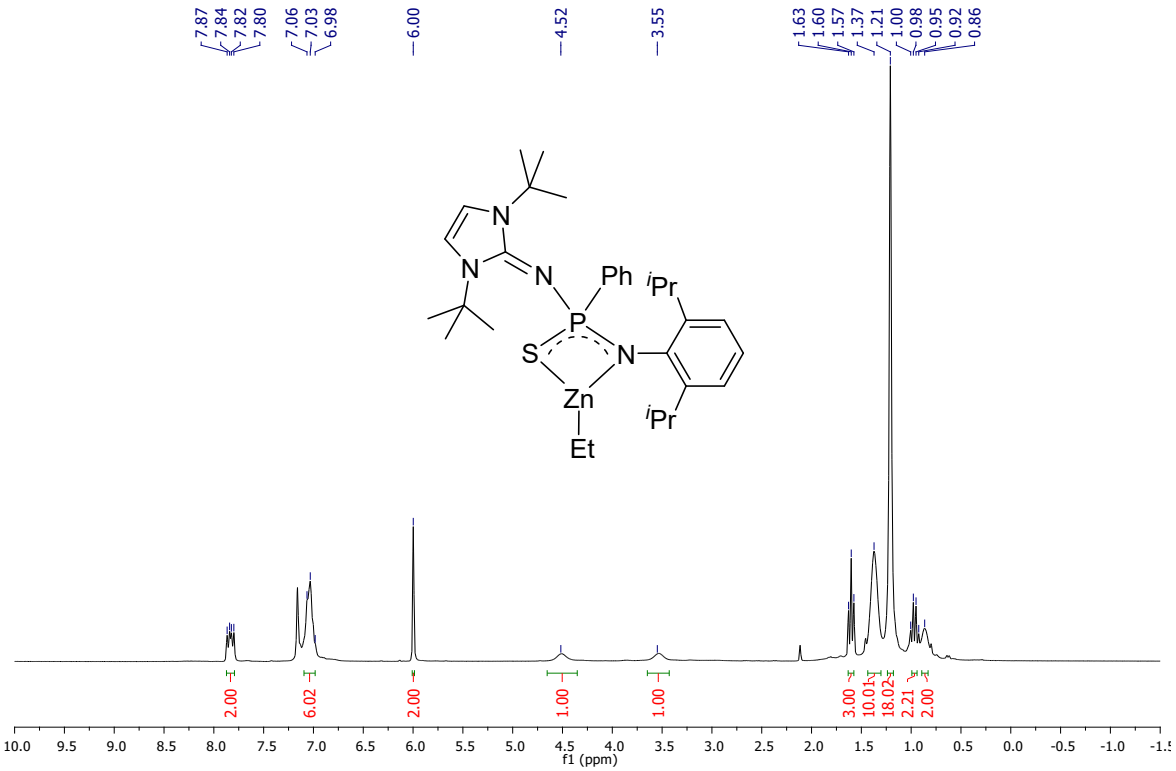

Figure FS8. ^{1}H NMR (300 MHz, C_6D_6, 298 K) spectrum of **4a**.

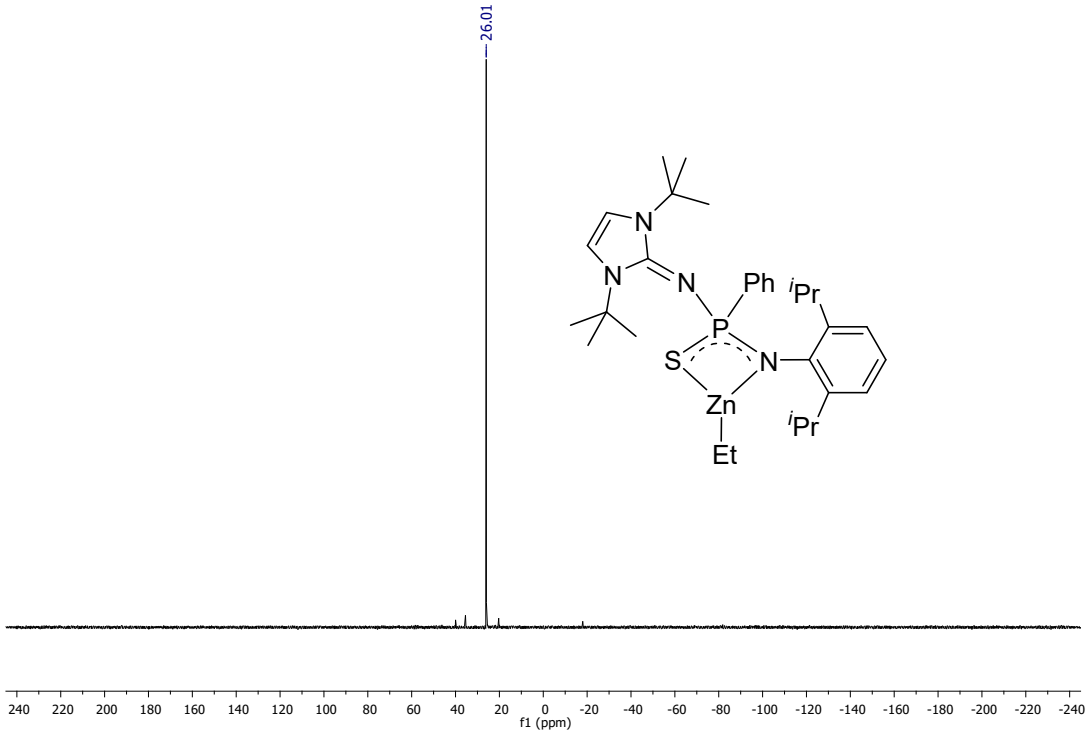

Figure FS9. $^{31}P\{^{1}H\}$ NMR (121.5 MHz, C_6D_6, 298 K) spectrum of **4a**.

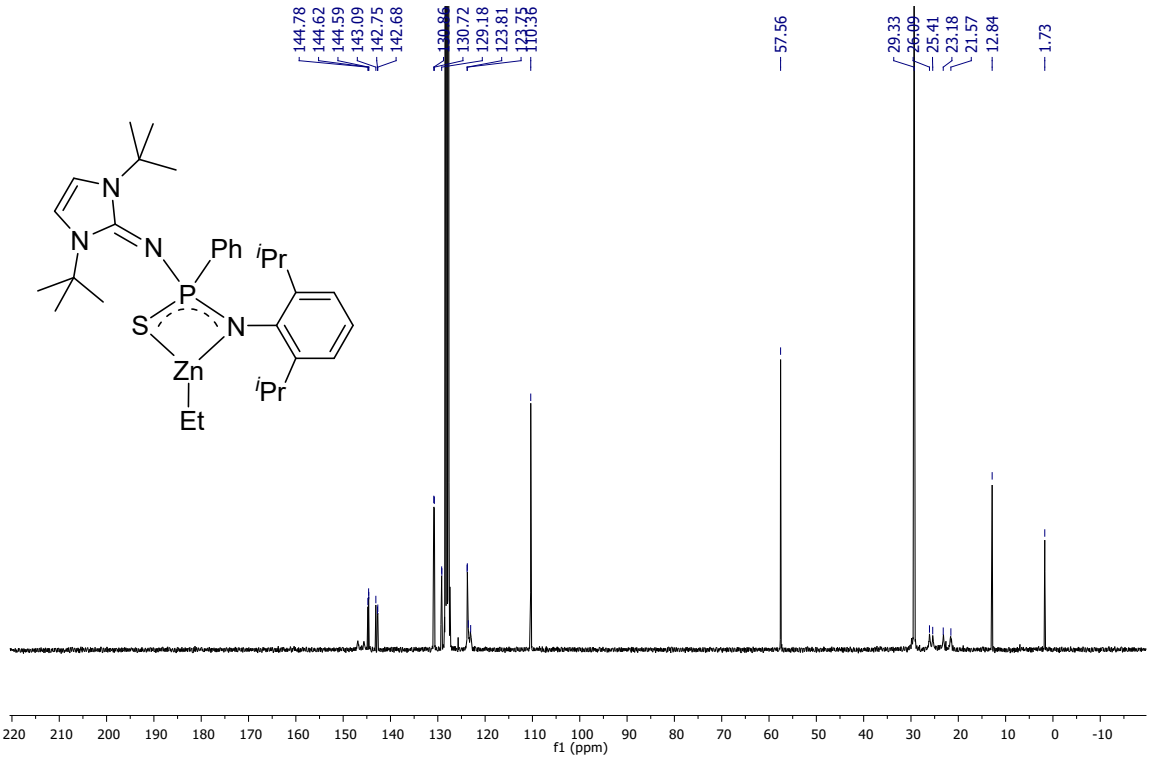

Figure FS10. $^{13}C\{^{1}H\}$ NMR (75 MHz, C_6D_6, 298 K) spectrum of **4a**.

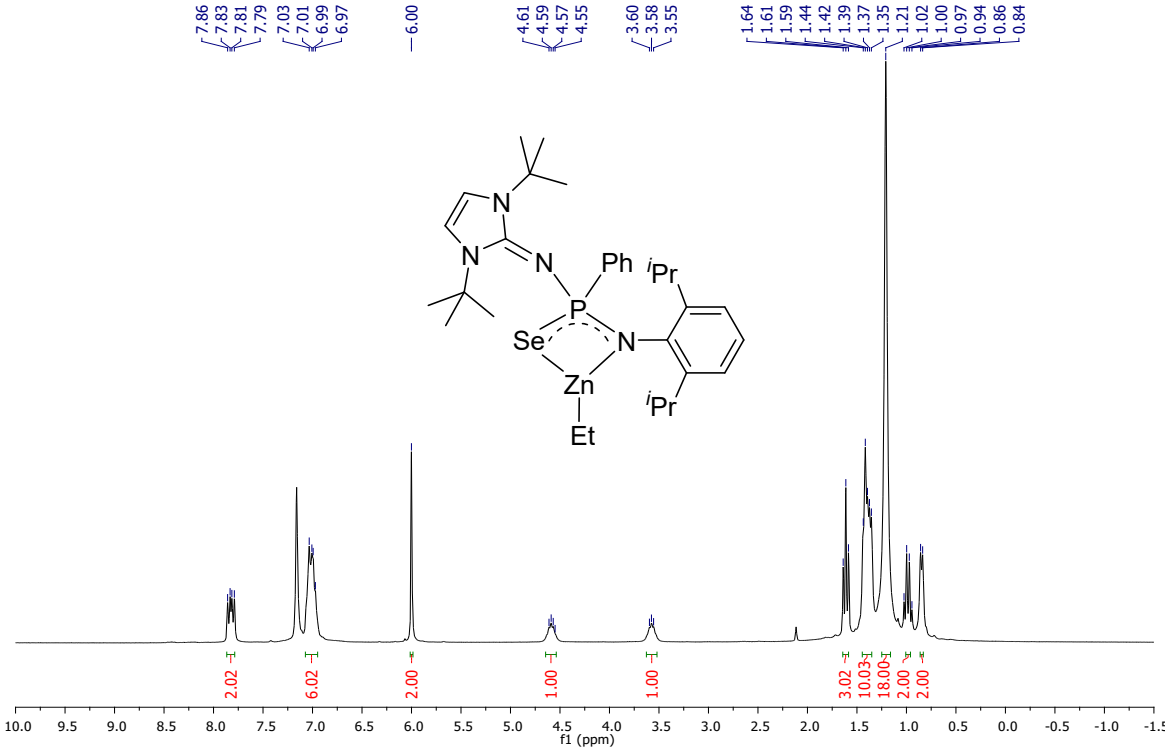

Figure FS11. ^{1}H NMR (300 MHz, C_6D_6, 298 K) spectrum of **4b**.

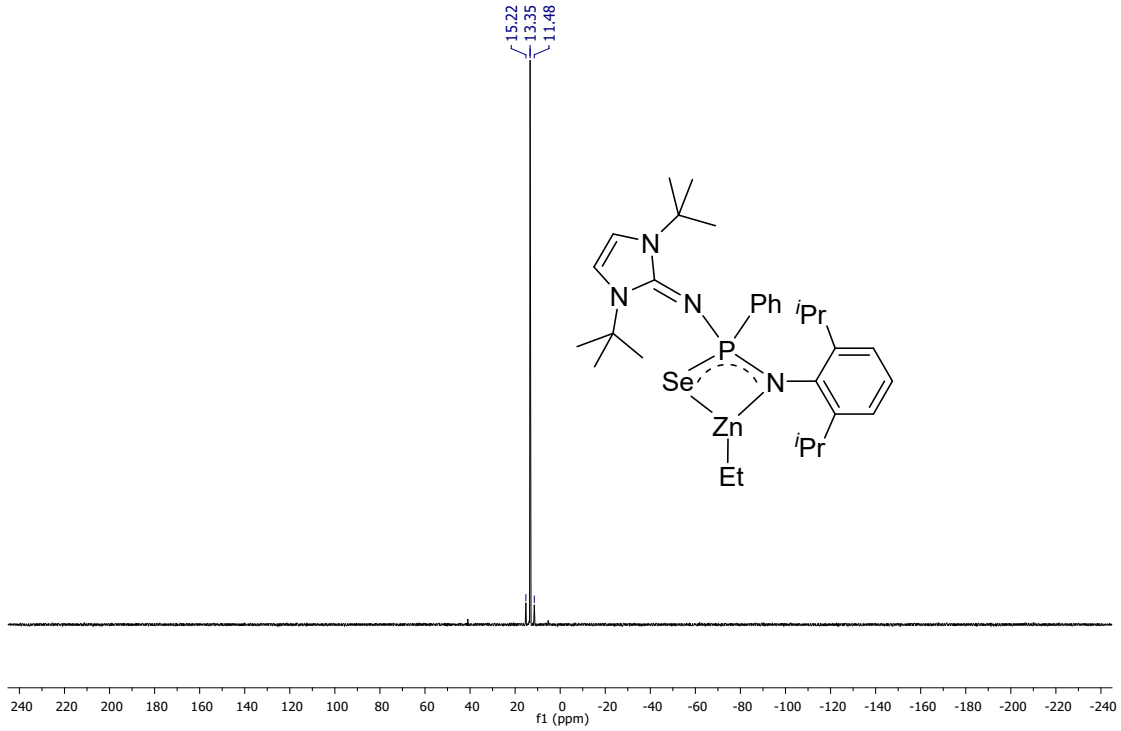

Figure FS12. $^{31}P\{^{1}H\}$ NMR (121.5 MHz, C_6D_6, 298 K) spectrum of **4b**.

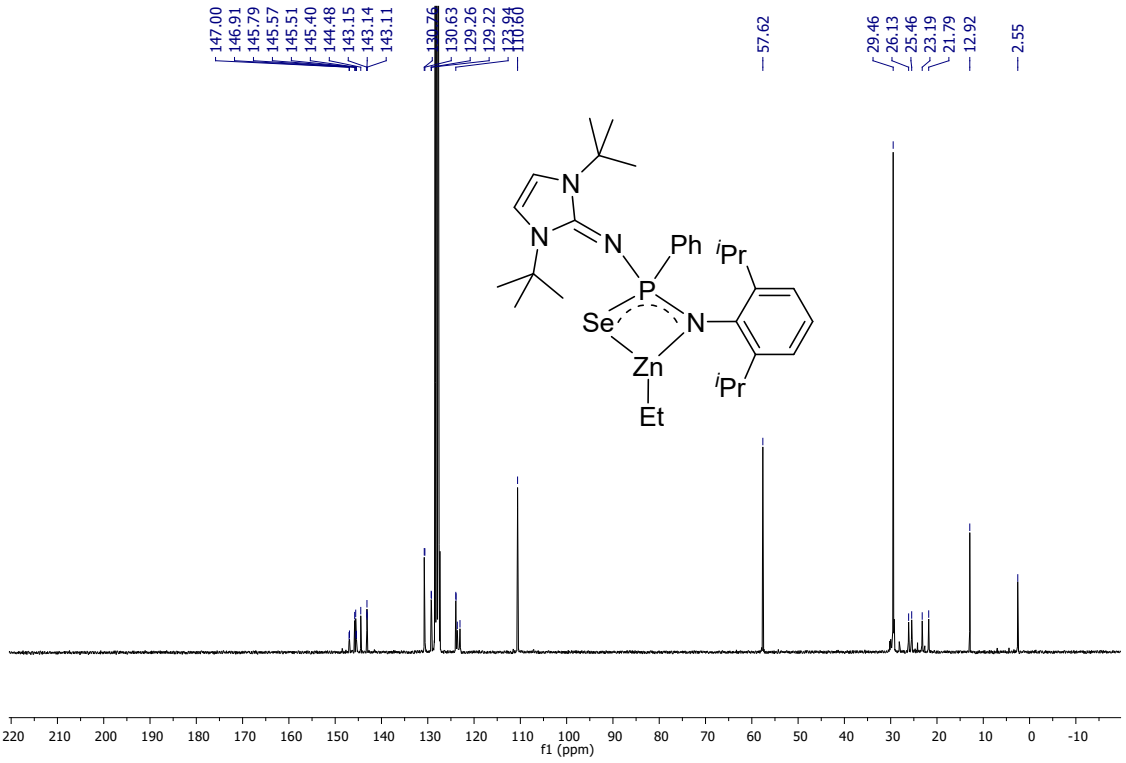

Figure FS13. $^{13}C\{^{1}H\}$ NMR (75 MHz, C_6D_6, 298 K) spectrum of **4b**.

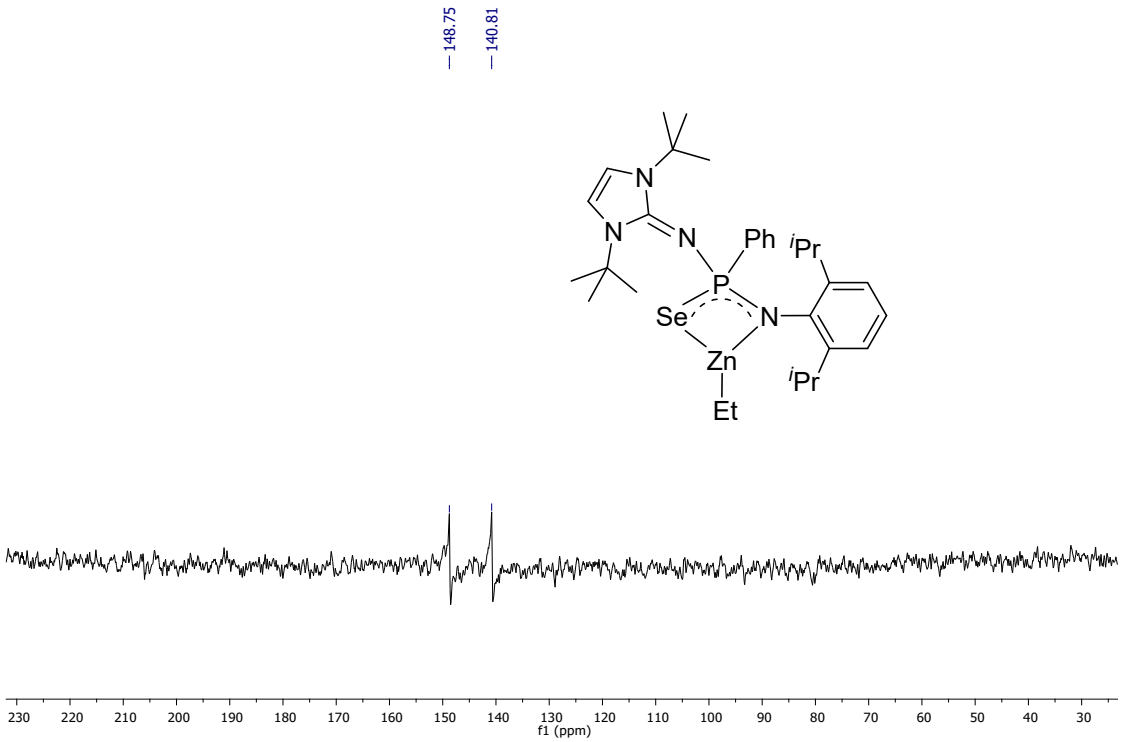

Figure FS14. $^{77}Se\{^{1}H\}$ NMR (57.4 MHz, C_6D_6, 298 K) spectrum of **4b**.

3. Catalytic hydroboration of nitriles

3.1 General procedure for the catalytic hydroboration of nitriles

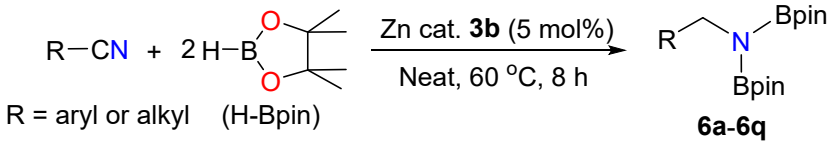

Inside the glove box, the Zn catalyst **3b** (5 mol %) and pinacolborane (HBpin, 1.1 mmol, 2.2 equiv) were added to a Schlenk tube followed by the addition of nitriles (0.5 mmol, 1 equiv). The Schlenk tube was taken out from the glove box and the reaction mixture was stirred at 60 °C for 8 hours. Finally, volatiles of the mixture were removed under reduced pressure to obtain the hydroboration product. The yield was calculated from ^{1}H NMR spectroscopy with the help of 1,3,5-trimethoxy benzene as the internal standard. The progress of the reaction was monitored by ^{1}H NMR, which indicated the completion of the reaction by the appearance of a new R-CH_2-N(Bpin)$_2$ resonance.

3.2 NMR data of *N*,*N*-diborylamines

_N_-benzyl-1,3,2-dioxaborolan-2-amine (6a)[2]

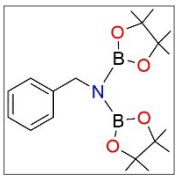

^{1}H NMR (400 MHz, $CDCl_3$, 298 K): δ_H 7.28 - 7.25 (m, 2H), 7.22 - 7.18 (m, 2H), 7.13 - 7.10 (m, 1H), 4.19 (s, 2H), 1.16 (s, 24H) ppm. ^{13}C{^{1}H} NMR (100 MHz, $CDCl_3$, 298 K): δ_C 143.1, 127.9, 127.6, 126.2, 82.4, 47.4, 24.6 ppm. ^{11}B{^{1}H} NMR (128.4 MHz, $CDCl_3$, 298 K): δ_B 25.9 ppm.

_N_-(4-methylbenzyl)-1,3,2-dioxaborolan-2-amine (6b)[2]

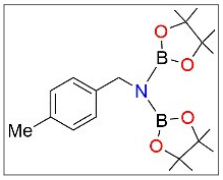

^{1}H NMR (400 MHz, $CDCl_3$, 298 K): δ_H 7.10 (d, 2H, J = 8 Hz), 6.95 (d, 2H, J = 8 Hz), 4.10 (s, 2H), 2.21 (s, 3H), 1.10 (s, 24H) ppm. ^{13}C{^{1}H} NMR (100 MHz, $CDCl_3$, 298 K): δ_C 140.2, 135.5, 128.6, 127.5, 82.4, 46.9, 24.6, 21.2 ppm. ^{11}B{^{1}H} NMR (128.4 MHz, $CDCl_3$, 298 K): δ_B 25.9 ppm.

_N_-(2-methylbenzyl)-1,3,2-dioxaborolan-2-amine (6c)[2]

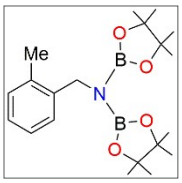

^{1}H NMR (400 MHz, $CDCl_3$, 298 K): δ_H 7.16 - 7.15 (m, 1H), 7.03 - 7.01 (m, 1H), 7.00 - 6.97 (m, 2H), 4.14 (s, 2H), 2.21 (s, 3H), 1.09 (s, 24H) ppm. ^{13}C{^{1}H} NMR (100 MHz, $CDCl_3$, 298 K): δ_C 140.7, 135.2, 129.5, 126.2, 125.8, 125.4, 82.4, 44.8, 24.6, 24.5, 19.2 ppm. ^{11}B{^{1}H} NMR (128.4 MHz, $CDCl_3$, 298 K): δ_B 25.9 ppm.

_N_-(4-(*tert*-butyl)benzyl)-1,3,2-dioxaborolan-2-amine (6d)[2]

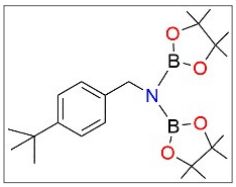

^{1}H NMR (400 MHz, $CDCl_3$, 298 K): δ_H 7.16 (s, 4H), 4.10 (s, 2H), 1.20 (s, 9H), 1.11 (s, 24H) ppm. ^{13}C{^{1}H} NMR (100 MHz, $CDCl_3$, 298 K): δ_C 148.9, 140.2, 127.4, 124.8, 82.4, 46.9, 34.5, 31.6, 24.6 ppm. ^{11}B{^{1}H} NMR (128.4 MHz, $CDCl_3$, 298 K): δ_B 25.7 ppm.

_N_-(4-(dimethylamino)benzyl)-1,3,2-dioxaborolan-2-amine (6e)[2]

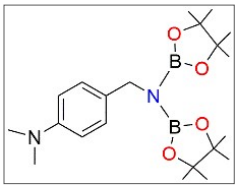

^{1}H NMR (400 MHz, $CDCl_3$, 298 K): δ_H 7.13 (d, 2H, J = 8.5 Hz), 6.57 (d, 2H, J = 8.6 Hz), 4.05 (s, 2H), 2.80 (s, 6H), 1.12 (s, 24H) ppm. ^{13}C{^{1}H} NMR (100 MHz, $CDCl_3$, 298 K): δ_C 149.4, 131.8, 128.7, 112.6, 82.2, 46.6, 40.9, 24.6 ppm. ^{11}B{^{1}H} NMR (128.4 MHz, $CDCl_3$, 298 K): δ_B 25.7 ppm.

***N*-(4-(methoxy)benzyl)-1,3,2-dioxaborolan-2-amine (6f)**[2]

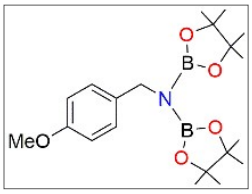

^{1}H NMR (400 MHz, $CDCl_3$, 298 K): δ_H 7.15 (d, 2H, J = 8 Hz), 6.67 (d, 2H, J = 8 Hz), 4.06 (s, 2H), 3.68 (s, 3H), 1.10 (s, 24H) ppm. ^{13}C{^{1}H} NMR (100 MHz, $CDCl_3$, 298 K): δ_C 157.8, 130.2, 129.9, 113.6, 82.1, 55.4, 45.4, 38.5, 24.5 ppm. ^{11}B{^{1}H} NMR (128.4 MHz, $CDCl_3$, 298 K): δ_B 25.9 ppm.

***N*-(4-(methylthio)benzyl)-1,3,2-dioxaborolan-2-amine (6g)**[2]

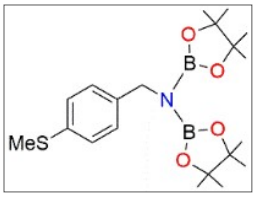

^{1}H NMR (400 MHz, $CDCl_3$, 298 K): δ_H 7.20 (d, 2H, J = 8 Hz), 7.13 (d, 2H, J = 8 Hz), 4.14 (s, 2H), 2.42 (s, 3H), 1.16 (s, 24H) ppm. ^{13}C{^{1}H} NMR (100 MHz, $CDCl_3$, 298 K): δ_C 140.3, 135.5, 128.2, 126.6, 82.4, 46.8, 24.5, 16.3 ppm. ^{11}B{^{1}H} NMR (128.4 MHz, $CDCl_3$, 298 K): δ_B 25.9 ppm.

***N*-(4-(trifluoromethyl)benzyl)-1,3,2-dioxaborolan-2-amine (6h)**[2]

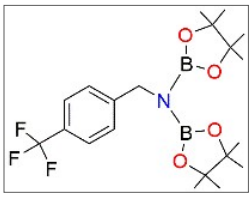

^{1}H NMR (400 MHz, $CDCl_3$, 298 K): δ_H 7.42 (d, 2H, J = 8 Hz), 7.32 (d, 2H, J = 8 Hz), 4.19 (s, 2H), 1.10 (s, 24H) ppm. ^{13}C{^{1}H} NMR (100 MHz, $CDCl_3$, 298 K): δ_C 147.1, 127.6, 126.9, 124.8, 124.8, 124.8, 124.7, 82.5, 46.9, 24.5, 24.5 ppm. ^{11}B{^{1}H} NMR (128.4 MHz, $CDCl_3$, 298 K): δ_B 25.7 ppm.

***N*-(4-fluorobenzyl)-1,3,2-dioxaborolan-2-amine (6i)**[2]

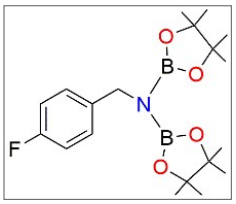

^{1}H NMR (400 MHz, $CDCl_3$, 298 K): δ_H 7.20 - 7.16 (m, 2H), 6.85 - 6.83 (m, 2H), 4.09 (s, 2H), 1.11 (s, 24H) ppm. ^{13}C{^{1}H} NMR (100 MHz, $CDCl_3$, 298 K): δ_C 138.9, 129.3, 129.2, 114.7, 114.5, 82.5, 46.7, 24.7, 24.6 ppm. ^{11}B{^{1}H} NMR (128.4 MHz, $CDCl_3$, 298 K): δ_B 25.9 ppm.

***N*-(4-chlorobenzyl)-1,3,2-dioxaborolan-2-amine (6j)**[2]

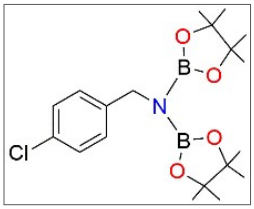

^{1}H NMR (400 MHz, $CDCl_3$, 298 K): δ_H 7.20 - 7.16 (m, 2H), 6.85 - 6.83 (m, 2H), 4.09 (s, 2H), 1.11 (s, 24H) ppm. ^{13}C{^{1}H} NMR (100 MHz, $CDCl_3$, 298 K): δ_C 141.7, 129.0, 128.5, 128.2, 128.0, 82.5, 46.7, 24.7, 24.6 ppm. ^{11}B{^{1}H} NMR (128.4 MHz, $CDCl_3$, 298 K): δ_B 25.6 ppm.

***N*-(4-bromobenzyl)-1,3,2-dioxaborolan-2-amine (6k)**[2]

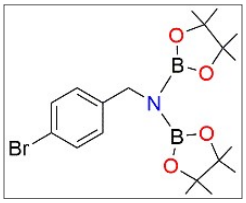

^{1}H NMR (400 MHz, $CDCl_3$, 298 K): δ_H 7.27 (d, 2H, J = 8 Hz), 7.09 (d, 2H, J = 8 Hz), 4.07 (s, 2H), 1.10 (s, 24H) ppm. $^{13}C\{^{1}H\}$ NMR (100 MHz, $CDCl_3$, 298 K): δ_C 142.2, 130.9, 129.4, 119.9, 82.5, 46.8, 24.6 ppm. $^{11}B\{^{1}H\}$ NMR (128.4 MHz, $CDCl_3$, 298 K): δ_B 25.9 ppm.

***N*-(4-iodobenzyl)-1,3,2-dioxaborolan-2-amine (6l)**[2]

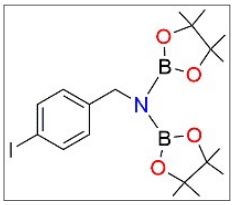

^{1}H NMR (400 MHz, $CDCl_3$, 298 K): δ_H 7.48 (d, 2H, J = 8 Hz), 6.97 (d, 2H, J = 8 Hz), 4.07 (s, 2H), 1.10 (s, 24H) ppm. $^{13}C\{^{1}H\}$ NMR (100 MHz, $CDCl_3$, 298 K): δ_C 142.9, 137.4, 136.9, 129.7, 82.6, 46.9, 24.7, 24.6 ppm. $^{11}B\{^{1}H\}$ NMR (128.4 MHz, $CDCl_3$, 298 K): δ_B 25.6 ppm.

***N*-(4-methoxyphenethyl)-1,3,2-dioxaborolan-2-amine (6m)**[2]

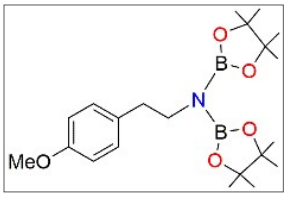

^{1}H NMR (400 MHz, $CDCl_3$, 298 K): δ_H 7.01 (d, 2H, J = 8 Hz), 6.71 (d, 2H, J = 8 Hz), 3.68 (s, 3H), 2.16 (t, 2H), 2.56 (t, 2H), 1.09 (s, 24H) ppm. $^{13}C\{^{1}H\}$ NMR (100 MHz, $CDCl_3$, 298 K): δ_C 157.7, 132.7, 130.2, 113.6, 82.1, 55.4, 45.4, 38.6, 25.0, 24.6 ppm. $^{11}B\{^{1}H\}$ NMR (128.4 MHz, $CDCl_3$, 298 K): δ_B 25.9 ppm.

***N*-(4-fluorophenethyl)-1,3,2-dioxaborolan-2-amine (6n)**[2]

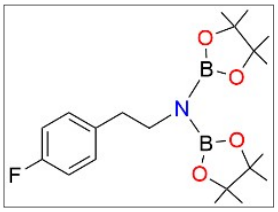

^{1}H NMR (400 MHz, $CDCl_3$, 298 K): δ_H 7.13 - 7.11 (m, 2H), 6.94 - 6.91 (m, 2H), 3.26 (t, 2H), 2.67 (t, 2H), 1.16 (s, 24H) ppm. $^{13}C\{^{1}H\}$ NMR (100 MHz, $CDCl_3$, 298 K): δ_C 162.2, 160.6, 130.7, 130.6, 114.8, 114.8, 114.6, 113.7, 92.9, 82.1, 55.3, 45.1, 38.4, 24.6, 24.5, 24.4 ppm. $^{11}B\{^{1}H\}$ NMR (128.4 MHz, $CDCl_3$, 298 K): δ_B 25.7 ppm.

_N_-(2,2-diphenylethyl)-1,3,2-dioxaborolan-2-amine (6o)[2]

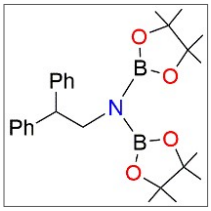

^{1}H NMR (400 MHz, $CDCl_3$, 298 K): δ_H 7.19 - 7.06 (m, 10H), 4.13 (t, 1H, J = 6 Hz), 3.63 (d, 2H, J = 8 Hz), 1.08 (s, 24H) ppm. ^{13}C{^{1}H} NMR (100 MHz, $CDCl_3$, 298 K): δ_C 143.4, 130.5, 129.2, 128.7, 128.5, 128.3, 128.2, 126.0, 125.9, 82.2, 53.6, 48.4, 24.6, 24.5 ppm. ^{11}B{^{1}H} NMR (128.4 MHz, $CDCl_3$, 298 K): δ_B 25.9 ppm.

_N_-(2-methoxyethyl)-1,3,2-dioxaborolan-2-amine (6p)[2]

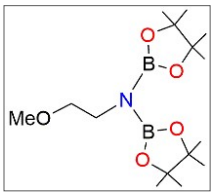

^{1}H NMR (400 MHz, $CDCl_3$, 298 K): δ_H 3.24 (m, 2H), 3.22 (s, 3H), 3.12 (t, 2H, 6 Hz), 1.14 (s, 24H) ppm. ^{13}C{^{1}H} NMR (100 MHz, $CDCl_3$, 298 K): δ_C 82.2, 74.1, 58.5, 42.8, 24.9 ppm. ^{11}B{^{1}H} NMR (128.4 MHz, $CDCl_3$, 298 K): δ_B 25.9 ppm.

_N_-(thiophen-2-ylmethyl)-1,3,2-dioxaborolan-2-amine (6q)[2]

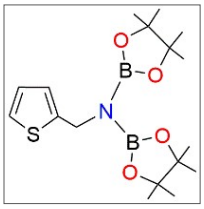

^{1}H NMR (400 MHz, $CDCl_3$, 298 K): δ_H 7.02 - 7.00 (m, 1H), 6.84 - 6.83 (m, 1H), 6.80 - 6.77 (m, 1H), 4.29 (s, 2H), 1.14 (s, 24H) ppm. ^{13}C{^{1}H} NMR (100 MHz, $CDCl_3$, 298 K): δ_C 146.9, 126.3, 124.6, 123.6, 82.6, 42.2, 24.6. ^{11}B{^{1}H} NMR (128.4 MHz, $CDCl_3$, 298 K): δ_B 25.7 ppm.

3.3 NMR spectra of *N*,*N*-diborylamines

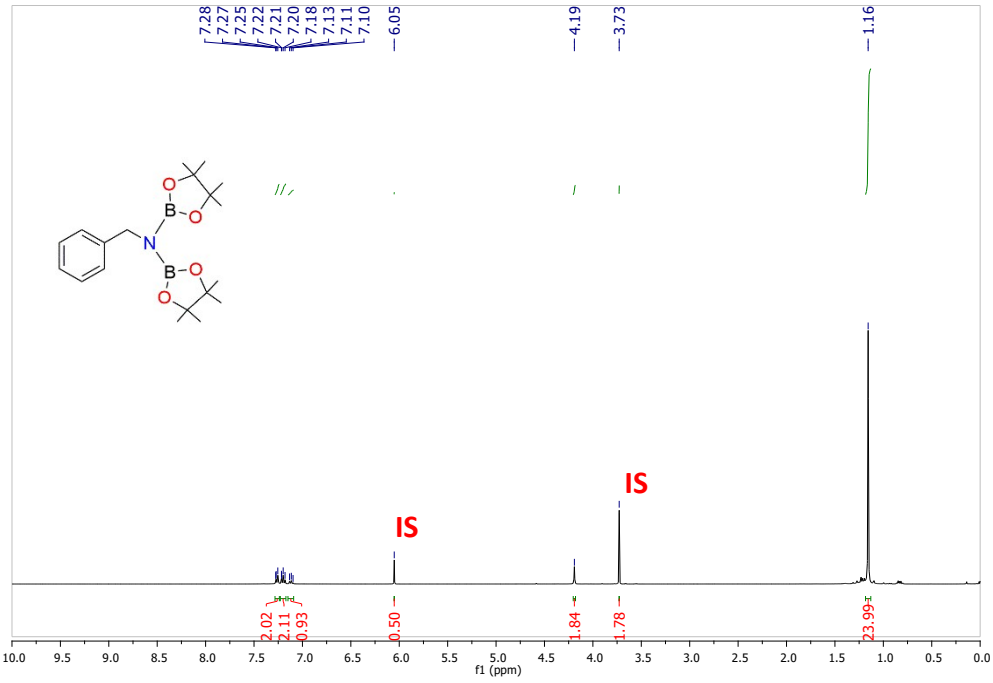

Figure FS 15. ^{1}H NMR (400 MHz, $CDCl_3$, 298 K) spectrum of **6a**.

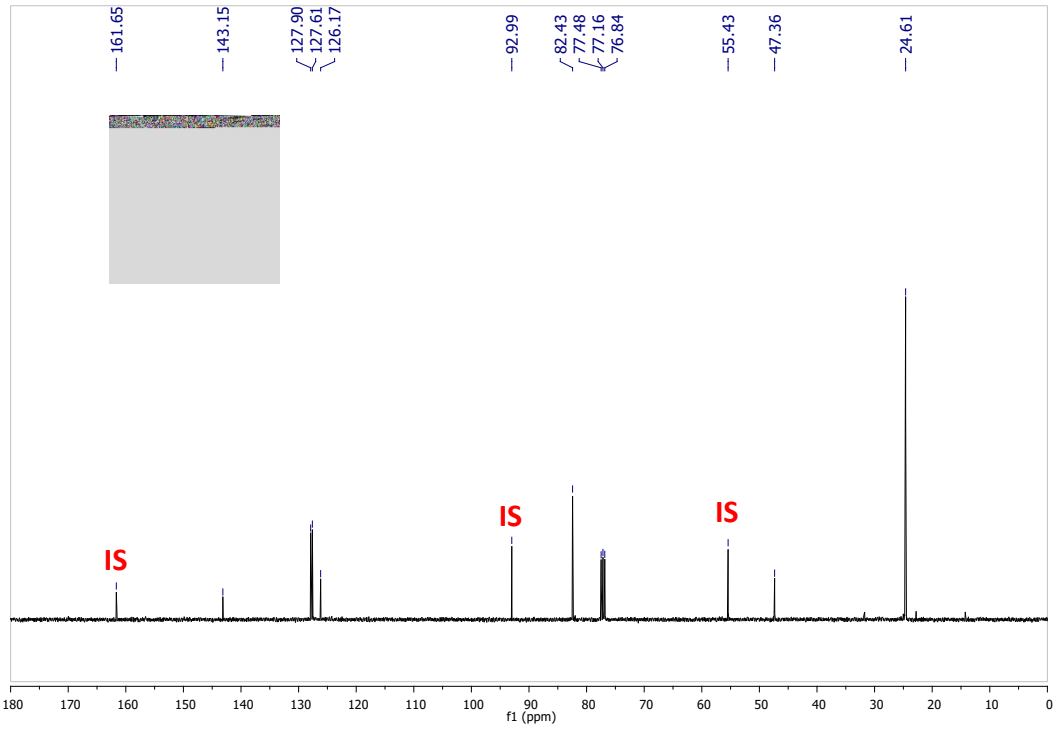

Figure FS 16. ^{13}C{^{1}H} NMR (100 MHz, $CDCl_3$, 298 K) spectrum of **6a**.

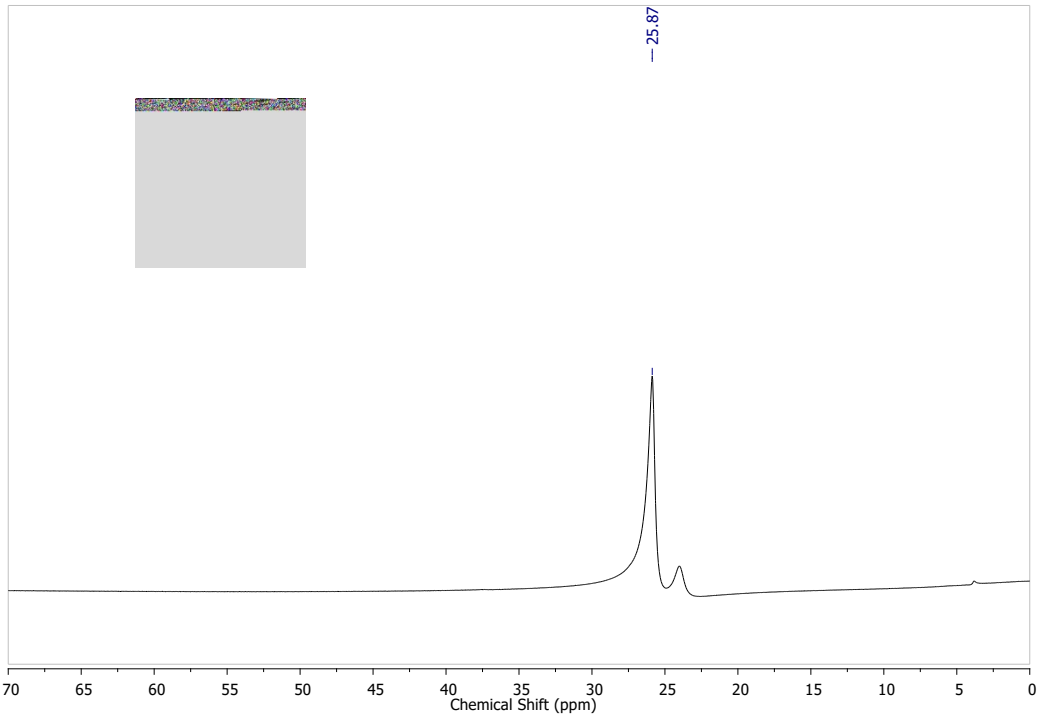

Figure FS 17. $^{11}B\{^{1}H\}$ NMR (128.4 MHz, $CDCl_3$, 298 K) spectrum of **6a**.

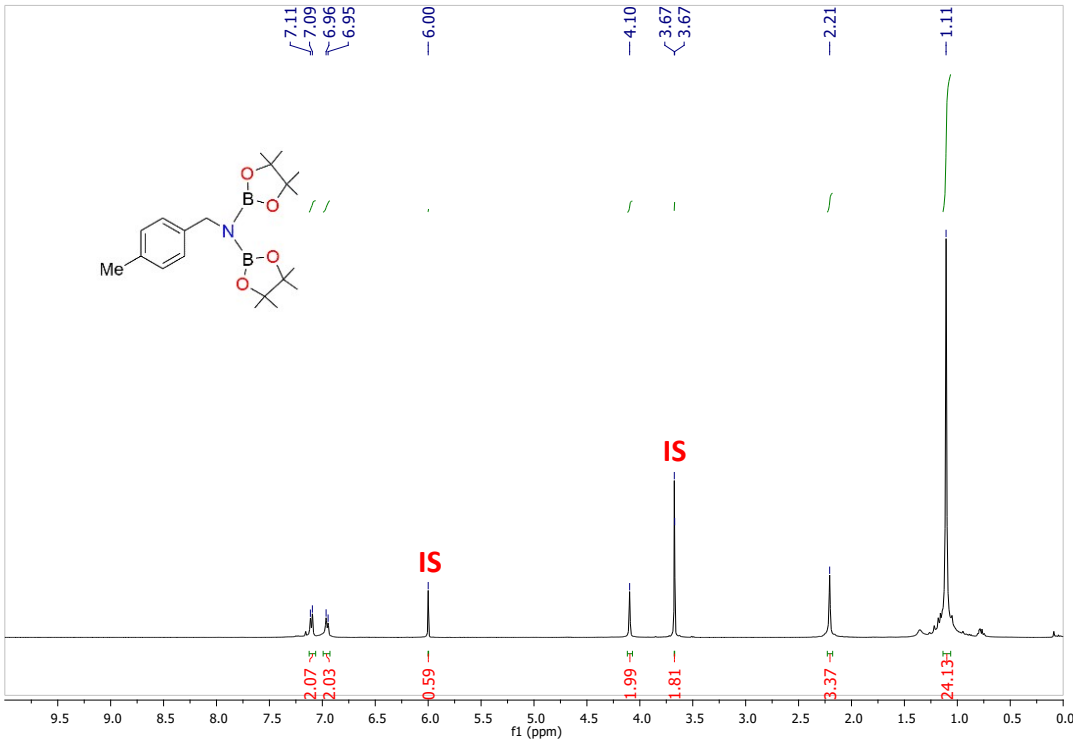

Figure FS 18. ^{1}H NMR (400 MHz, $CDCl_3$, 298 K) spectrum of **6b**.

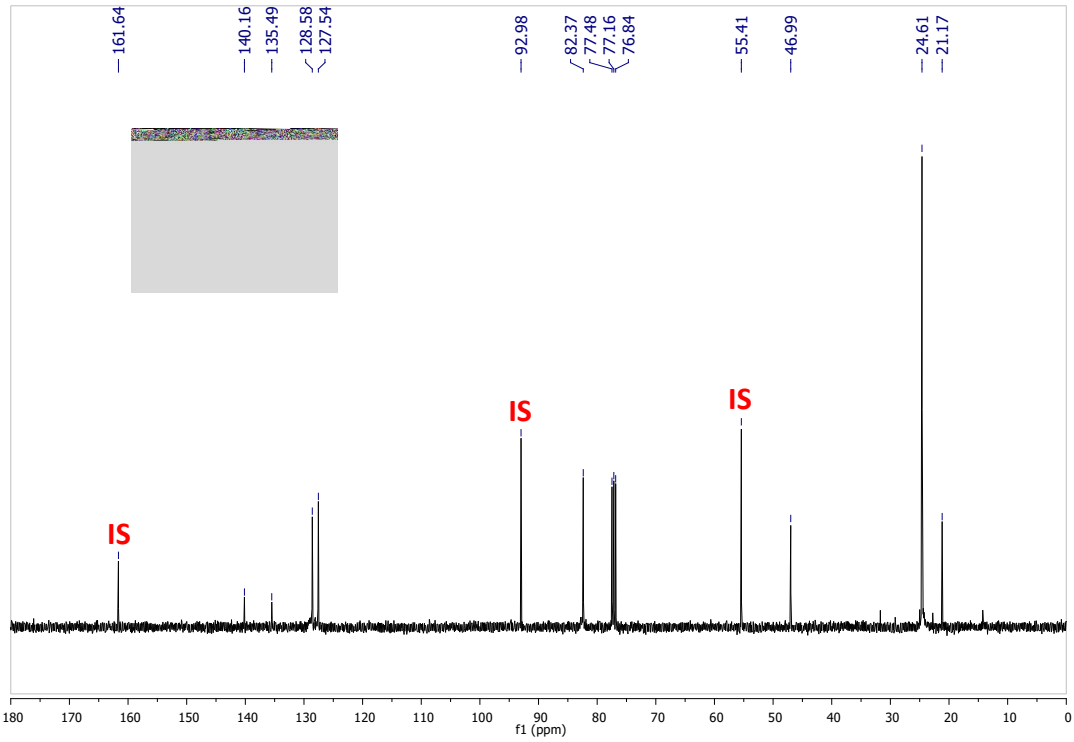

Figure FS 19. $^{13}C\{^{1}H\}$ NMR (100 MHz, $CDCl_3$, 298 K) spectrum of **6b**.

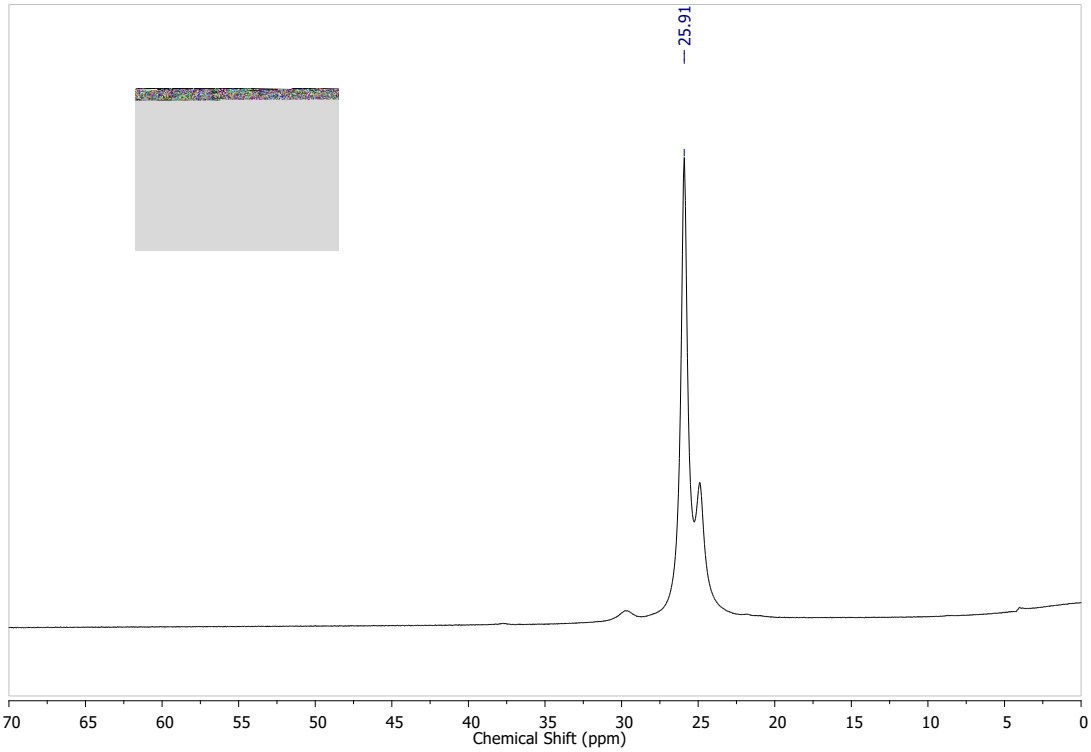

Figure FS 20. $^{11}B\{^{1}H\}$ NMR (128.4 MHz, $CDCl_3$, 298 K) spectrum of **6b**.

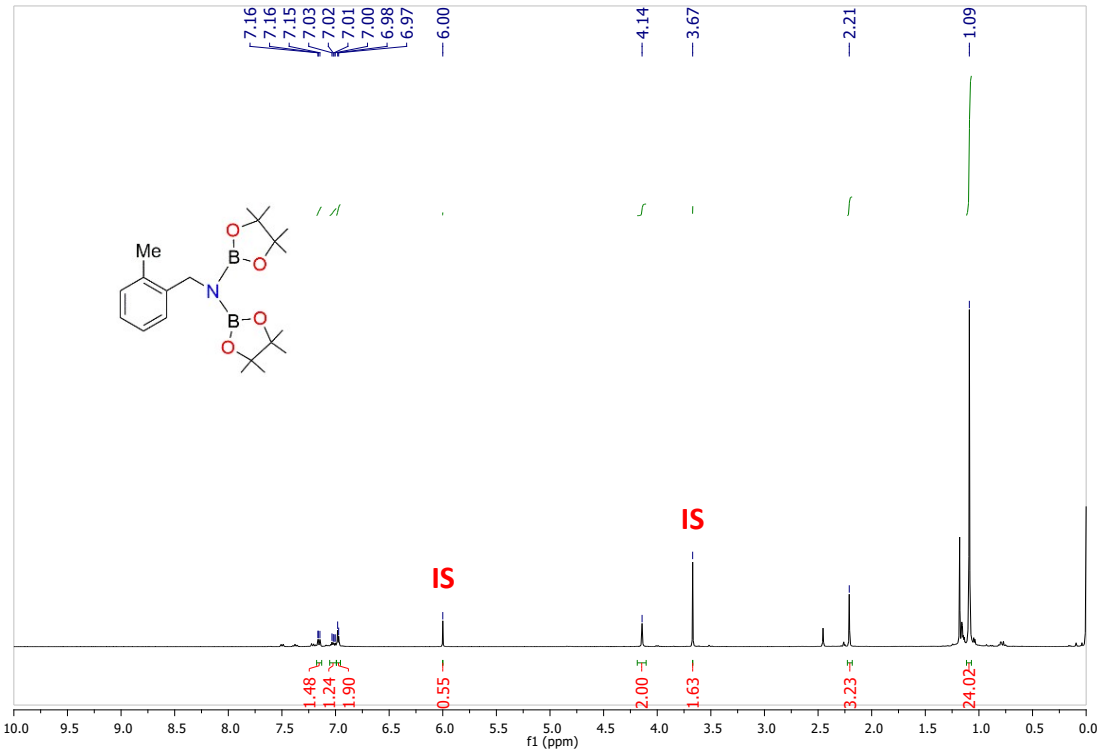

Figure FS 21. ^{1}H NMR (400 MHz, $CDCl_3$, 298 K) spectrum of **6c**.

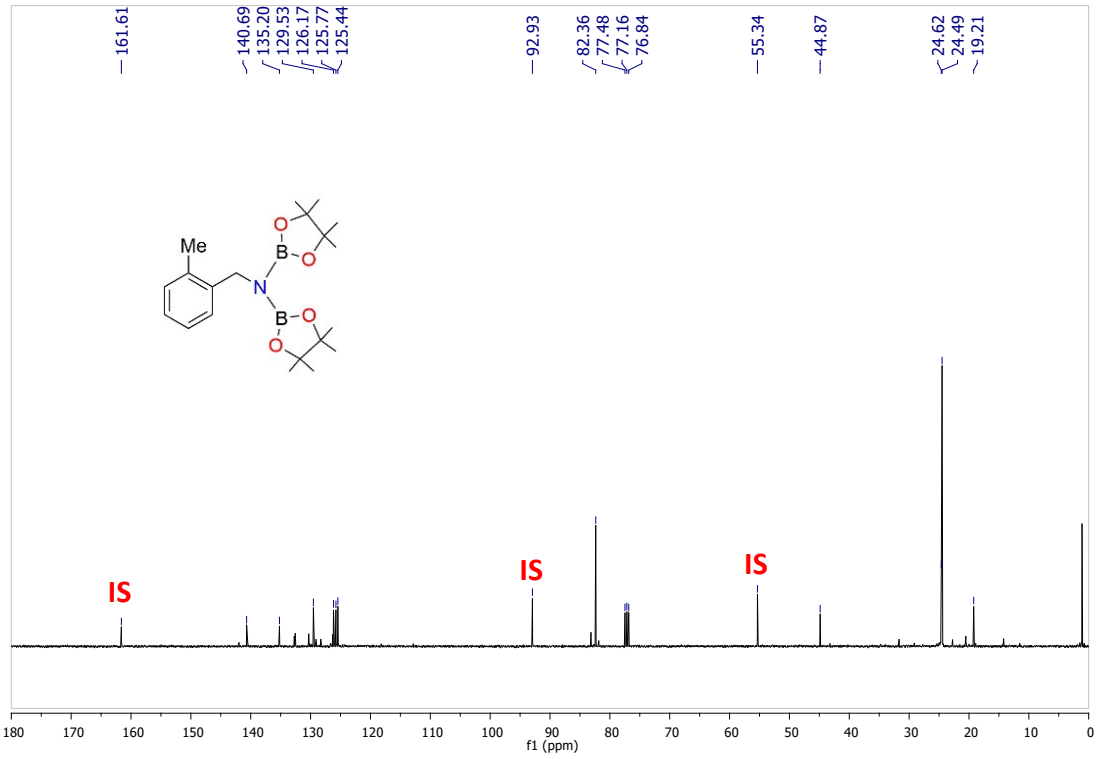

Figure FS 22. $^{13}C\{^{1}H\}$ NMR (100 MHz, $CDCl_3$, 298 K) spectrum of **6c**.

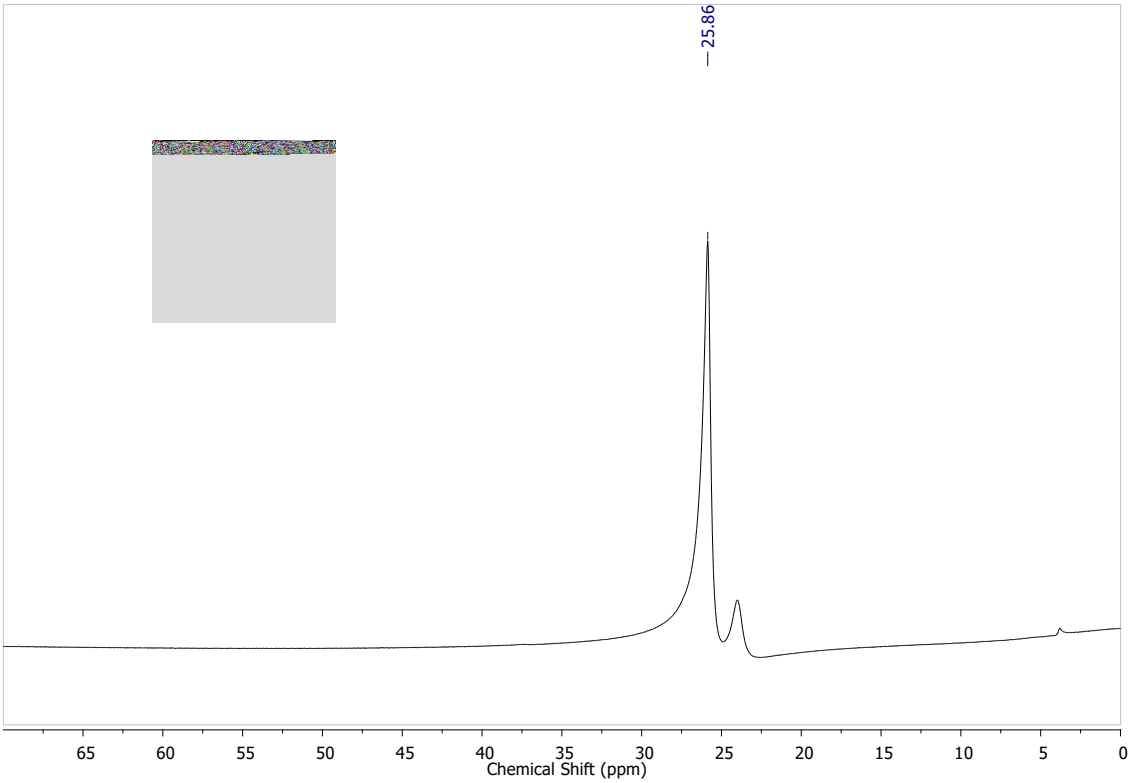

Figure FS 23. $^{11}B\{^{1}H\}$ NMR (128.4 MHz, $CDCl_3$, 298 K) spectrum of **6c**.

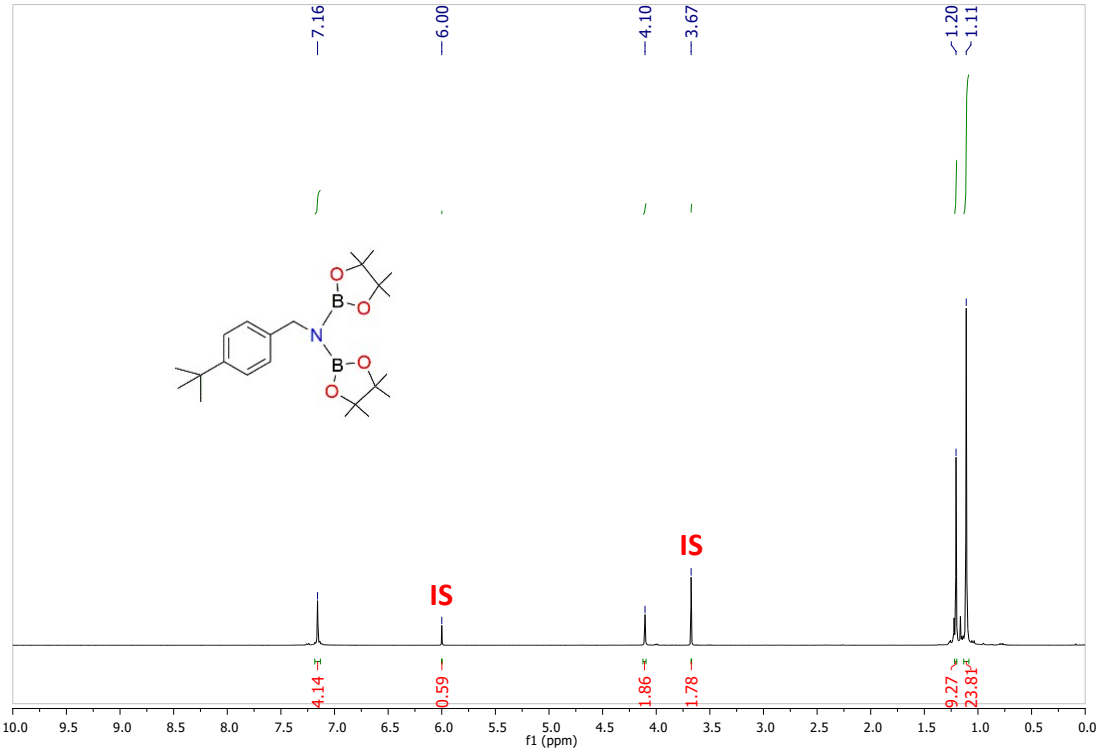

Figure FS 24. ^{1}H NMR (400 MHz, $CDCl_3$, 298 K) spectrum of **6d**.

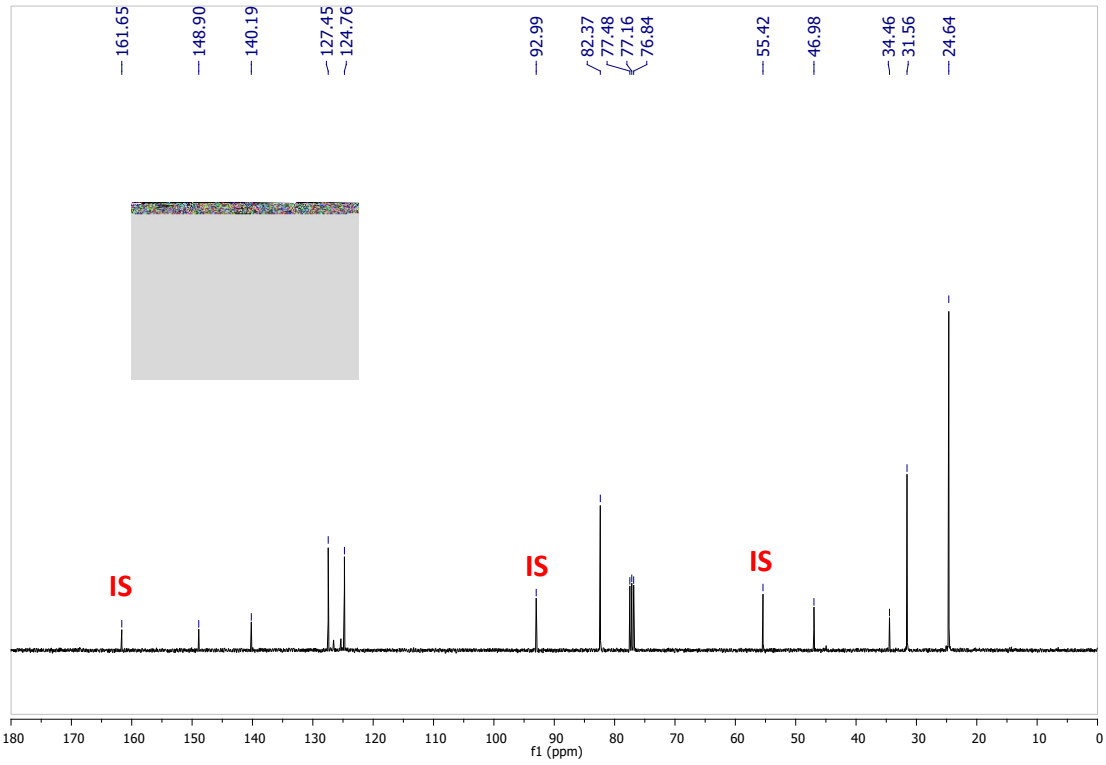

Figure FS 25. $^{13}C\{^{1}H\}$ NMR (100 MHz, $CDCl_3$, 298 K) spectrum of **6d**.

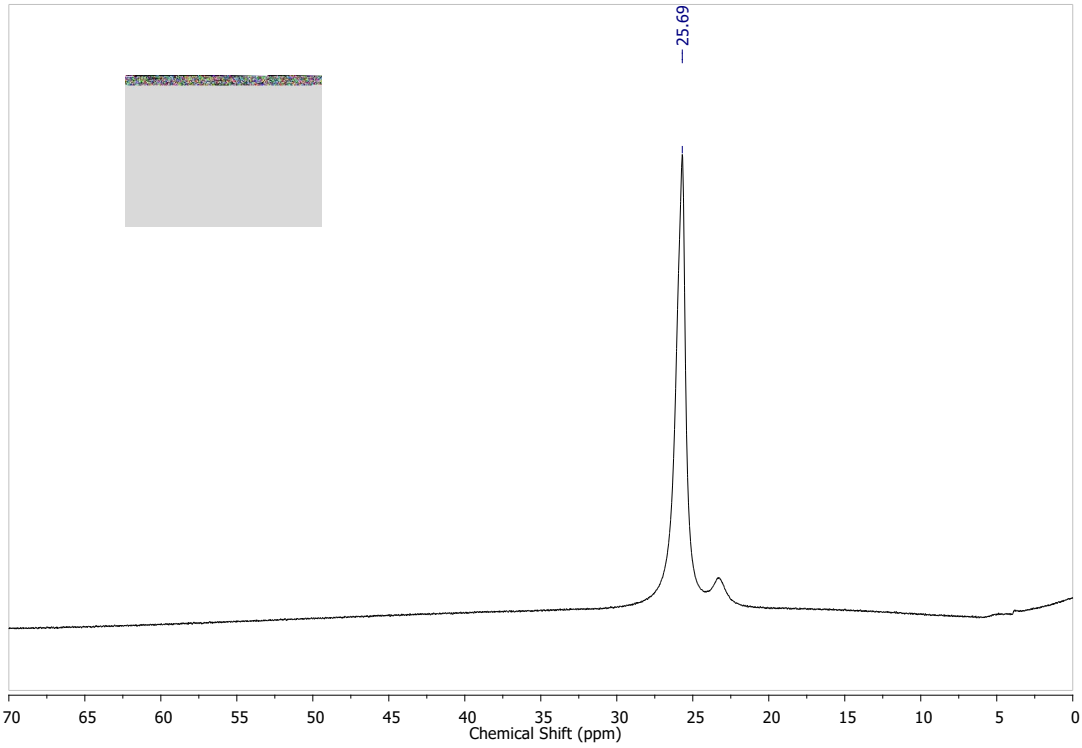

Figure FS 26. $^{11}B\{^{1}H\}$ NMR (128.4 MHz, $CDCl_3$, 298 K) spectrum of **6d**.

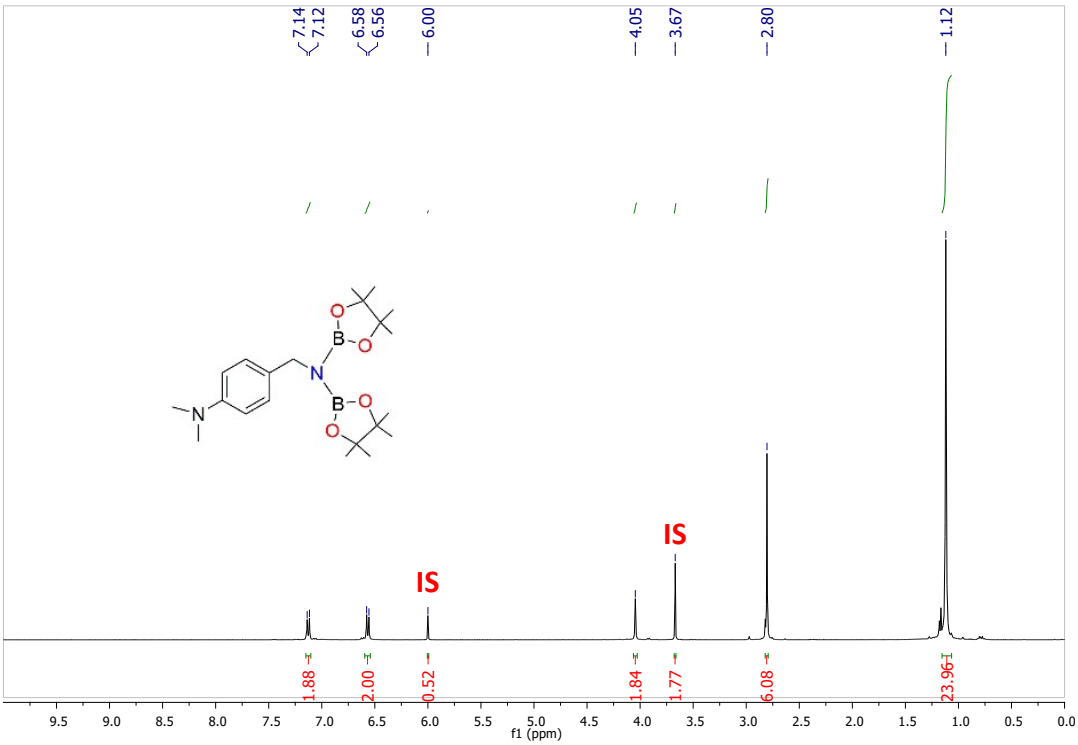

Figure FS 27. ^{1}H NMR (400 MHz, $CDCl_3$, 298 K) spectrum of **6e**.

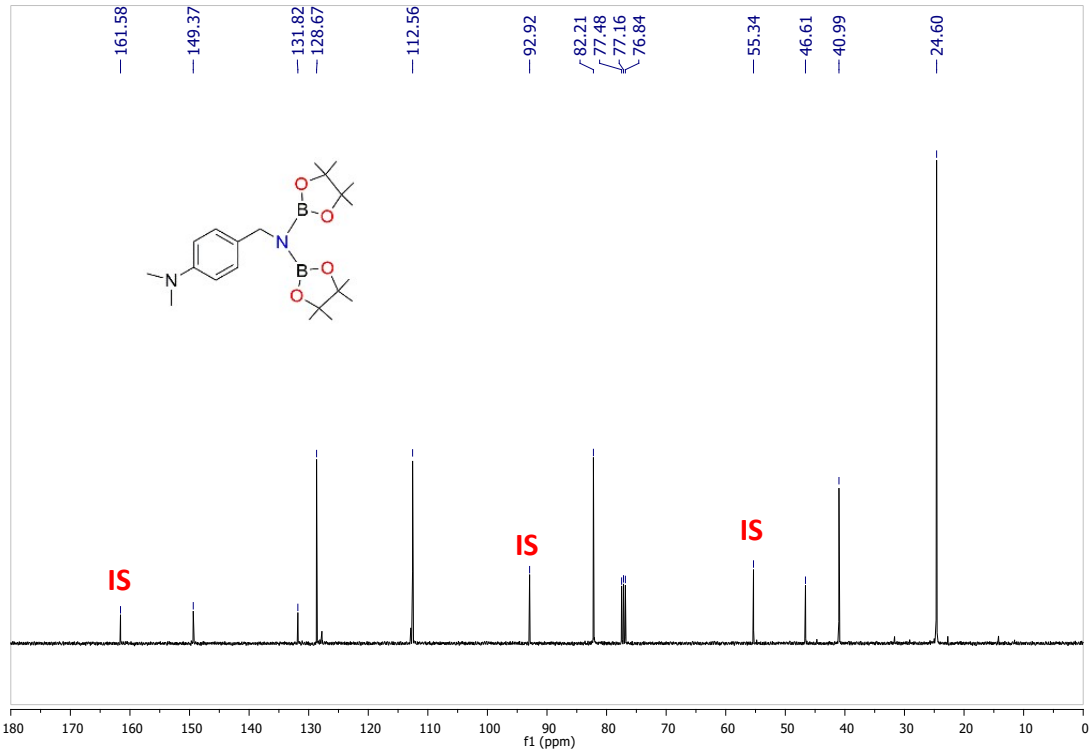

Figure FS 28. ^{13}C{^{1}H} NMR (100 MHz, $CDCl_3$, 298 K) spectrum of **6e**.

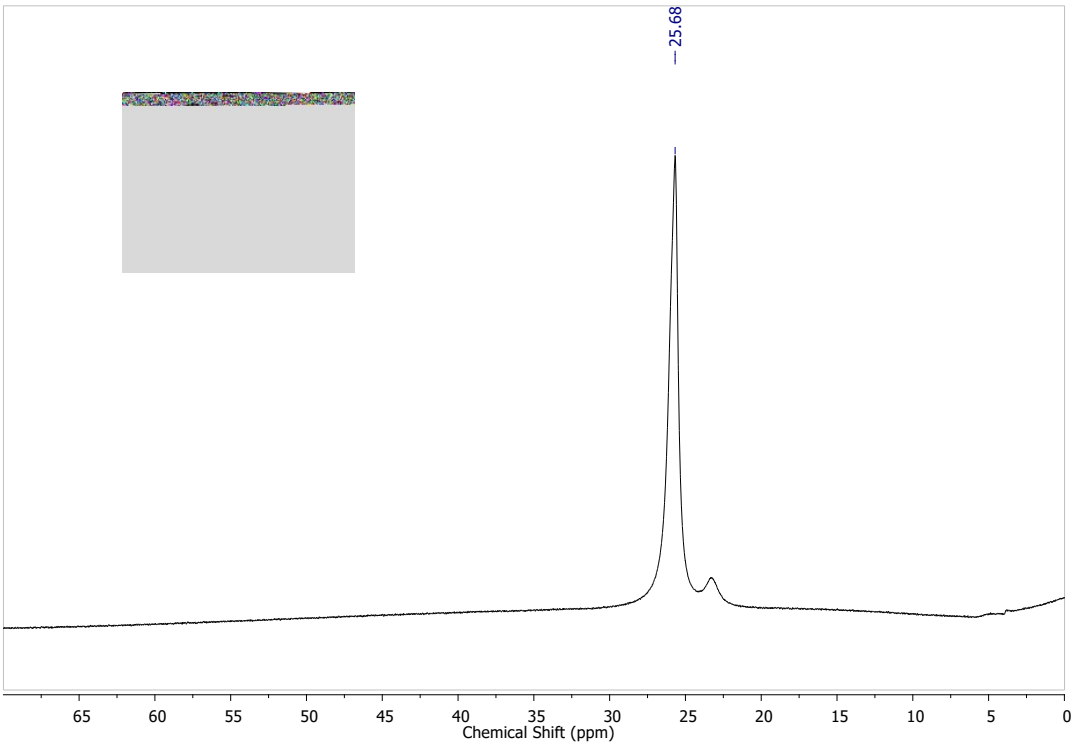

Figure FS 29. $^{11}B\{^{1}H\}$ NMR (128.4 MHz, $CDCl_3$, 298 K) spectrum of **6e**.

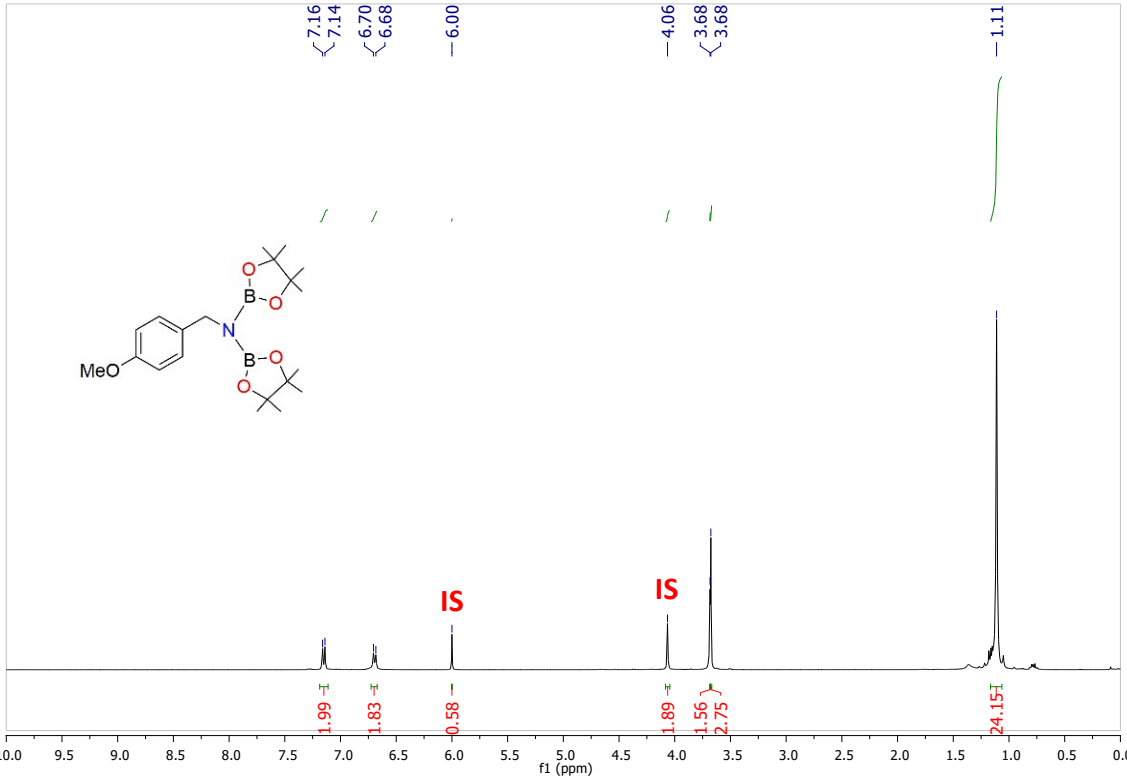

Figure FS 30. ^{1}H NMR (400 MHz, $CDCl_3$, 298 K) spectrum of **6f**.

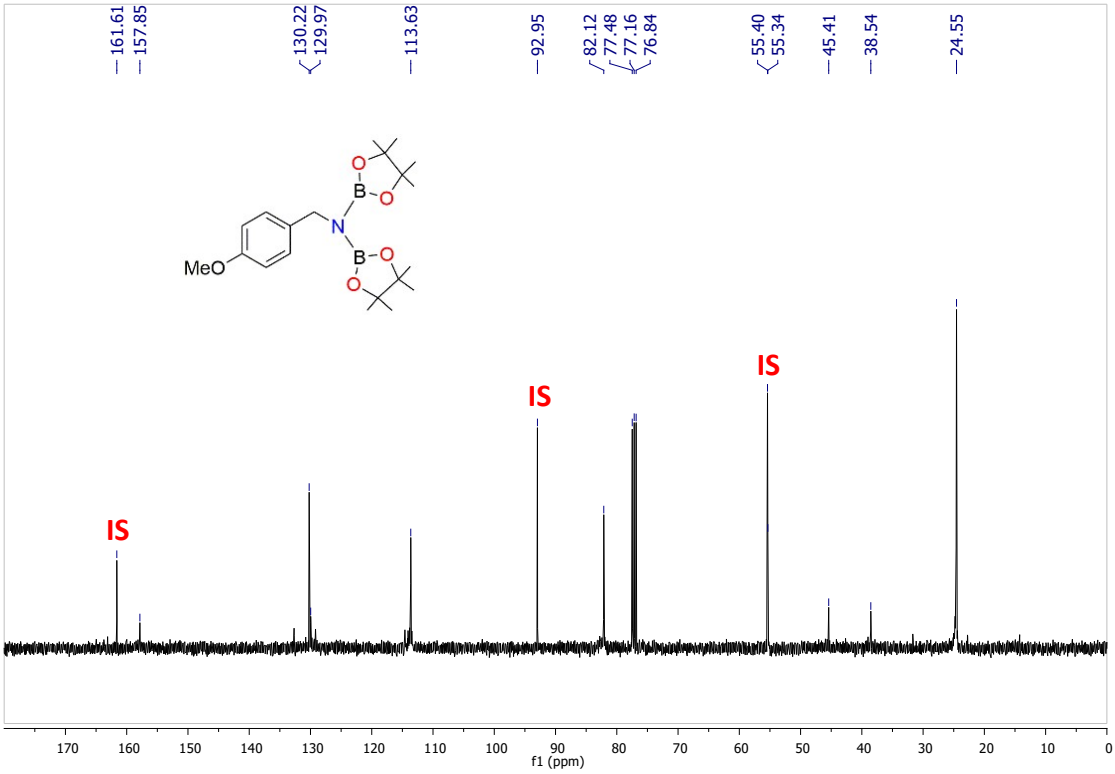

Figure FS 31. $^{13}C\{^{1}H\}$ NMR (100 MHz, $CDCl_3$, 298 K) spectrum of **6f**.

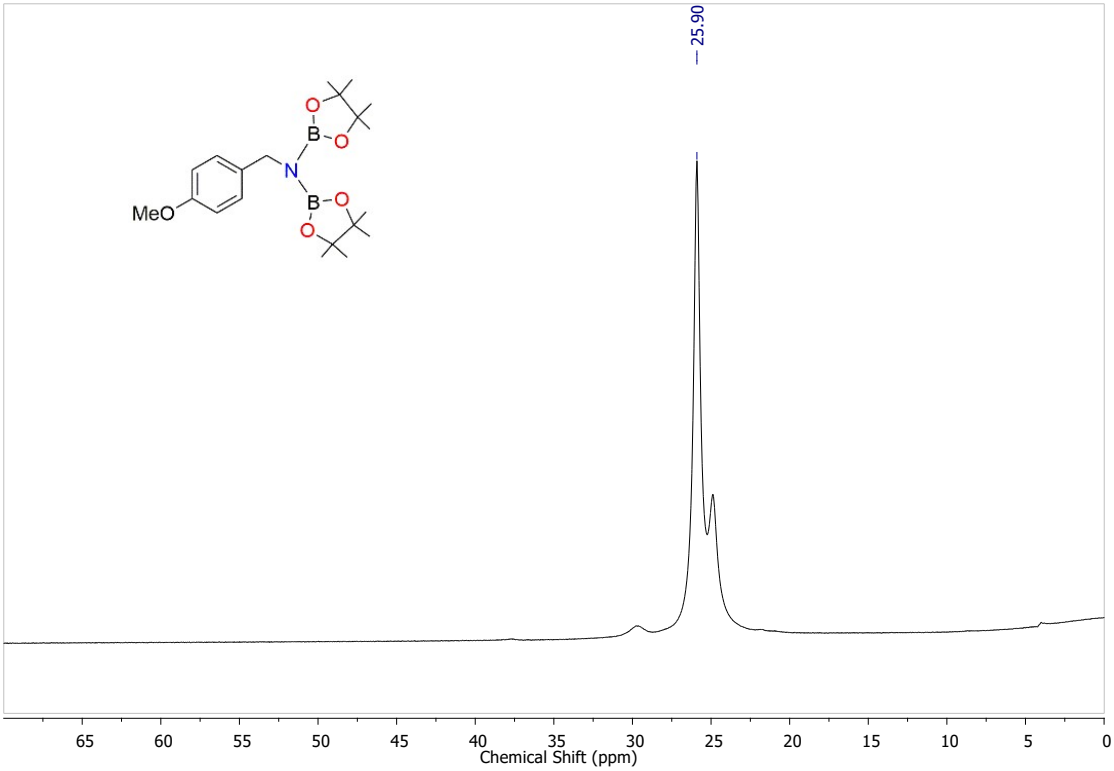

Figure FS 32. $^{11}B\{^{1}H\}$ NMR (128.4 MHz, $CDCl_3$, 298 K) spectrum of **6f**.

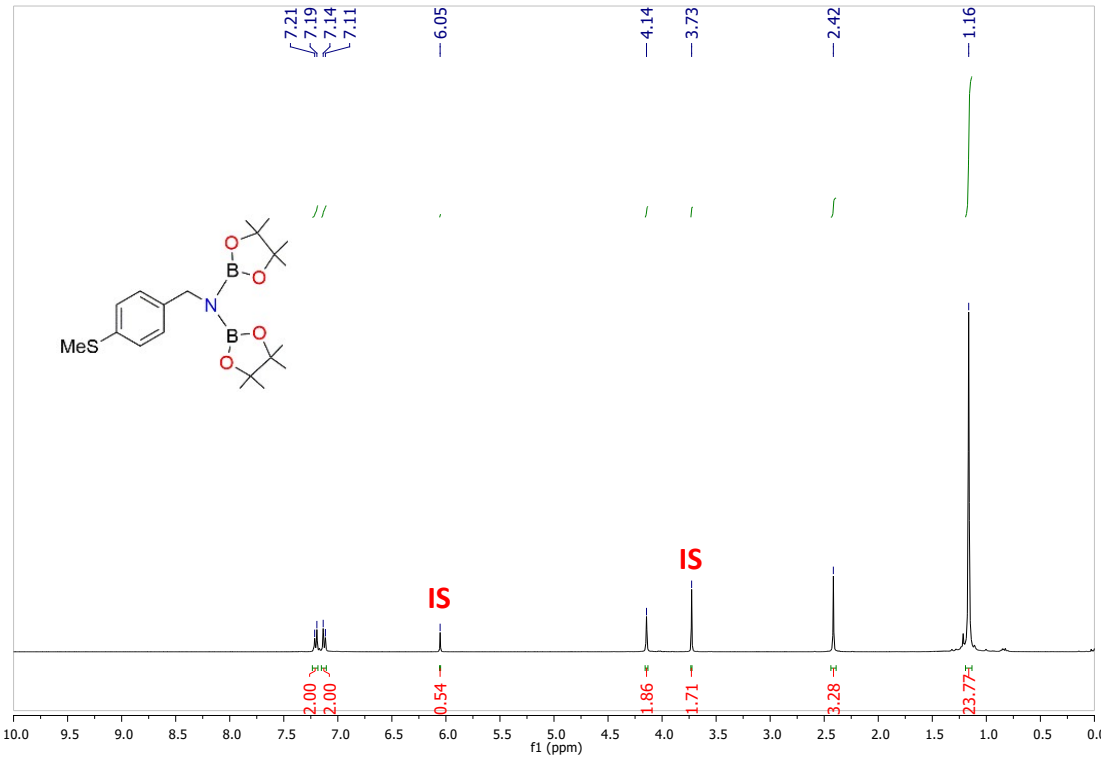

Figure FS 33. ^{1}H NMR (400 MHz, $CDCl_3$, 298 K) spectrum of **6g**.

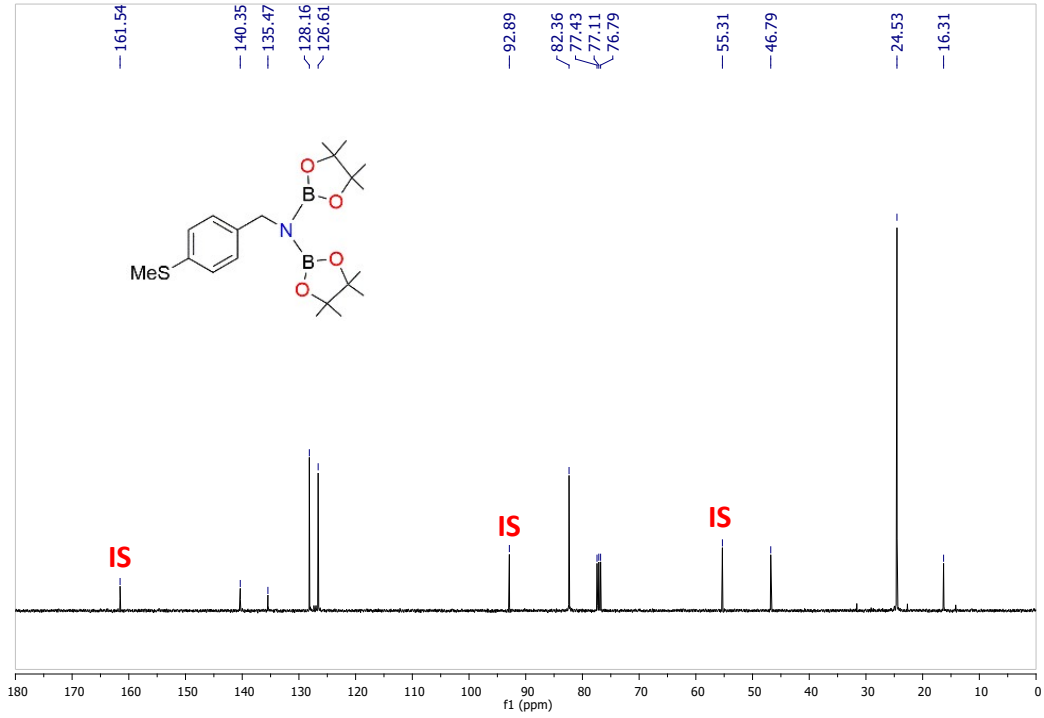

Figure FS 34. ^{13}C{^{1}H} NMR (100 MHz, $CDCl_3$, 298 K) spectrum of **6g**.

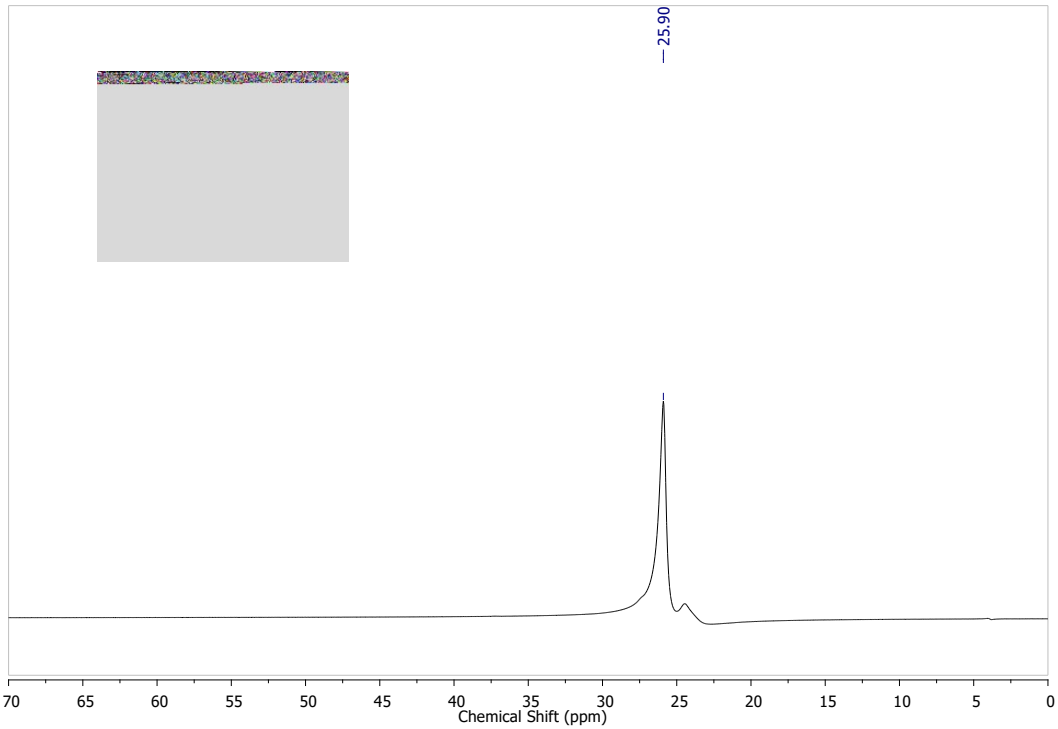

Figure FS 35. $^{11}B\{^{1}H\}$ NMR (128.4 MHz, $CDCl_3$, 298 K) spectrum of **6g**.

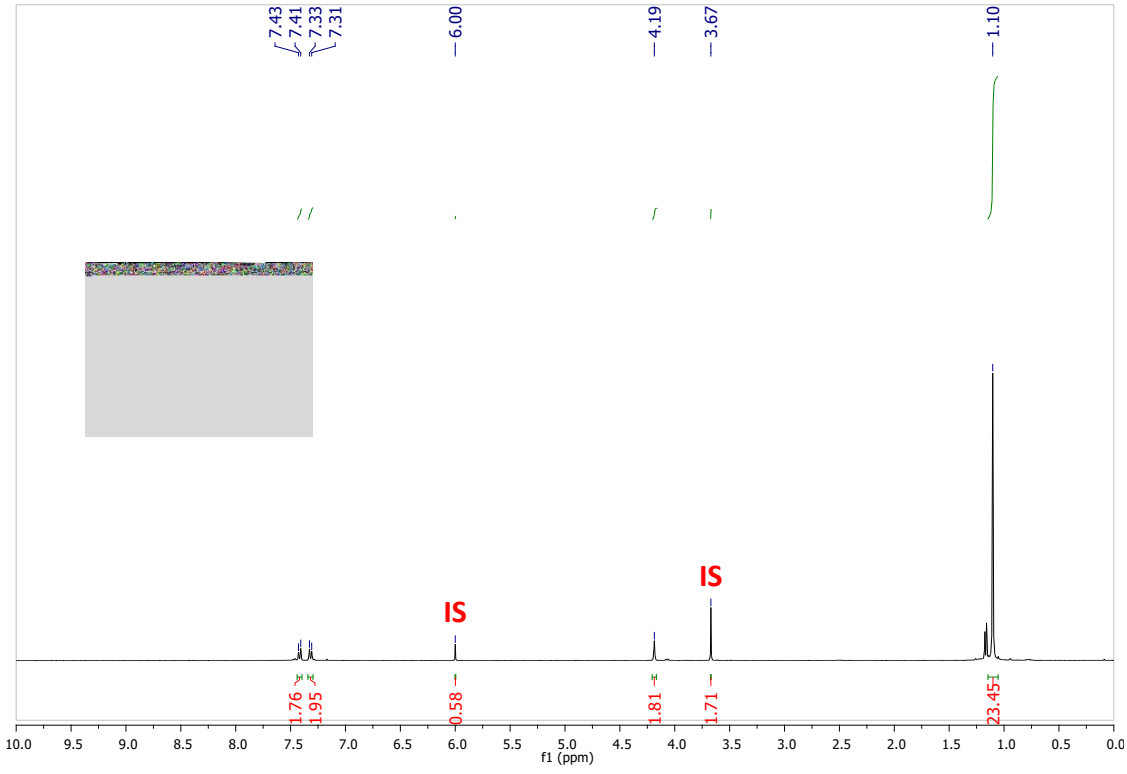

Figure FS 36. ^{1}H NMR (400 MHz, $CDCl_3$, 298 K) spectrum of **6h**.

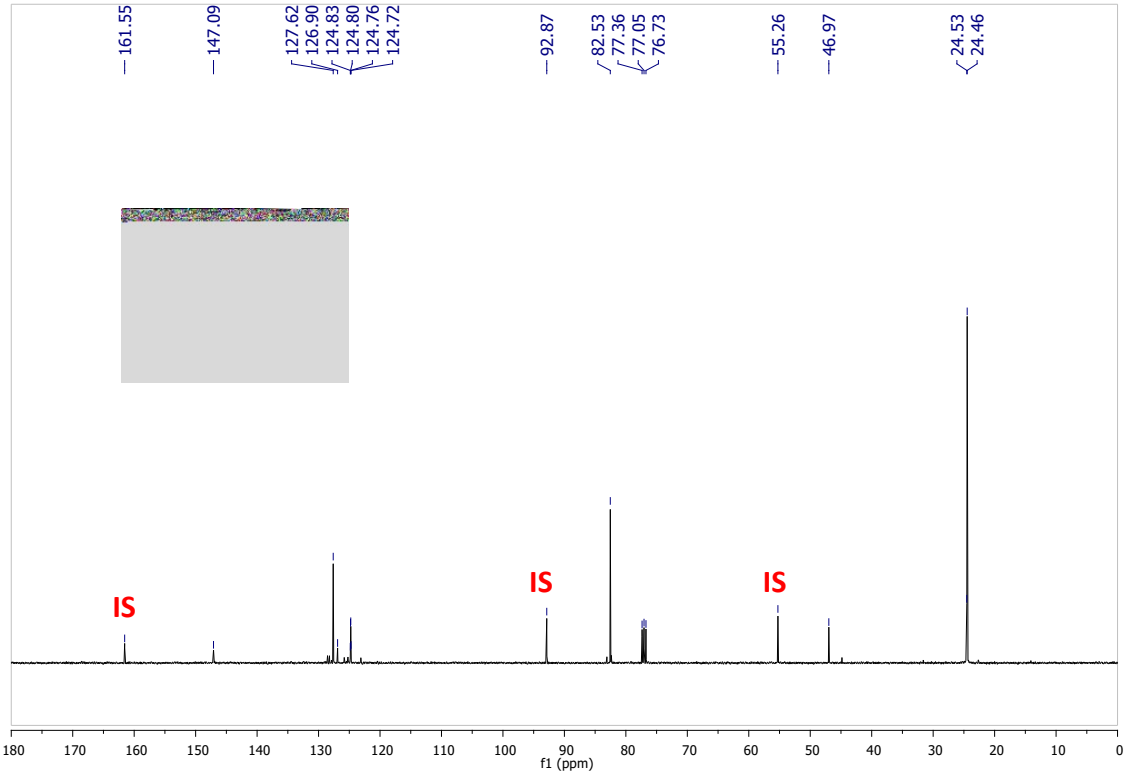

Figure FS 37. $^{13}C\{^{1}H\}$ NMR (100 MHz, $CDCl_3$, 298 K) spectrum of **6h**.

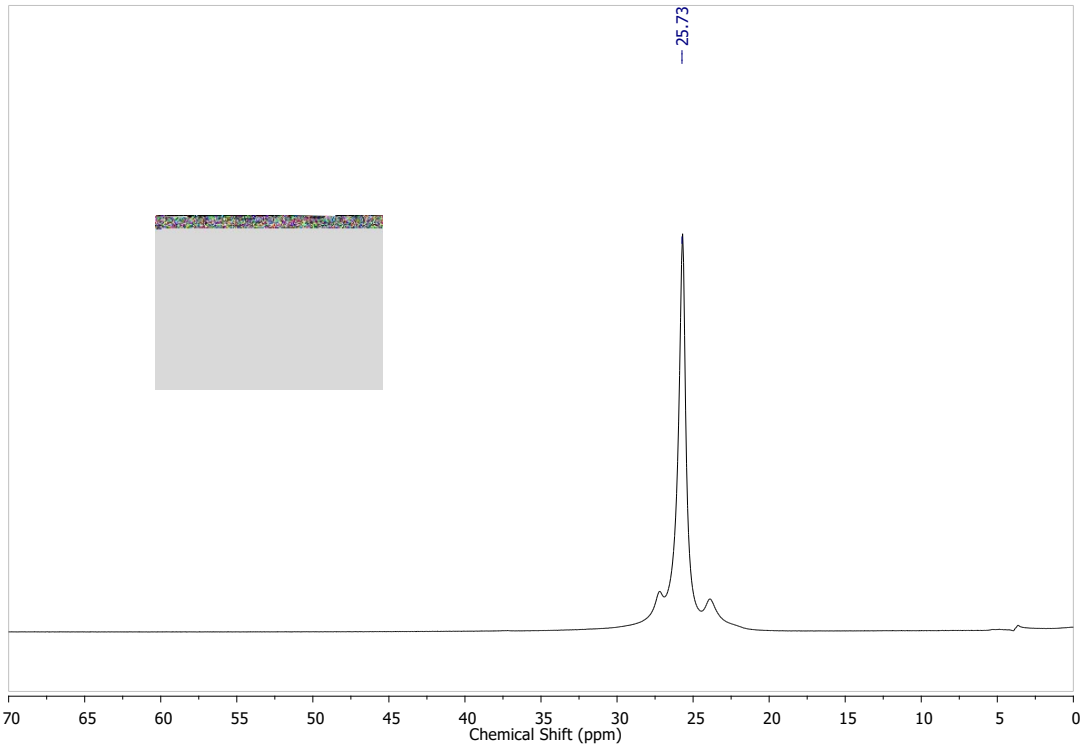

Figure FS 38. $^{11}B\{^{1}H\}$ NMR (128.4 MHz, $CDCl_3$, 298 K) spectrum of **6h**.

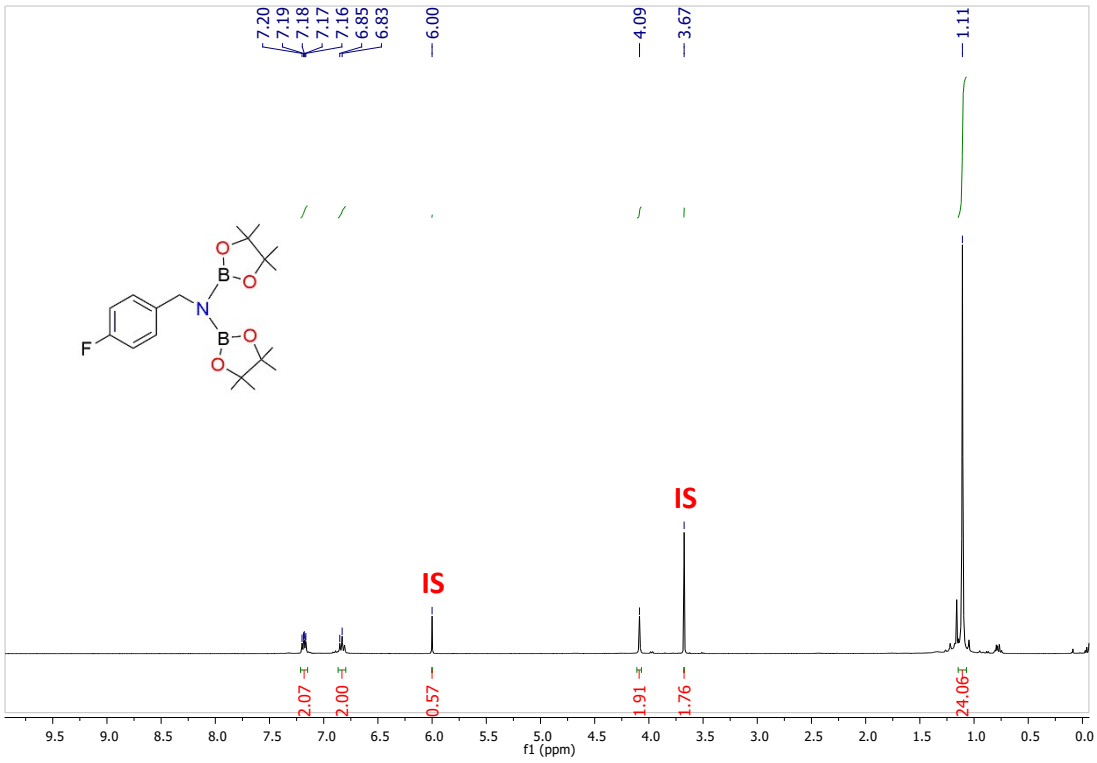

Figure FS 39. ^{1}H NMR (400 MHz, $CDCl_3$, 298 K) spectrum of **6i**.

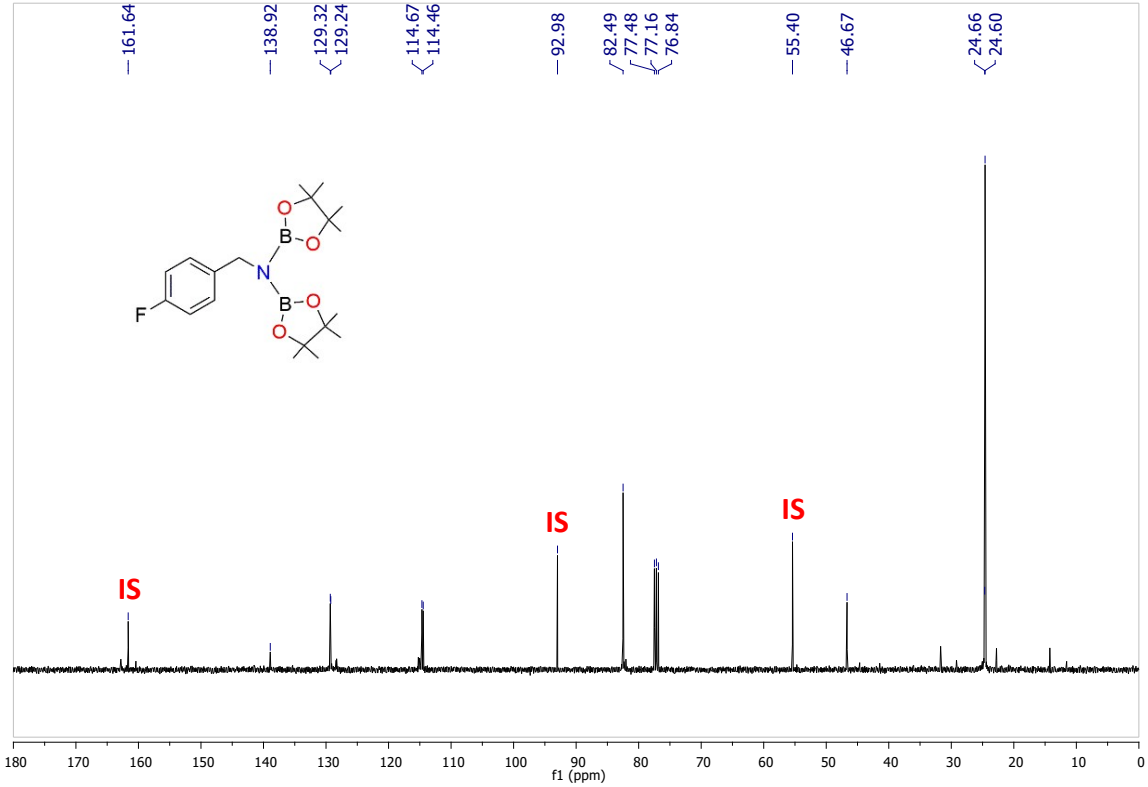

Figure FS 40. $^{13}C\{^{1}H\}$ NMR (100 MHz, $CDCl_3$, 298 K) spectrum of **6i**.

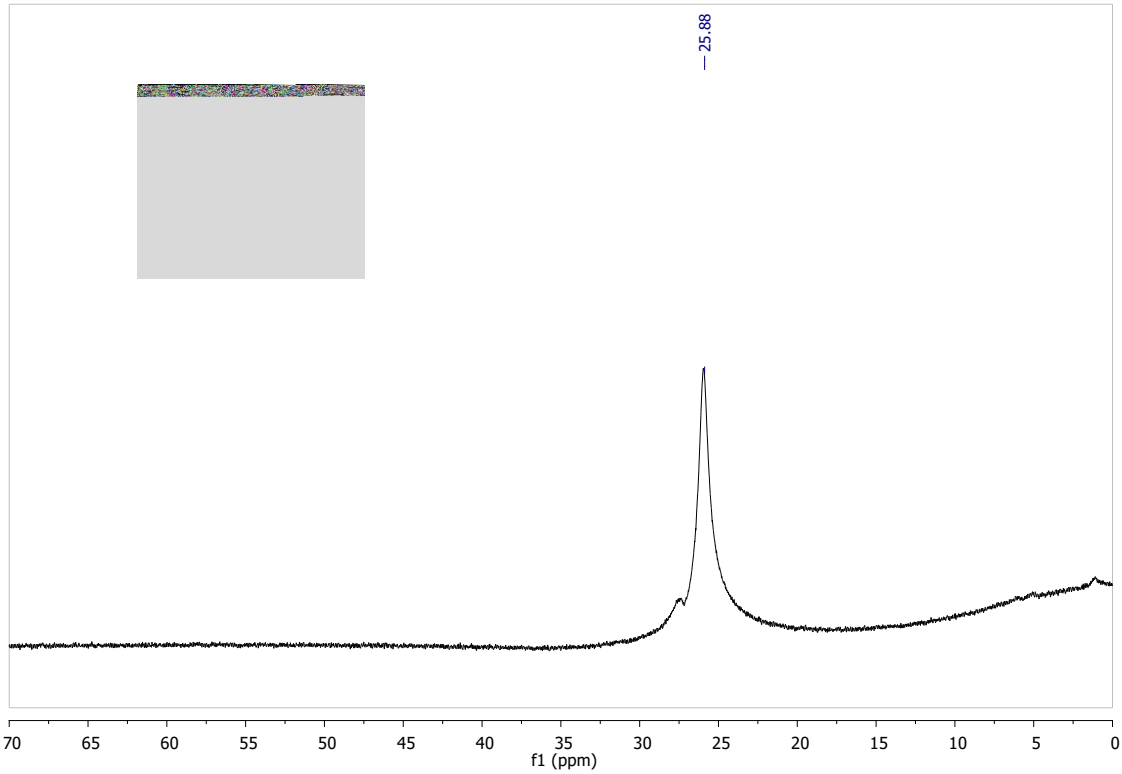

Figure FS 41. $^{11}B\{^{1}H\}$ NMR (128.4 MHz, $CDCl_3$, 298 K) spectrum of **6i**.

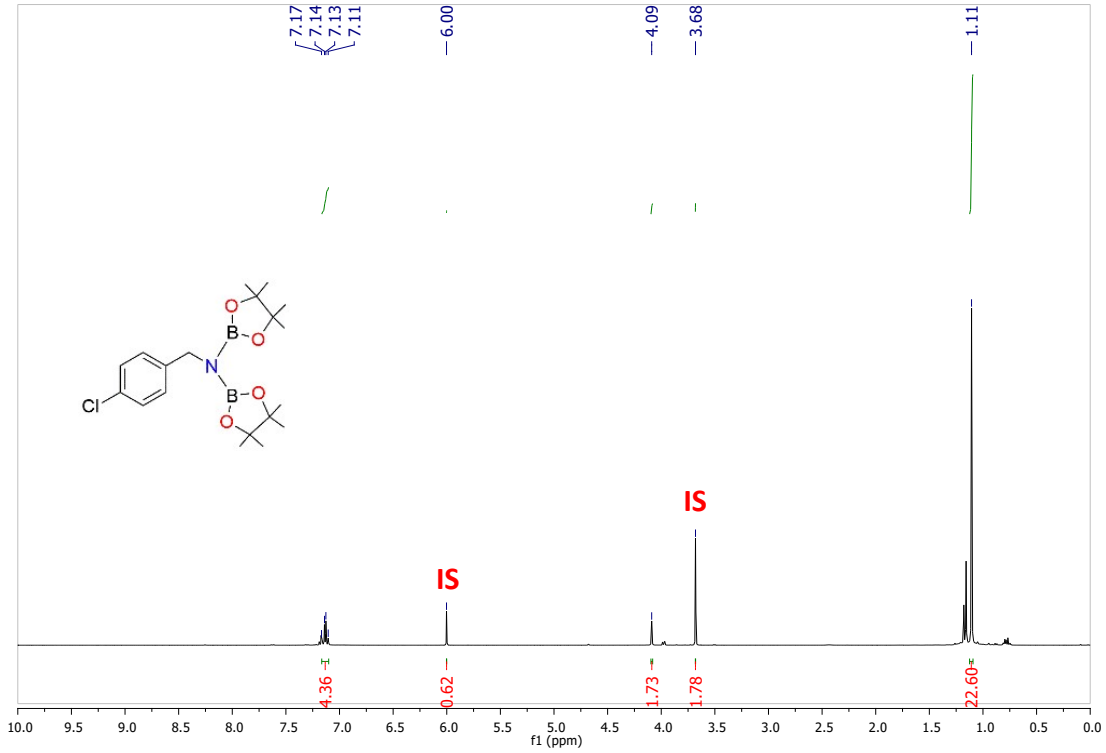

Figure FS 42. ^{1}H NMR (400 MHz, $CDCl_3$, 298 K) spectrum of **6j**.

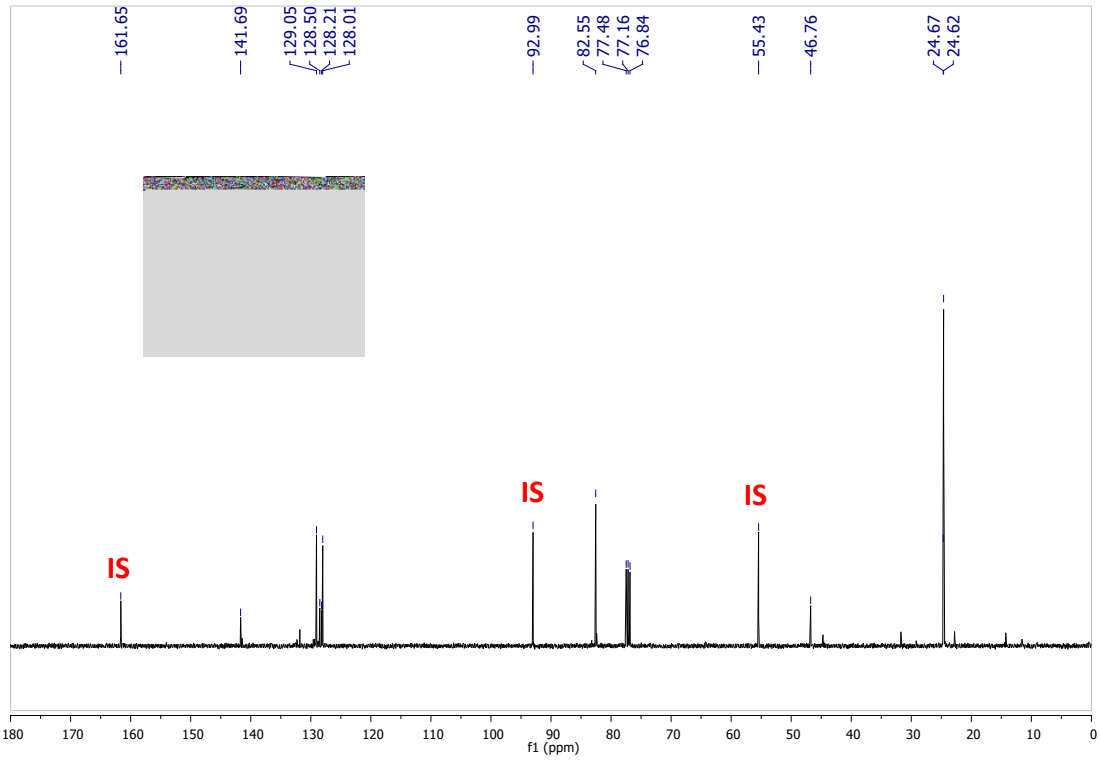

Figure FS 43. $^{13}C\{^{1}H\}$ NMR (100 MHz, $CDCl_3$, 298 K) spectrum of **6j**.

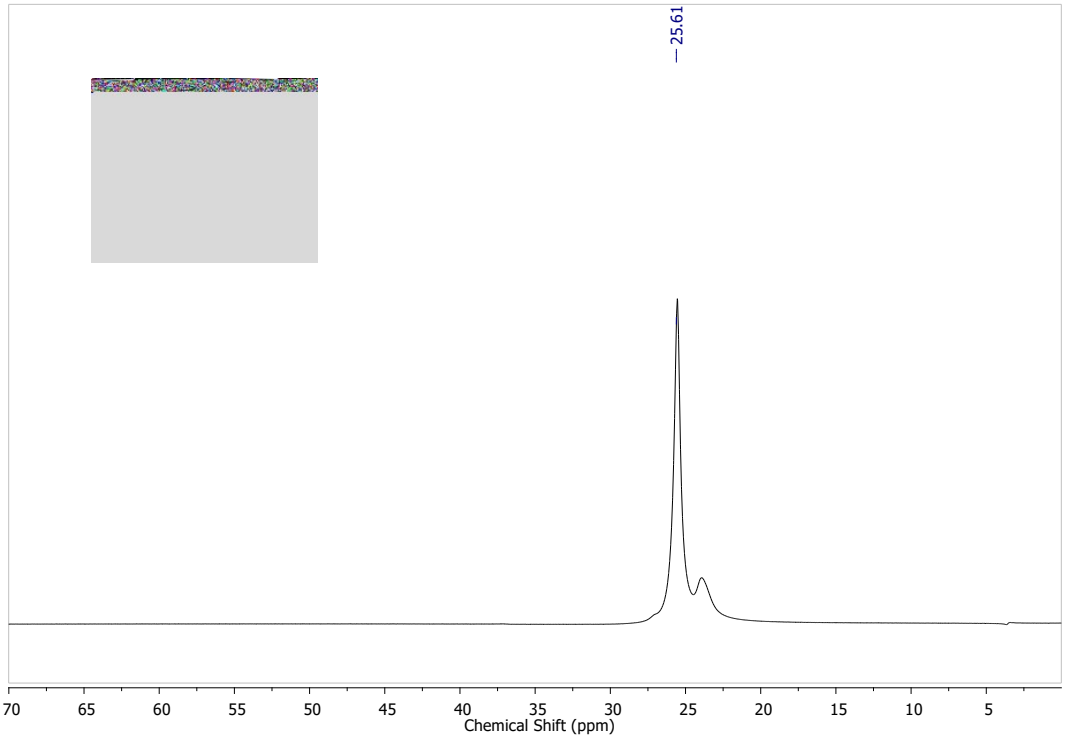

Figure FS 44. $^{11}B\{^{1}H\}$ NMR (128.4 MHz, $CDCl_3$, 298 K) spectrum of **6j**.

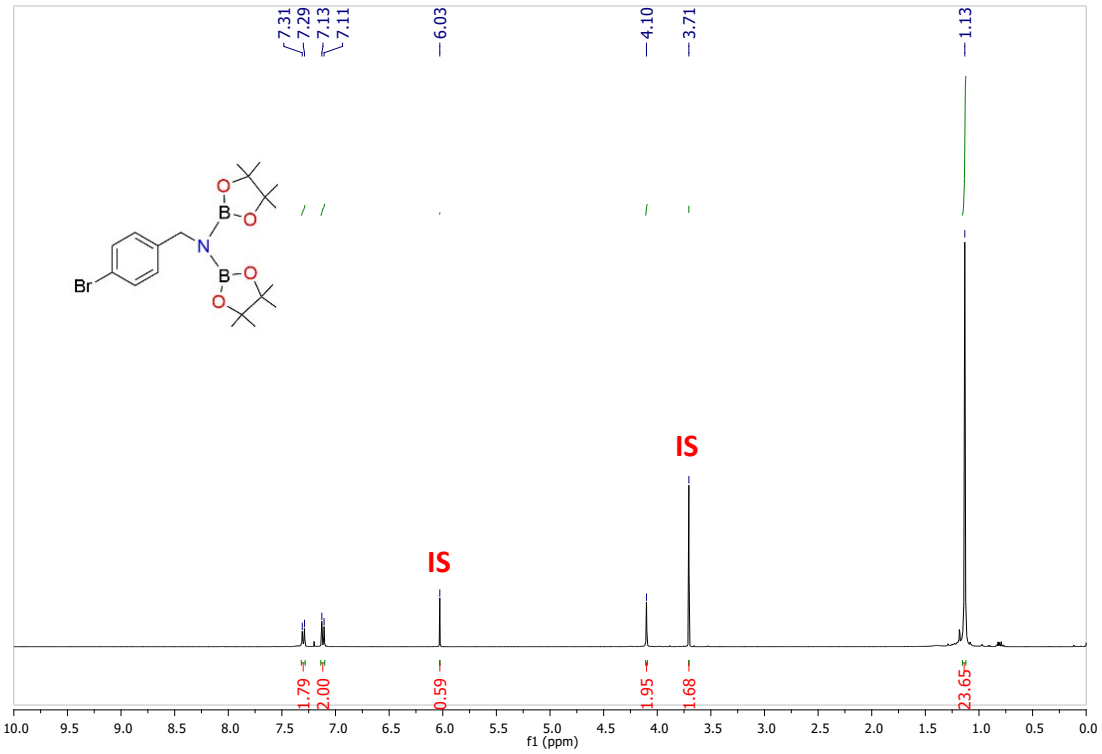

Figure FS 45. ^{1}H NMR (400 MHz, $CDCl_3$, 298 K) spectrum of **6k**.

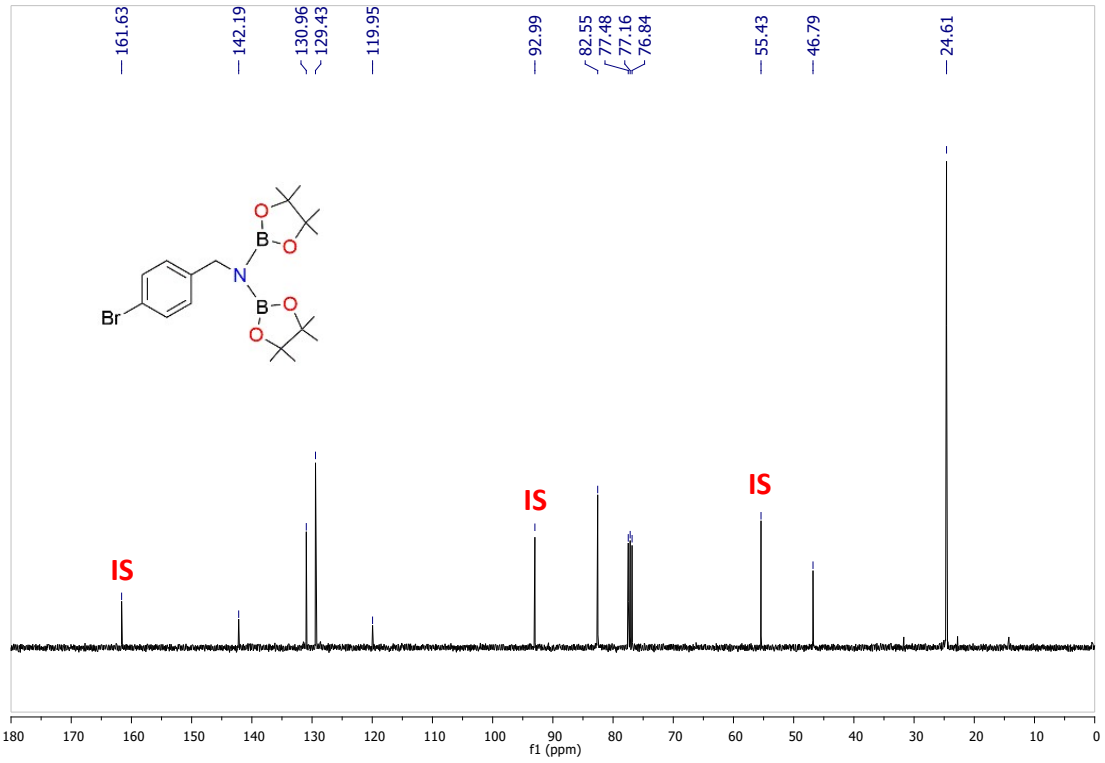

Figure FS 46. $^{13}C\{^{1}H\}$ NMR (100 MHz, $CDCl_3$, 298 K) spectrum of **6k**.

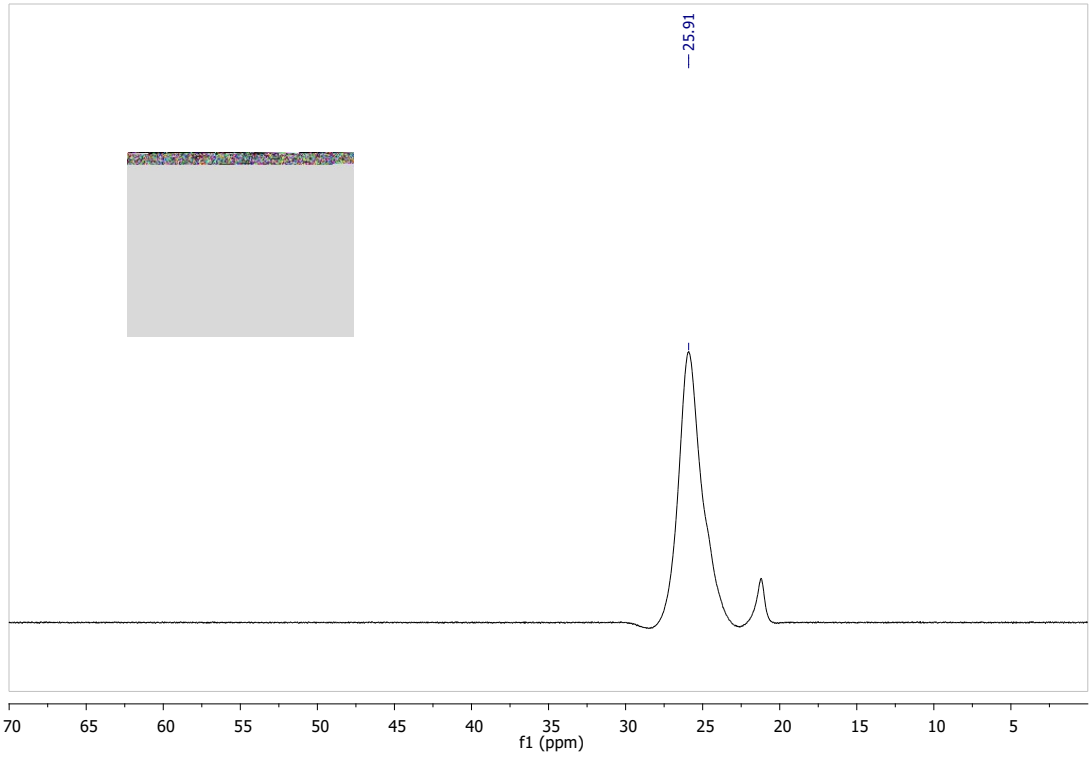

Figure FS 47. $^{11}B\{^{1}H\}$ NMR (128.4 MHz, $CDCl_3$, 298 K) spectrum of **6k**.

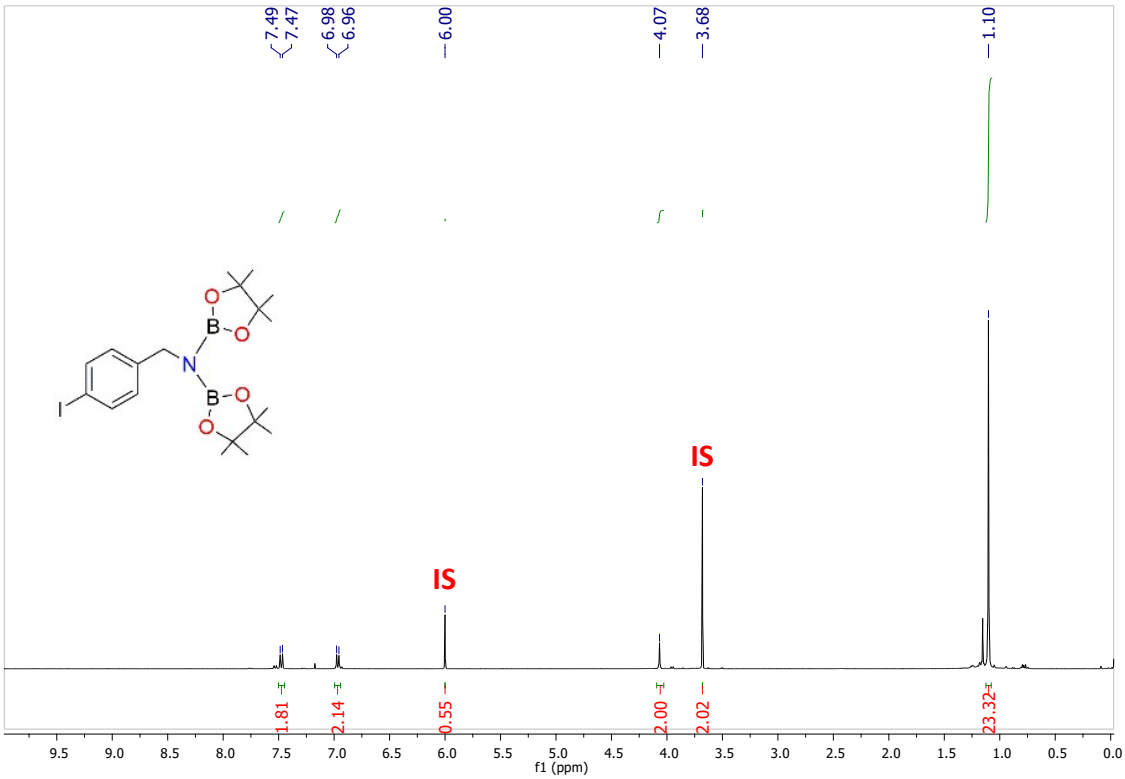

Figure FS 48. ^{1}H NMR (400 MHz, $CDCl_3$, 298 K) spectrum of **6l**.

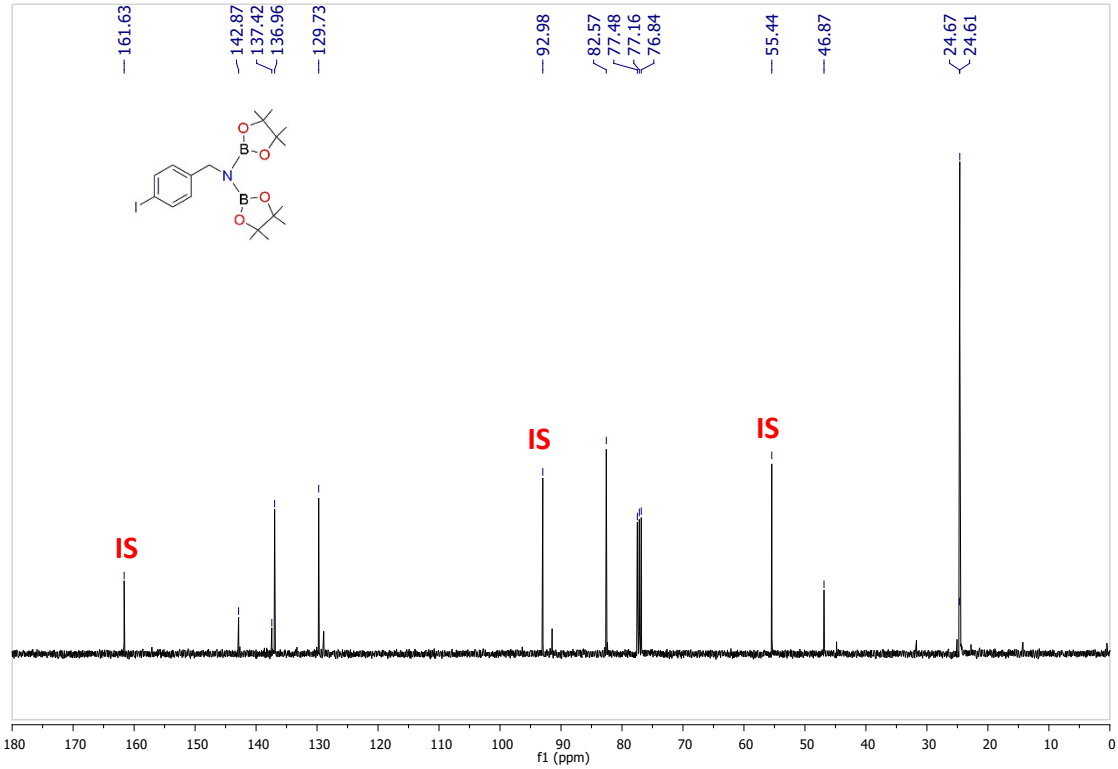

Figure FS 49. $^{13}C\{^{1}H\}$ NMR (100 MHz, $CDCl_3$, 298 K) spectrum of **6l**.

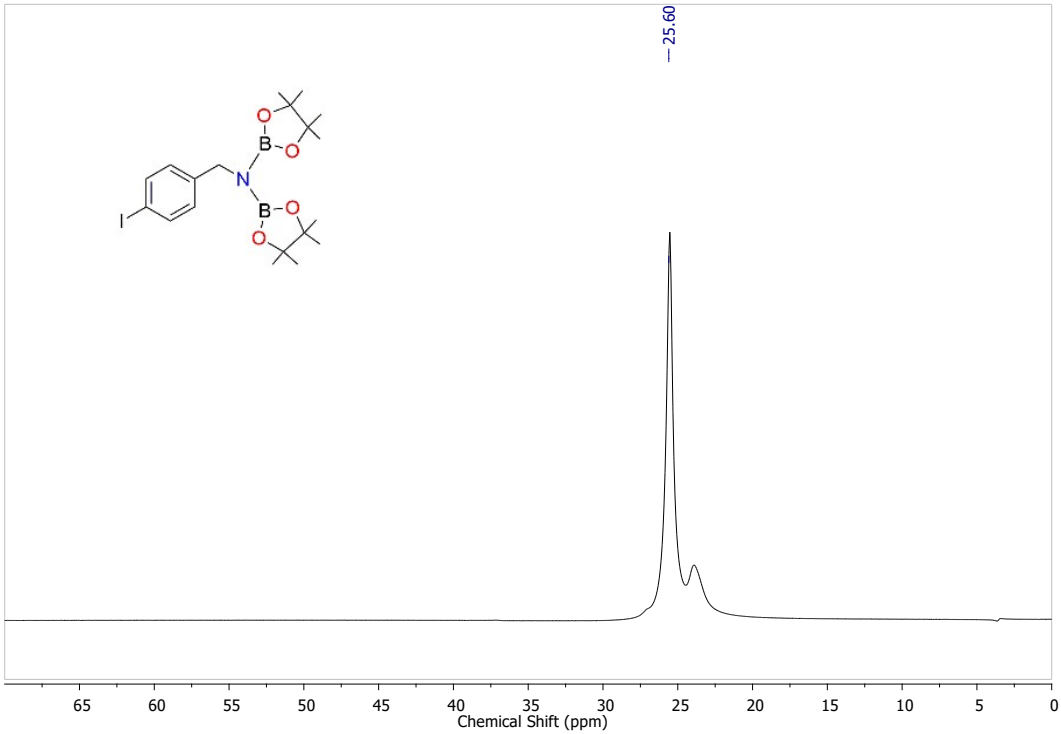

Figure FS 50. $^{11}B\{^{1}H\}$ NMR (128.4 MHz, $CDCl_3$, 298 K) spectrum of **6l**.

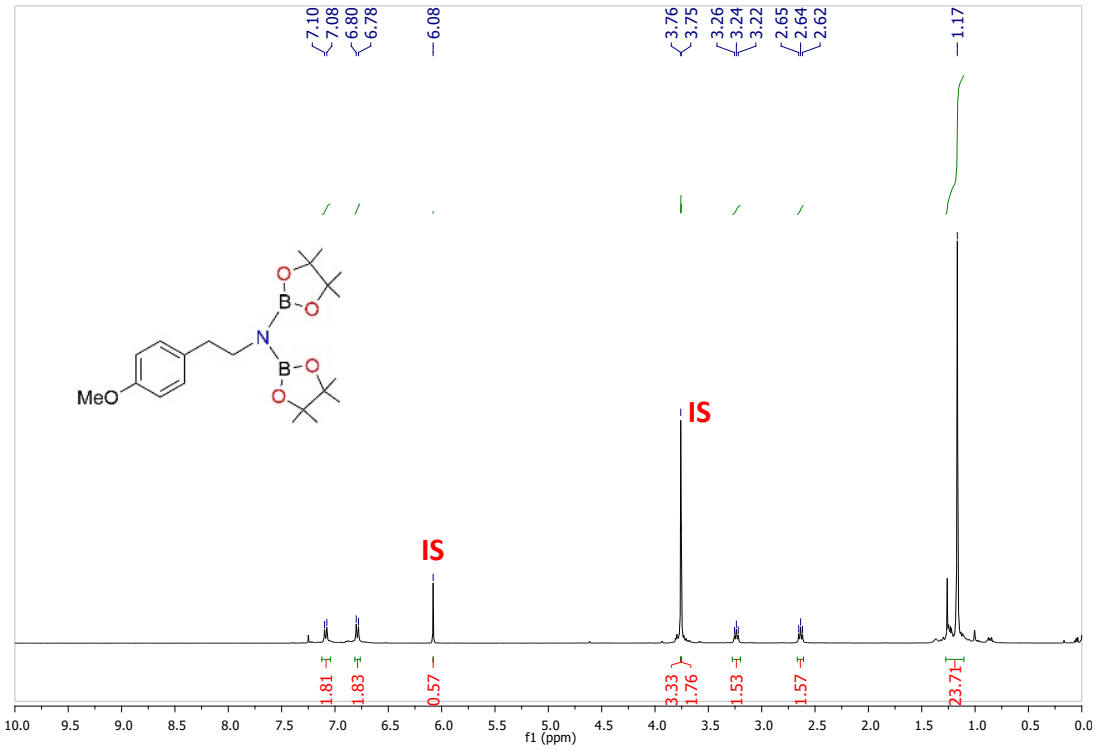

Figure FS 51. ^{1}H NMR (400 MHz, $CDCl_3$, 298 K) spectrum of **6m**.

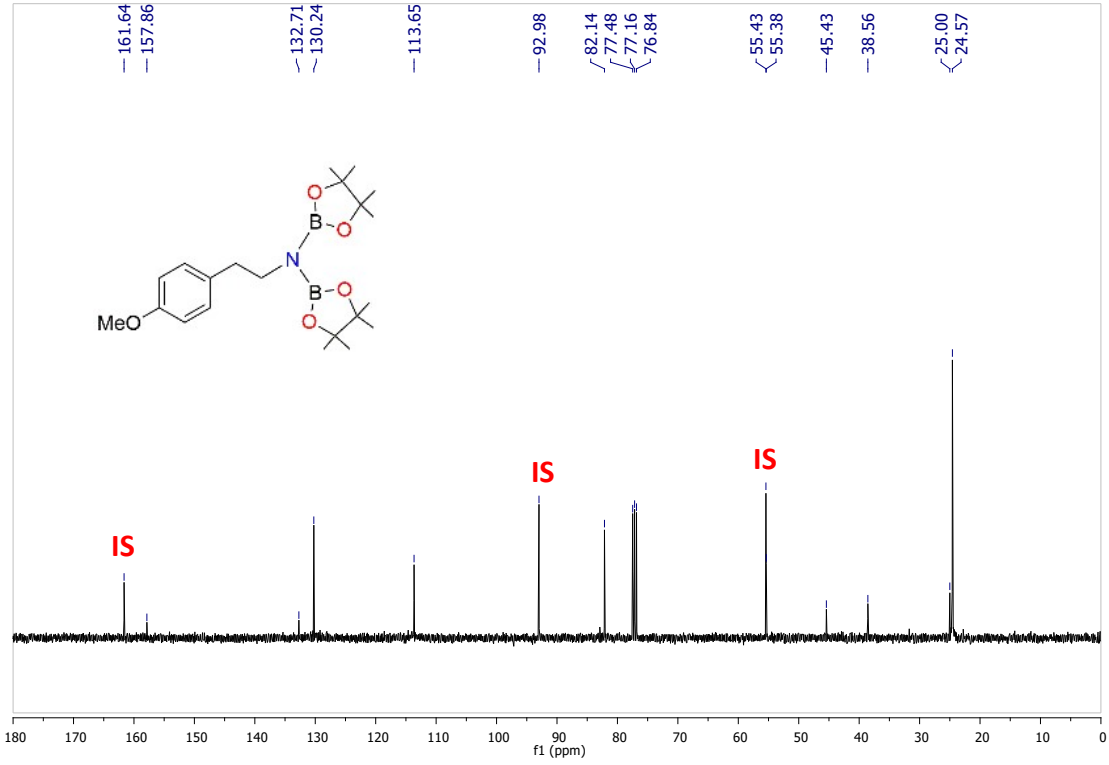

Figure FS 52. $^{13}C\{^{1}H\}$ NMR (100 MHz, $CDCl_3$, 298 K) spectrum of **6m**.

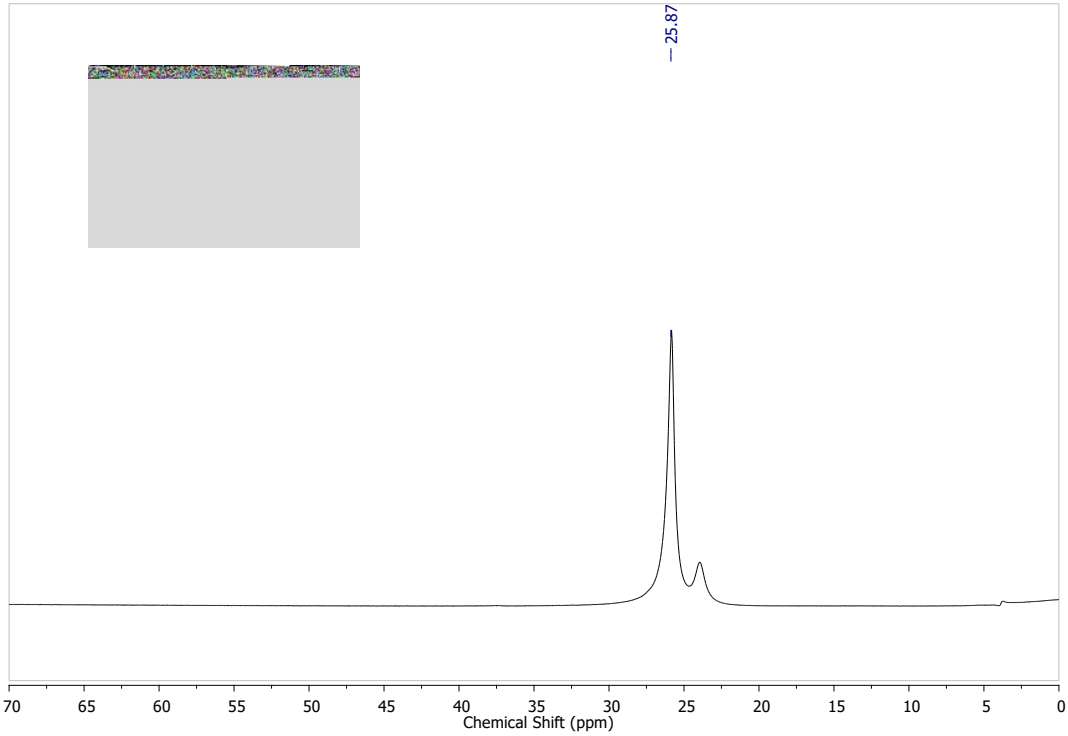

Figure FS 53. $^{11}B\{^{1}H\}$ NMR (128.4 MHz, $CDCl_3$, 298 K) spectrum of **6m**.

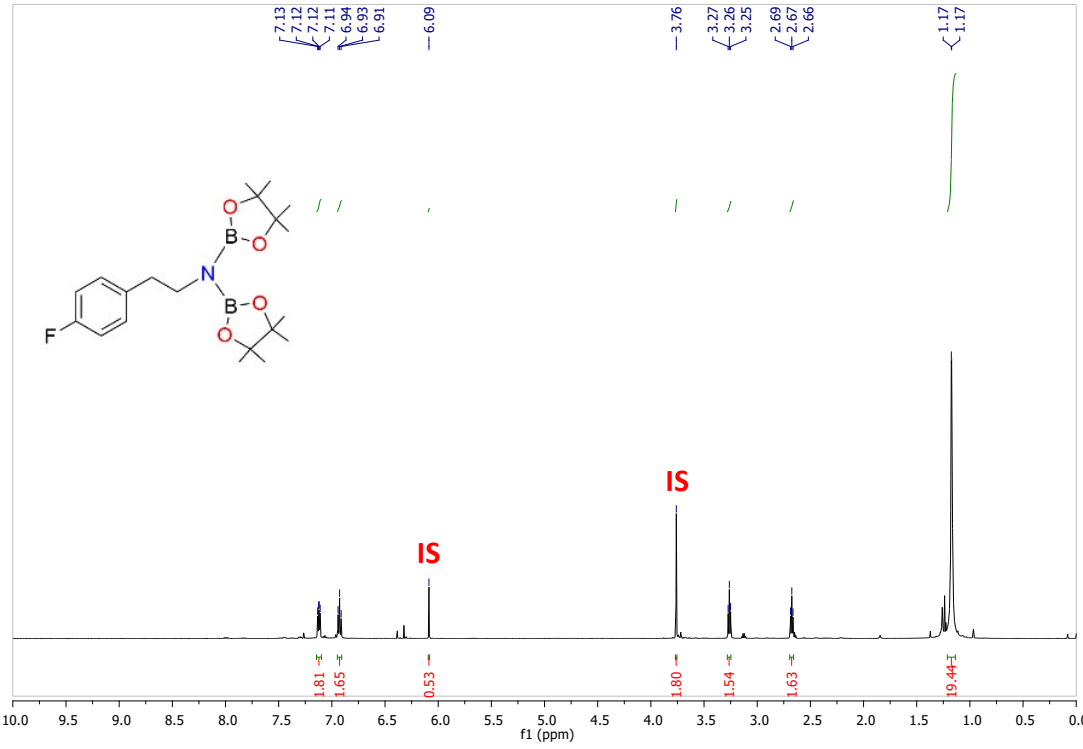

Figure FS 54. ^{1}H NMR (400 MHz, $CDCl_3$, 298 K) spectrum of **6n**.

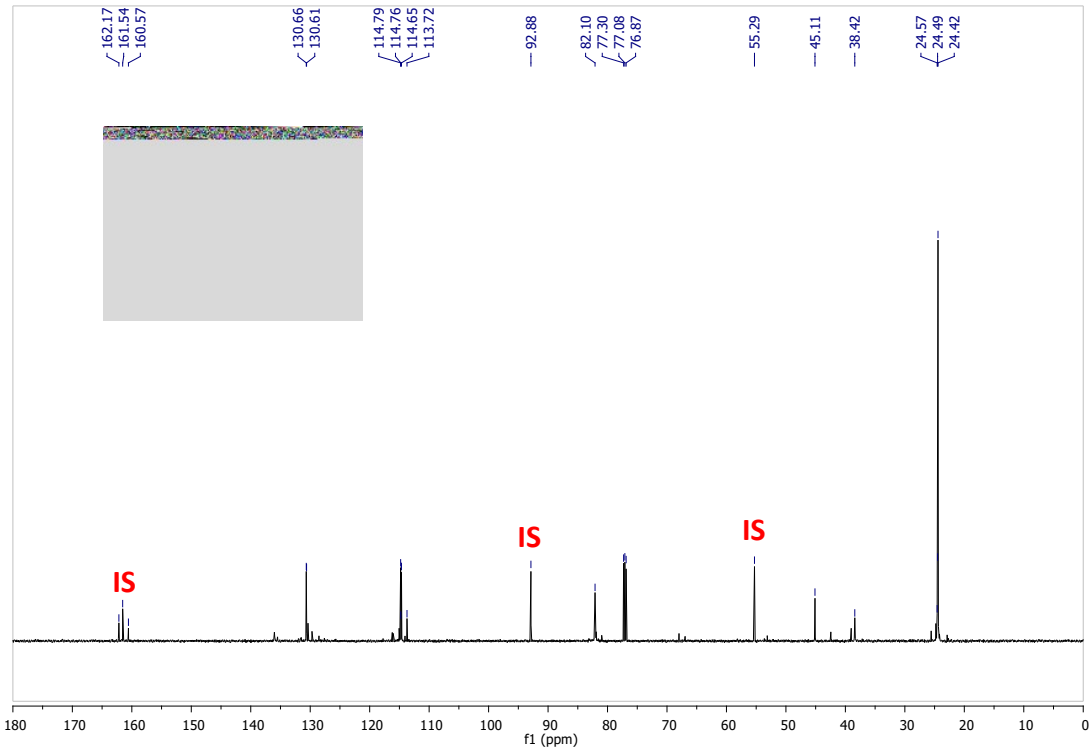

Figure FS 55. $^{13}C\{^{1}H\}$ NMR (100 MHz, $CDCl_3$, 298 K) spectrum of **6n**.

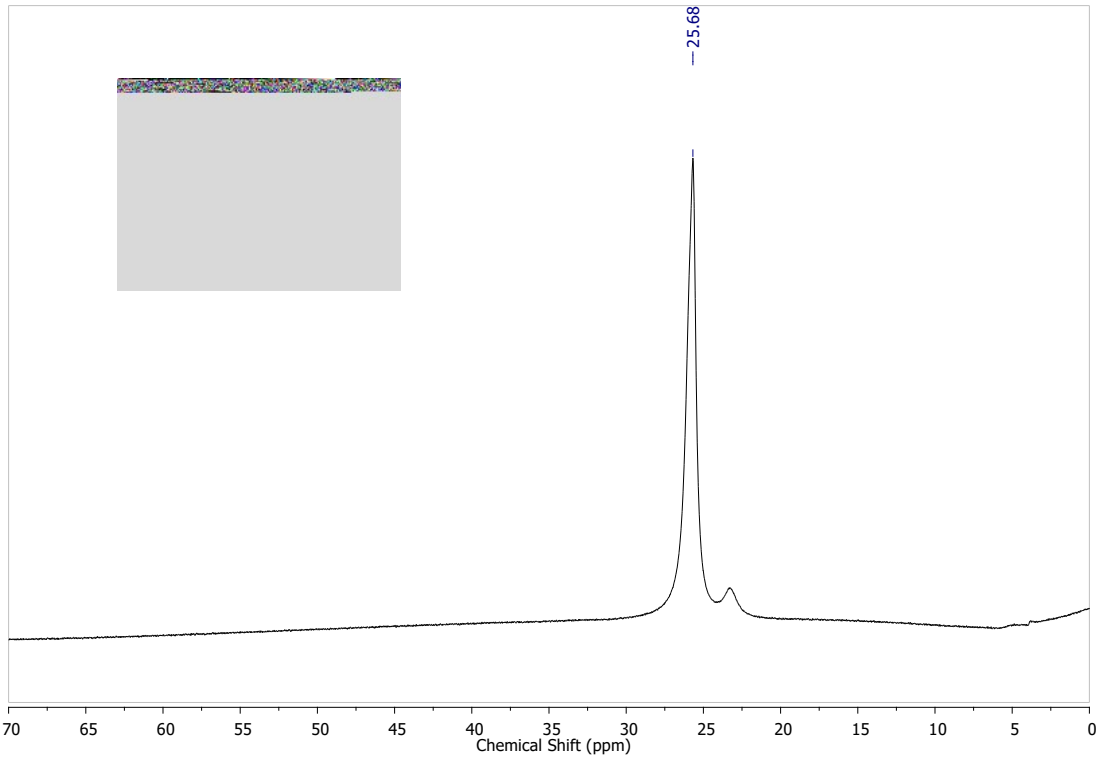

Figure FS 56. $^{11}B\{^{1}H\}$ NMR (128.4 MHz, $CDCl_3$, 298 K) spectrum of **6n**.

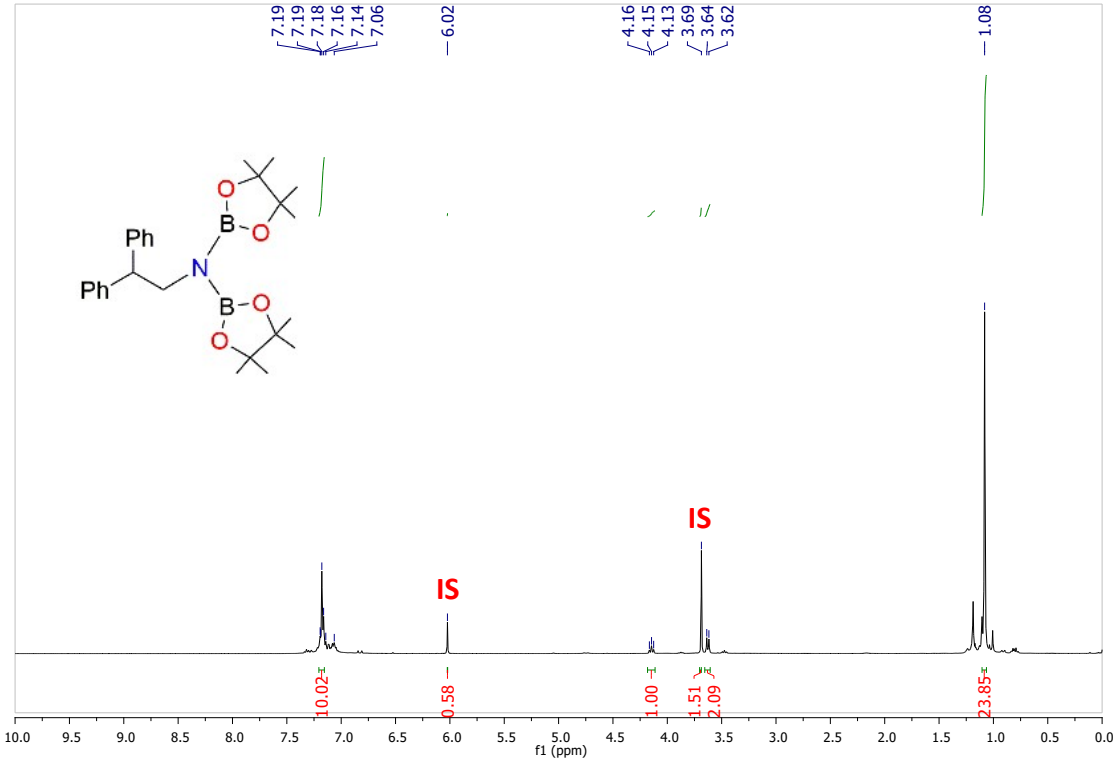

Figure FS 57. ^{1}H NMR (400 MHz, $CDCl_3$, 298 K) spectrum of **6o**.

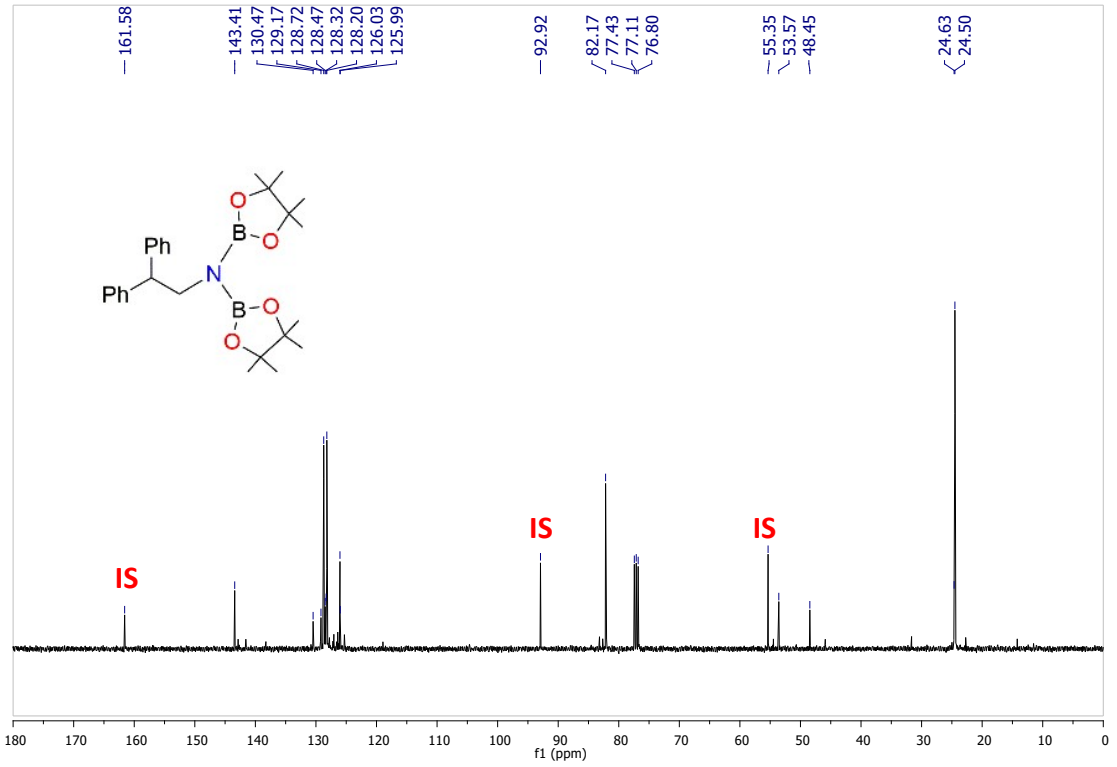

Figure FS 58. $^{13}C\{^{1}H\}$ NMR (100 MHz, $CDCl_3$, 298 K) spectrum of **6o**.

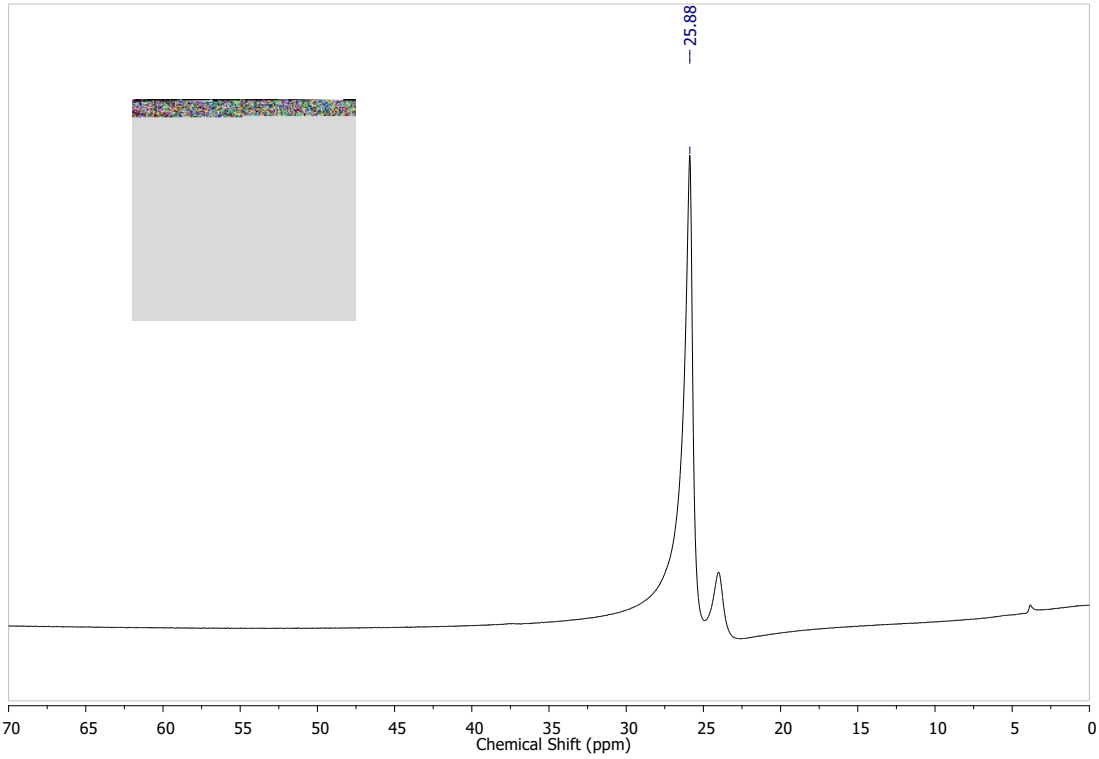

Figure FS 59. $^{11}B\{^{1}H\}$ NMR (128.4 MHz, $CDCl_3$, 298 K) spectrum of **6o**.

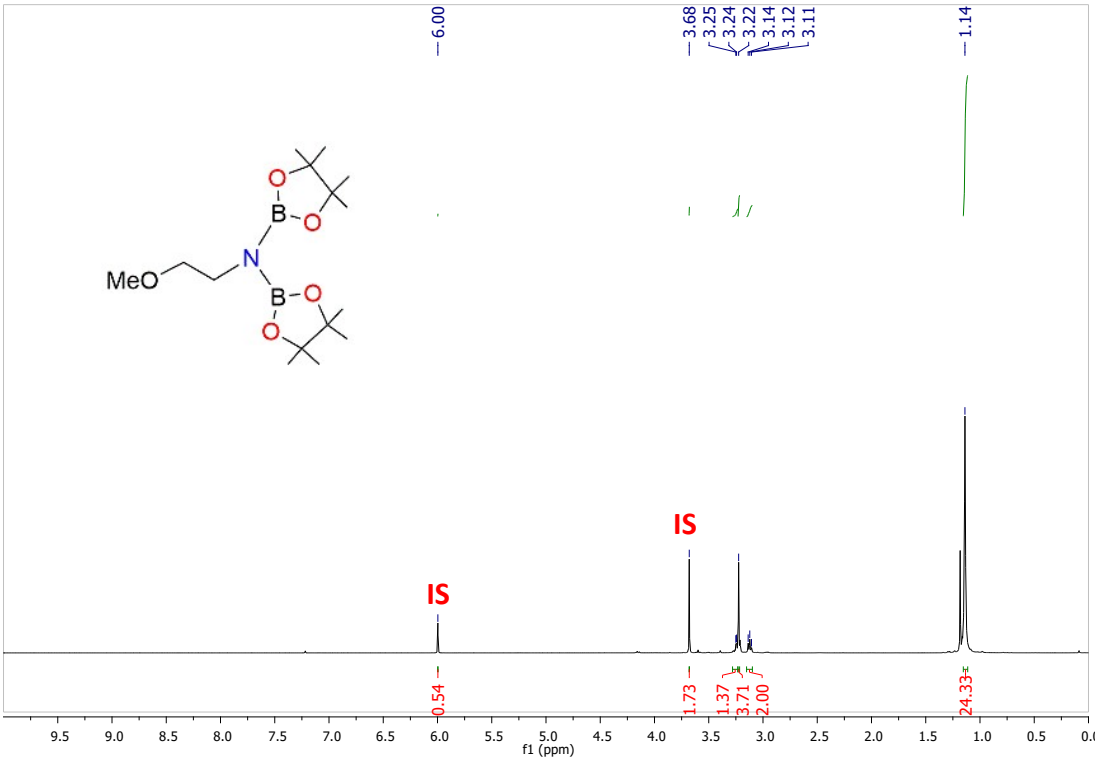

Figure FS 60. ^{1}H NMR (400 MHz, $CDCl_3$, 298 K) spectrum of **6p**.

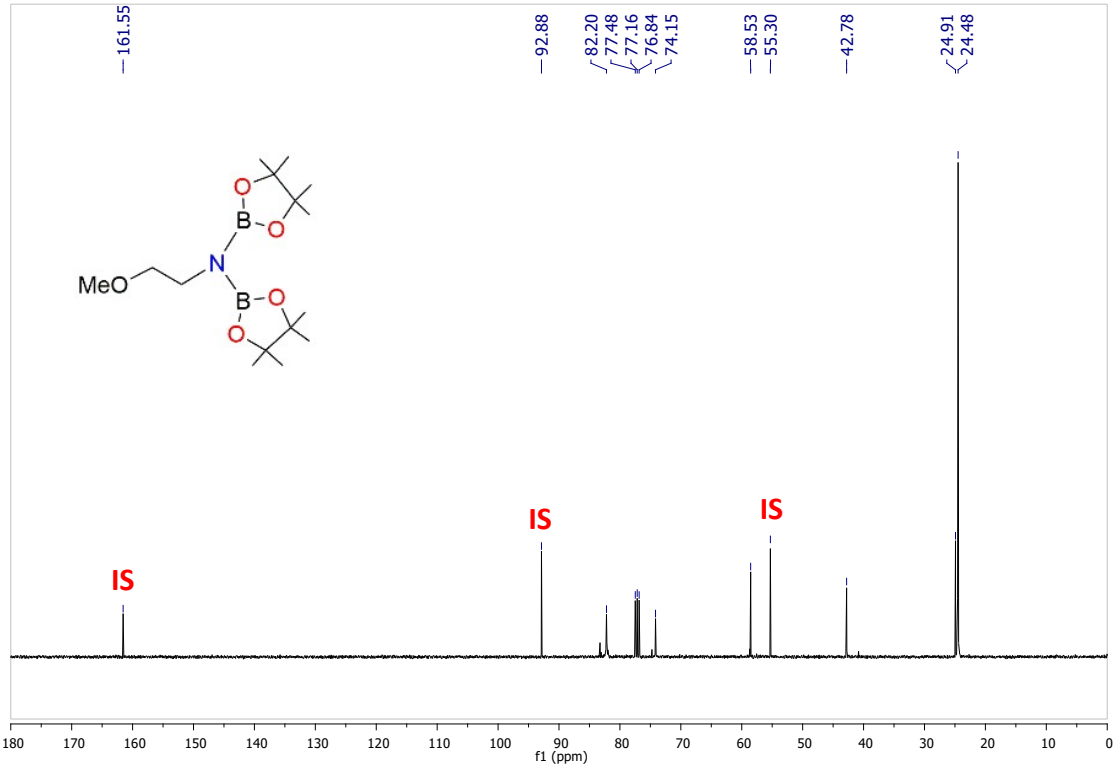

Figure FS 61. $^{13}C\{^{1}H\}$ NMR (100 MHz, $CDCl_3$, 298 K) spectrum of **6p**.

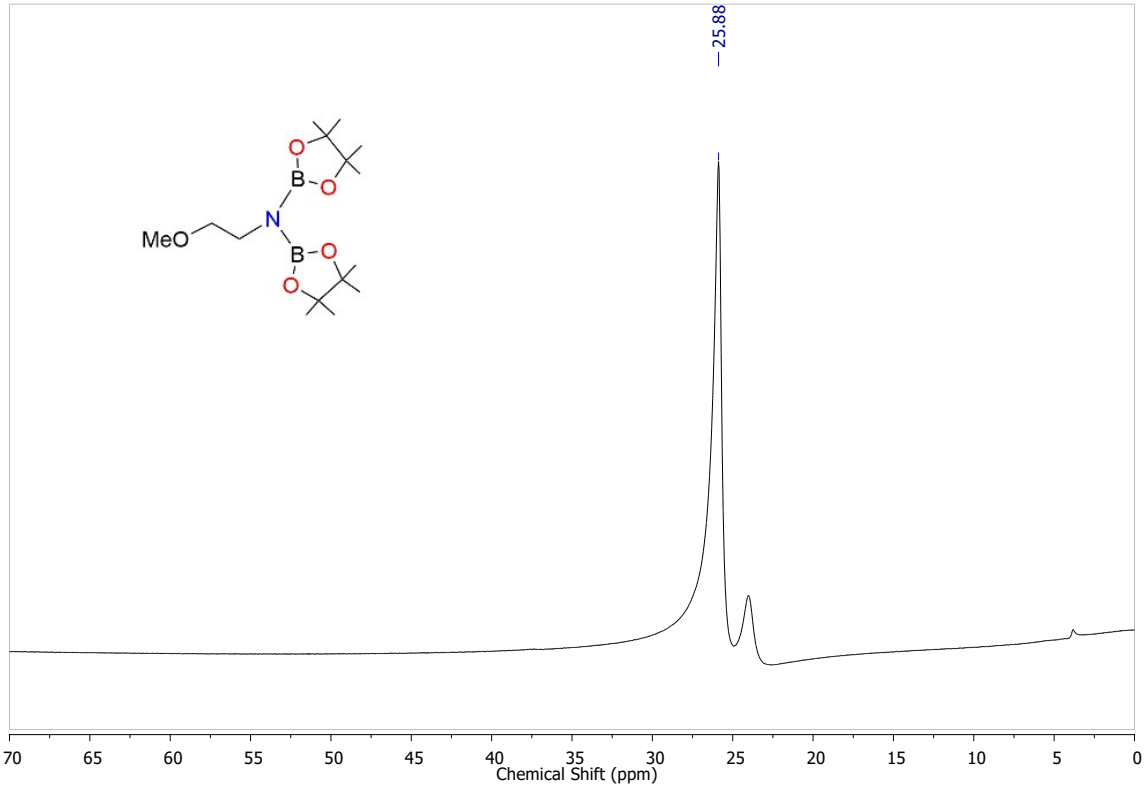

Figure FS 62. $^{11}B\{^{1}H\}$ NMR (128.4 MHz, $CDCl_3$, 298 K) spectrum of **6p**.

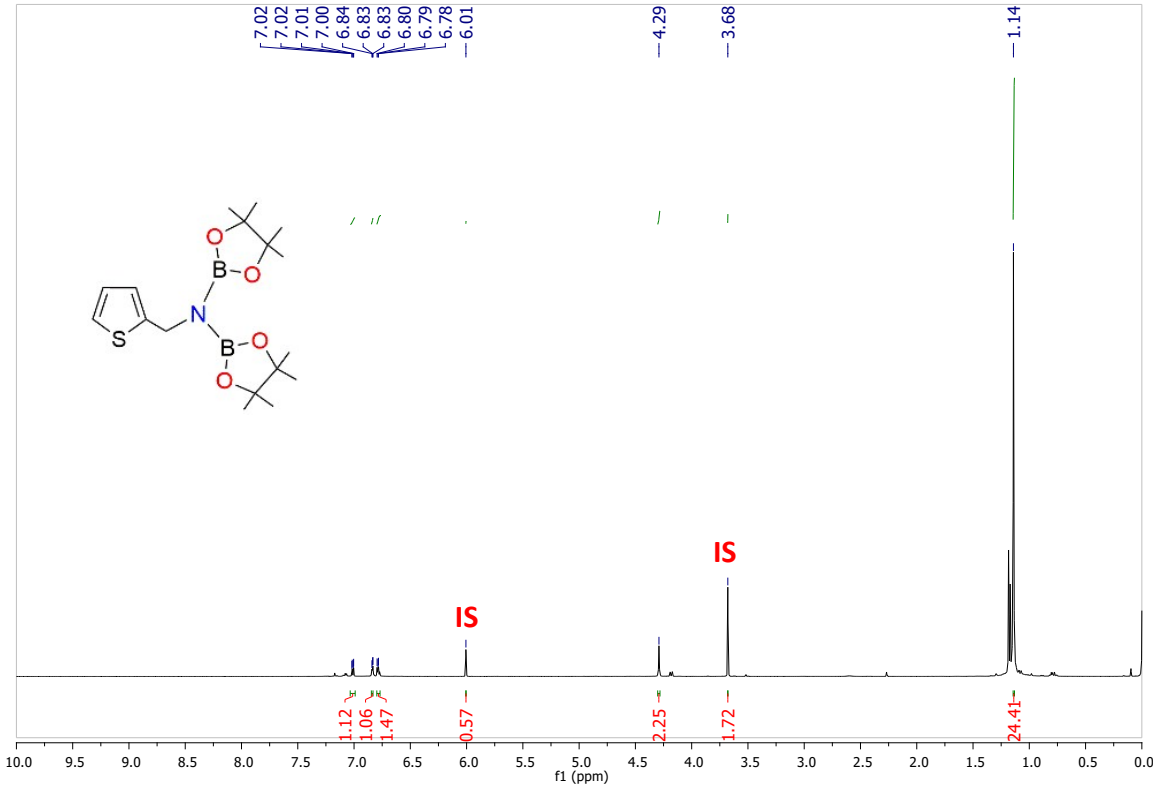

Figure FS 63. ^{1}H NMR (400 MHz, $CDCl_3$, 298 K) spectrum of **6q**.

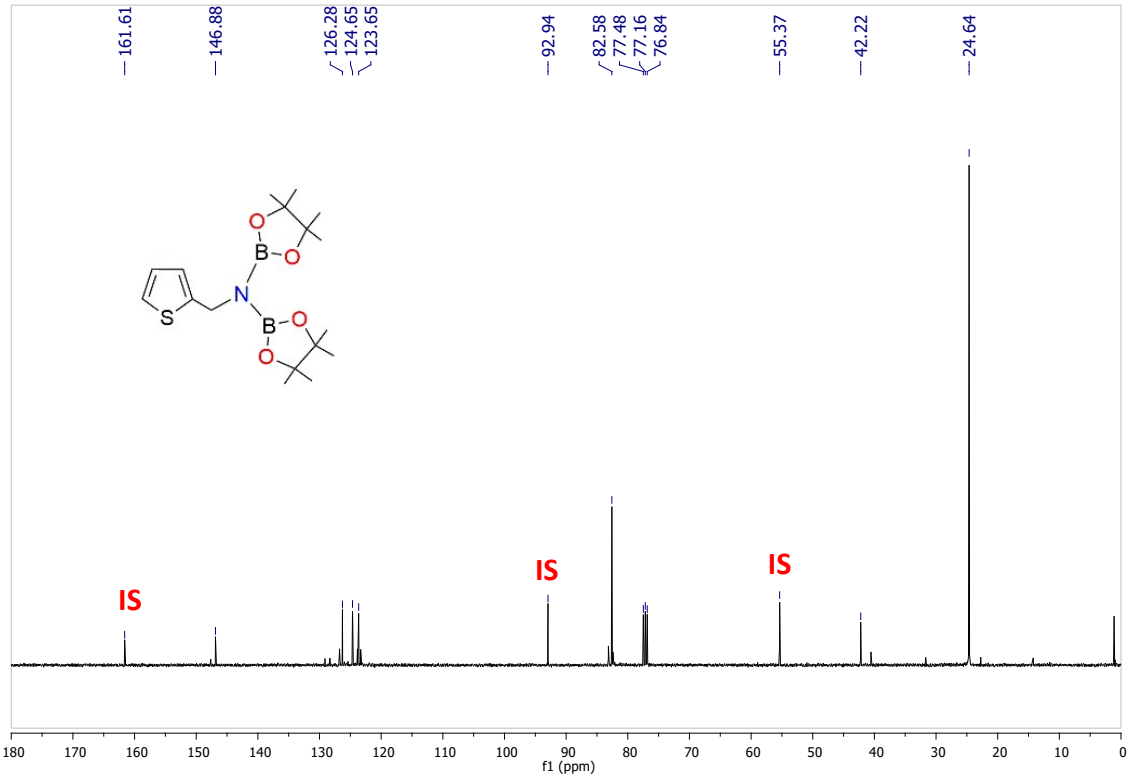

Figure FS 64. ^{13}C{^{1}H} NMR (100 MHz, $CDCl_3$, 298 K) spectrum of **6q**.

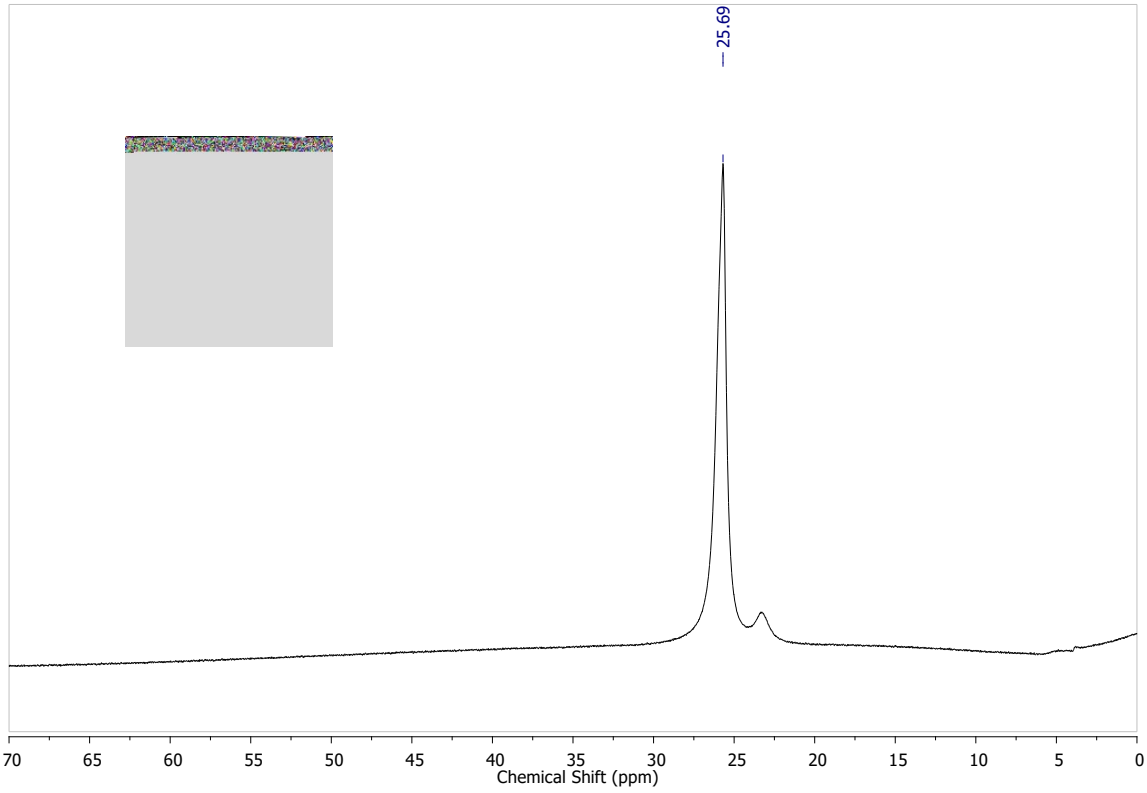

Figure FS 65. $^{11}B\{^{1}H\}$ NMR (128.4 MHz, $CDCl_3$, 298 K) spectrum of **6q**.

3.4. Hydrolysis of *N*,*N*-diborylamines

3.4.1 General procedure for the hydrolysis of *N*,*N*-diborylamines

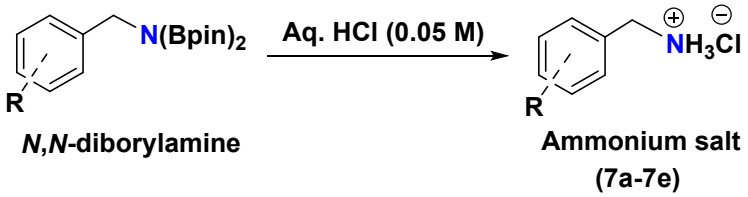

N,*N*-diborylamines, obtained from the hydroboration of organic nitriles were treated with 0.05 M HCl solution and kept in stirring for 4 h at room temperature. Next, the reaction mixture was washed with DCM (3-4 times). Finally, the aqueous part was collected and evaporated to obtain primary ammonium salts as hydrolyzed products and the compounds were characterized by NMR spectroscopy.

3.4.2 Characterization data of ammonium salts

Phenylmethanaminium chloride (7a)[2]

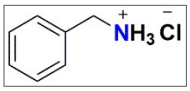

^{1}H NMR (400 MHz, D_2O, 298 K): δ_H 7.29 - 7.28 (m, 5H), 4.00 (s, 2H) ppm. $^{13}C\{^1H\}$ NMR (100 MHz, D_2O, 298 K): δ_C 131.8, 128.4, 128.0, 125.2, 42.3 ppm.

(4-tolyl)methanaminium chloride (7b)[2]

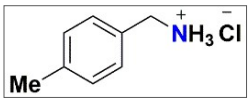

^{1}H NMR (400 MHz, D_2O, 298 K): δ_H 7.31 - 7.25 (m, 4H), 4.09 (s, 2H), 2.30 (s, 3H) ppm. $^{13}C\{^1H\}$ NMR (100 MHz, D_2O, 298 K): δ_C 139.5, 129.7, 129.5, 128.8, 42.8, 20.2 ppm.

2-(4-methoxyphenyl)ethan-1-aminium chloride (7c)[2]

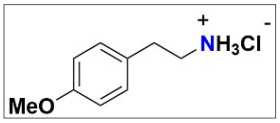

^{1}H NMR (400 MHz, D_2O, 298 K): δ_H 7.14 (d, 2H, J = 8 Hz), 6.86 (d, 2H, J = 8 Hz), 3.69 (s, 3H), 3.13 - 3.11 (m, 2H), 2.83 - 2.79 (m, 2H) ppm. $^{13}C\{^1H\}$ NMR (100 MHz, D_2O, 298 K): δ_C 157.8, 130.0, 129.0, 114.4, 55.3, 40.6, 31.8 ppm.

((4-trifluoromethyl)phenyl)methanaminium chloride (7d)[2]

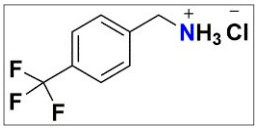

^{1}H NMR (400 MHz, D_2O, 298 K): δ_H 7.62 (d, 2H, J = 8 Hz), 7.33 (d, 2H, J = 8 Hz), 4.13 (s, 2H) ppm. $^{13}C\{^1H\}$ NMR (100 MHz, D_2O, 298 K): δ_C 136.6, 130.5, 129.2, 128.5, 126.0, 124.8, 42.5 ppm.

(4-iodophenyl)methanaminium chloride (7e)[2]

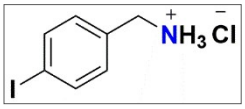

^{1}H NMR (400 MHz, D_2O, 298 K): δ_H 7.82 - 7.80 (m, 2H), 7.18 (d, 2H, J = 8 Hz), 4.10 (s, 2H) ppm. $^{13}C\{^1H\}$ NMR (100 MHz, D_2O, 298 K): δ_C 138.2, 132.2, 130.6, 42.5 ppm.

3.4.3 NMR spectra of ammonium salts

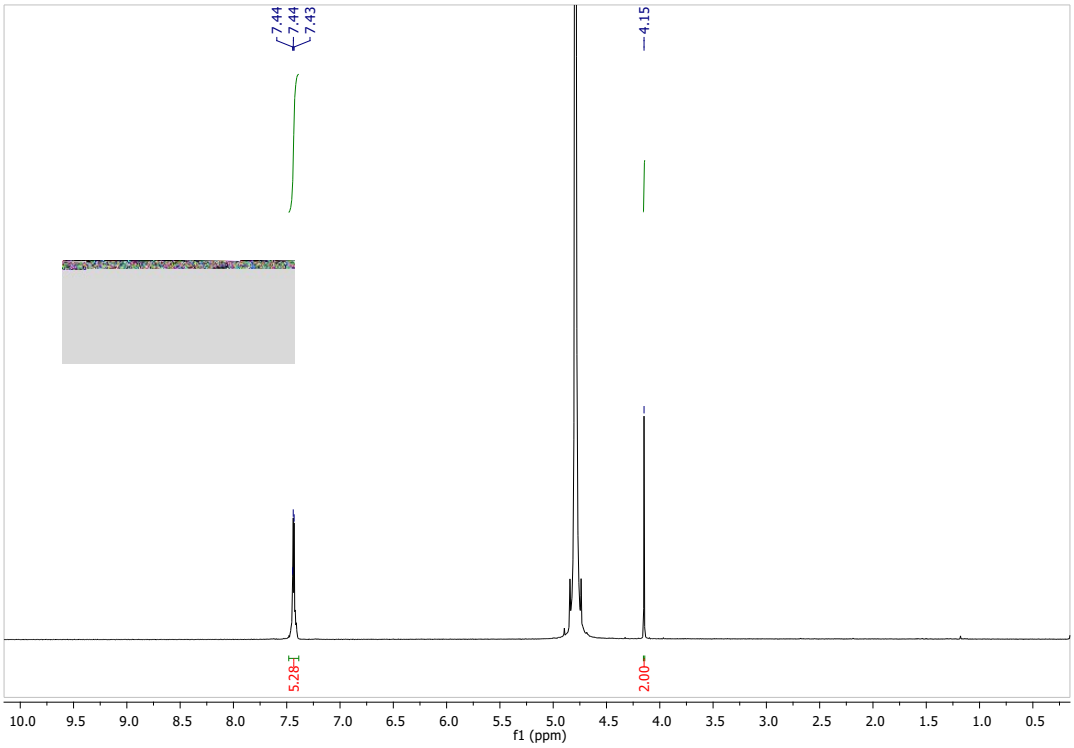

Figure FS 66. ^{1}H NMR (400 MHz, D_2O, 298 K) spectrum of **7a**.

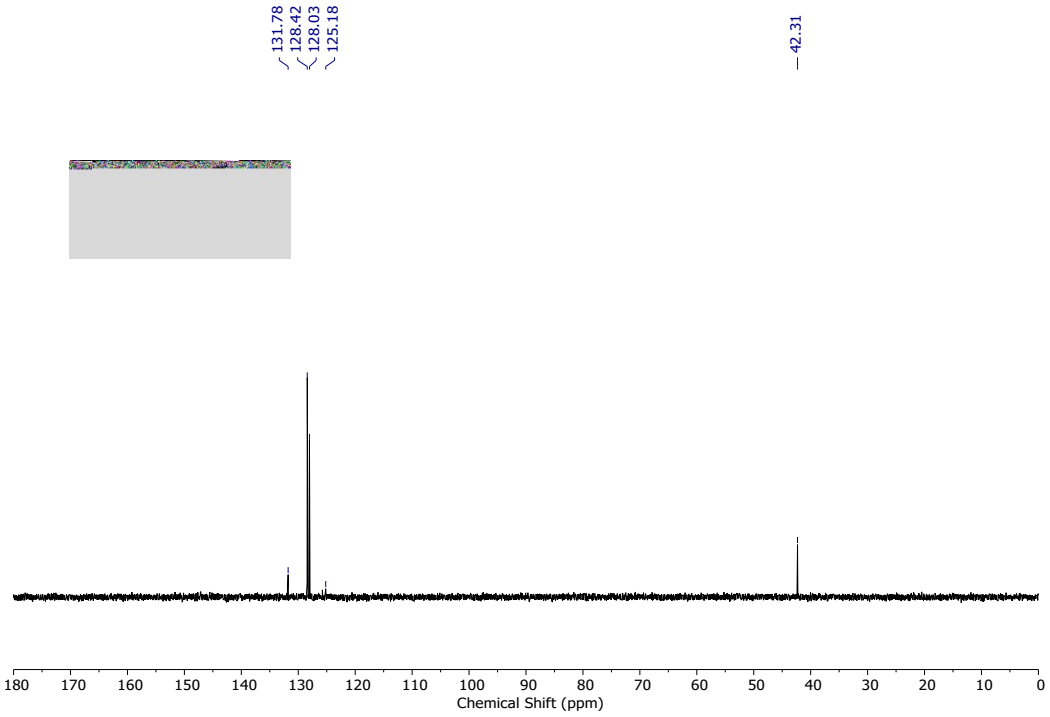

Figure FS 67. $^{13}C\{^{1}H\}$ NMR (100 MHz, D_2O, 298 k) spectrum of **7a**.

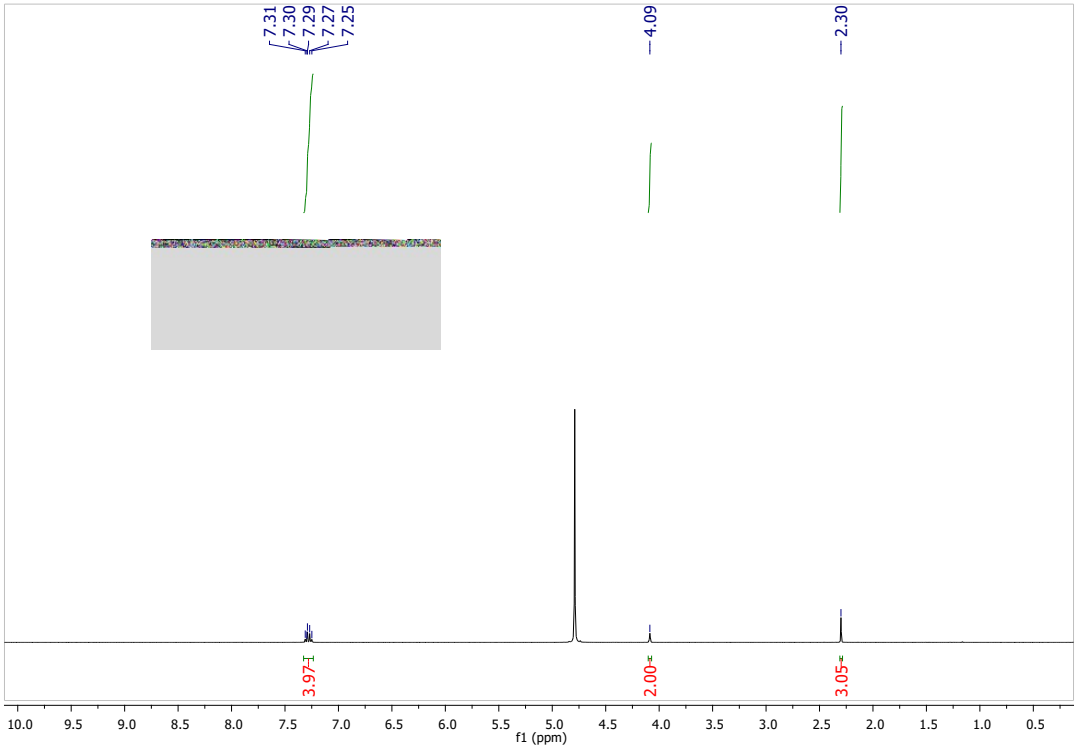

Figure FS 68. ^{1}H NMR (400 MHz, D_2O, 298 K) spectrum of **7b**.

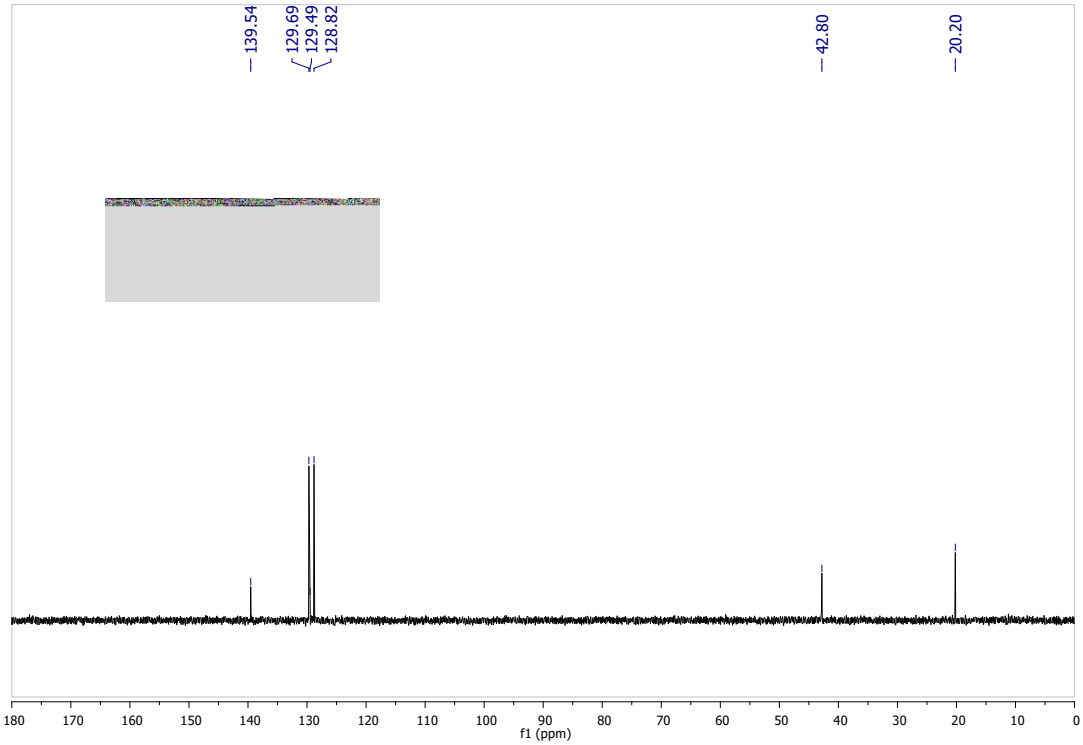

Figure FS 69. $^{13}C\{^{1}H\}$ NMR (100 MHz, D_2O, 298 k) spectrum of **7b**.

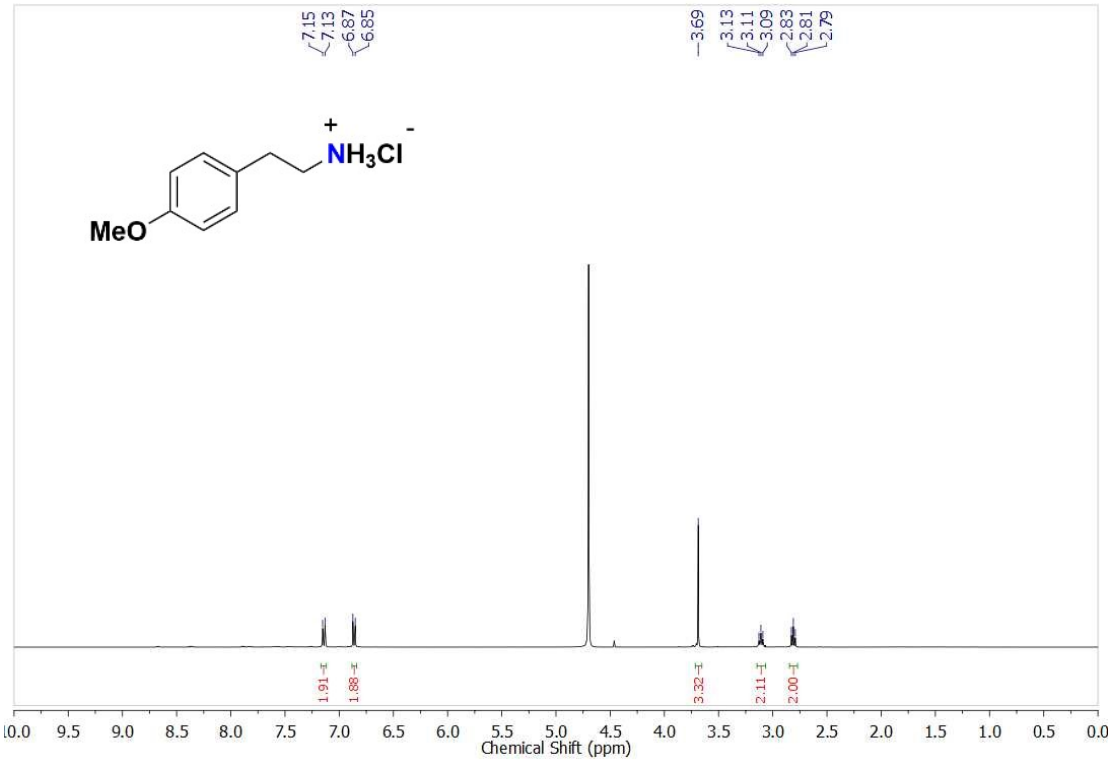

Figure FS 70. ^{1}H NMR (400 MHz, D_2O, 298 K) spectrum of **7c**.

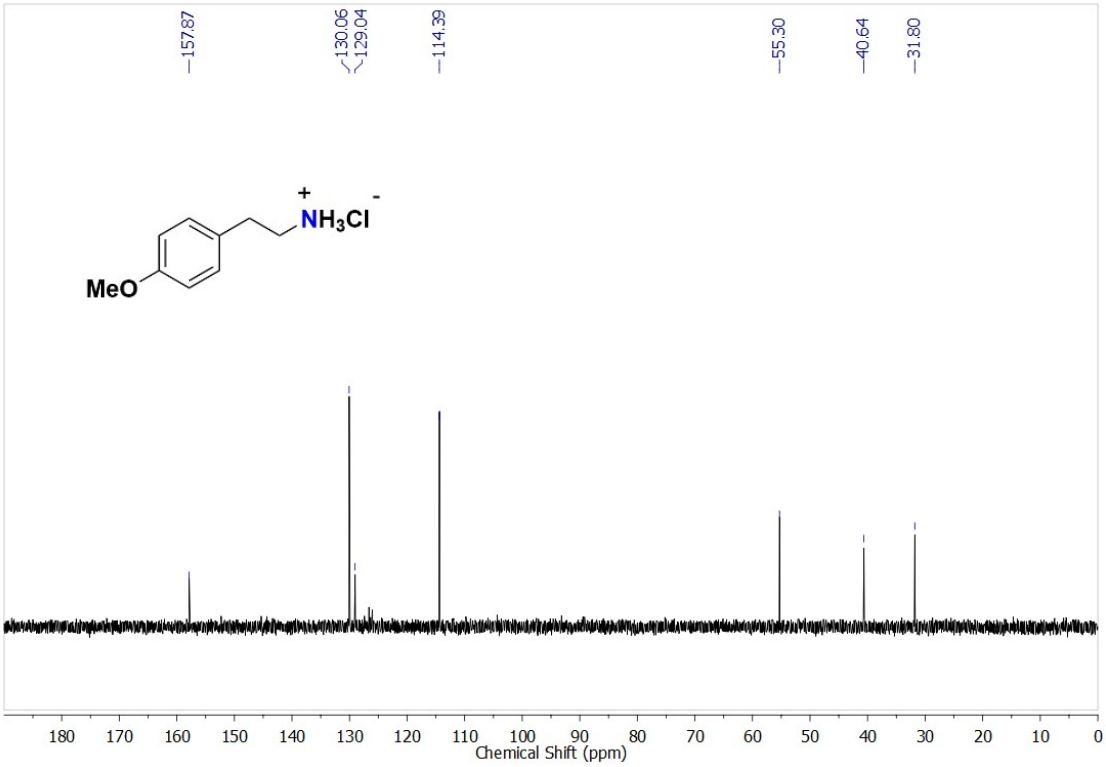

Figure FS 71. $^{13}C\{^{1}H\}$ NMR (100 MHz, D_2O, 298 k) spectrum of **7c**.

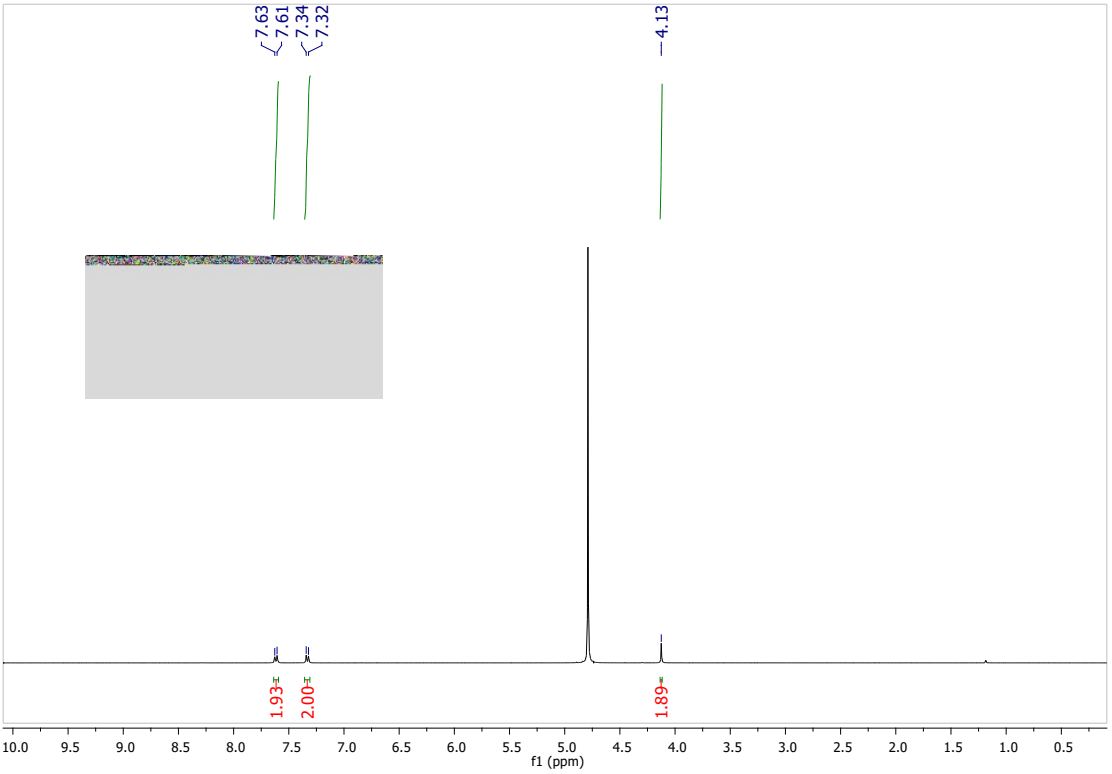

Figure FS 72. ^{1}H NMR (400 MHz, D_2O, 298 K) spectrum of **7d**.

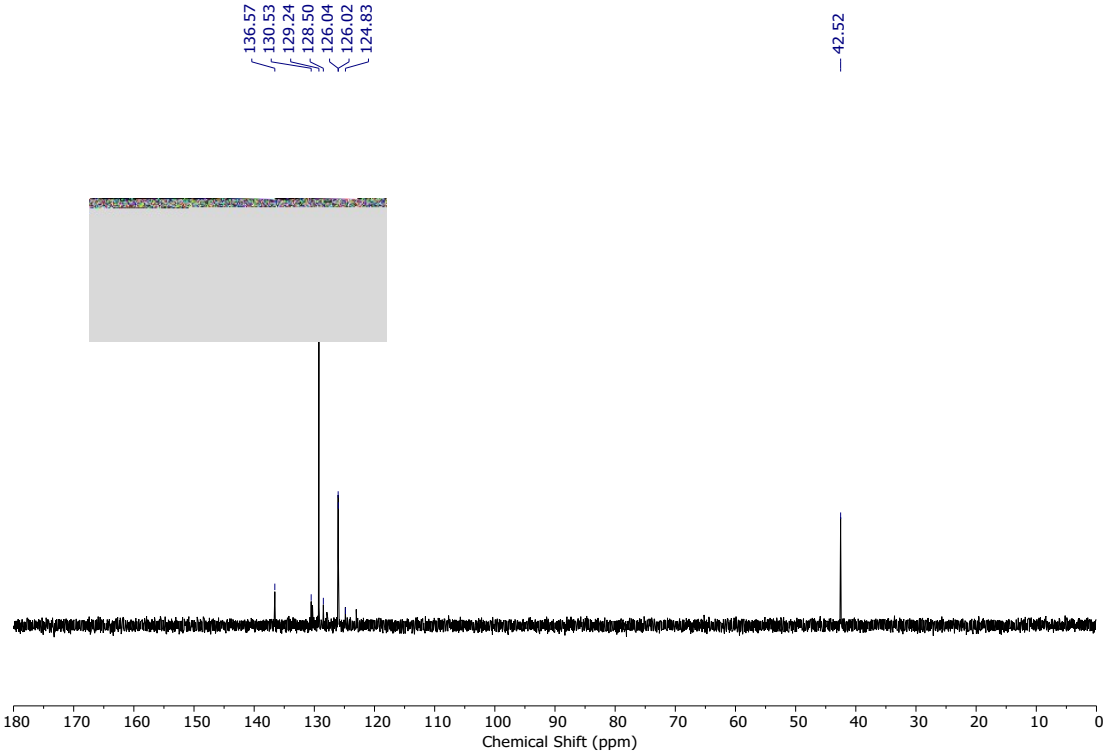

Figure FS 73. ^{13}C{^{1}H} NMR (100 MHz, D_2O, 298 k) spectrum of **7d**.

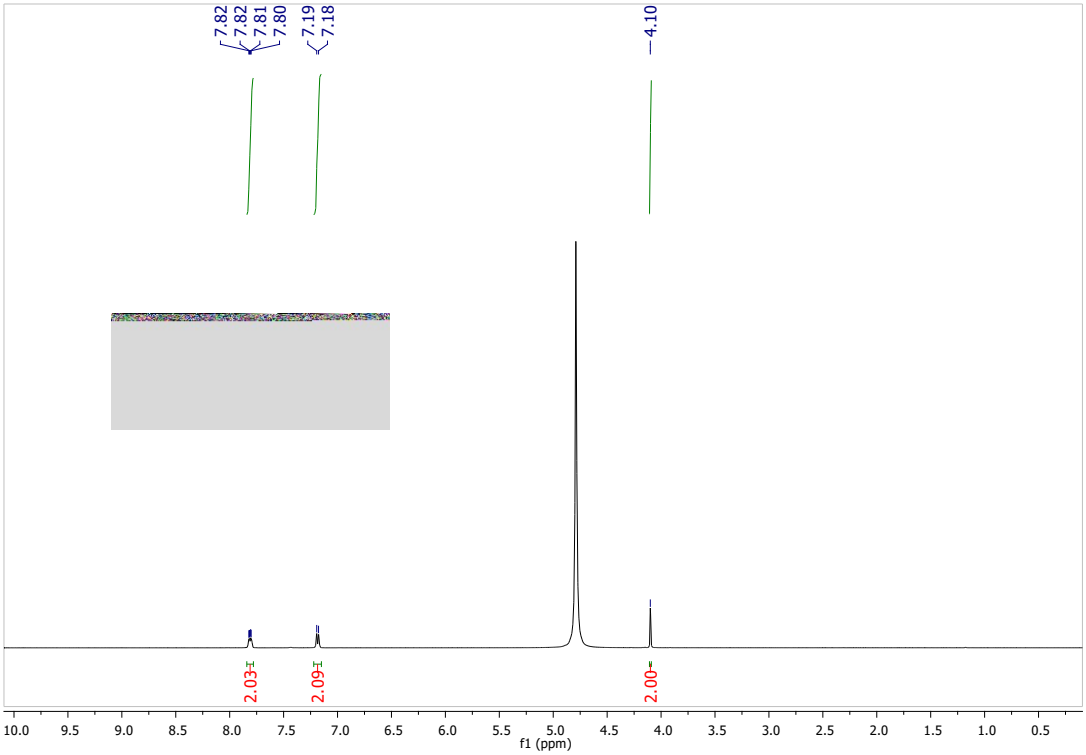

Figure FS 74. ^{1}H NMR (400 MHz, D_2O, 298 K) spectrum of **7e**.

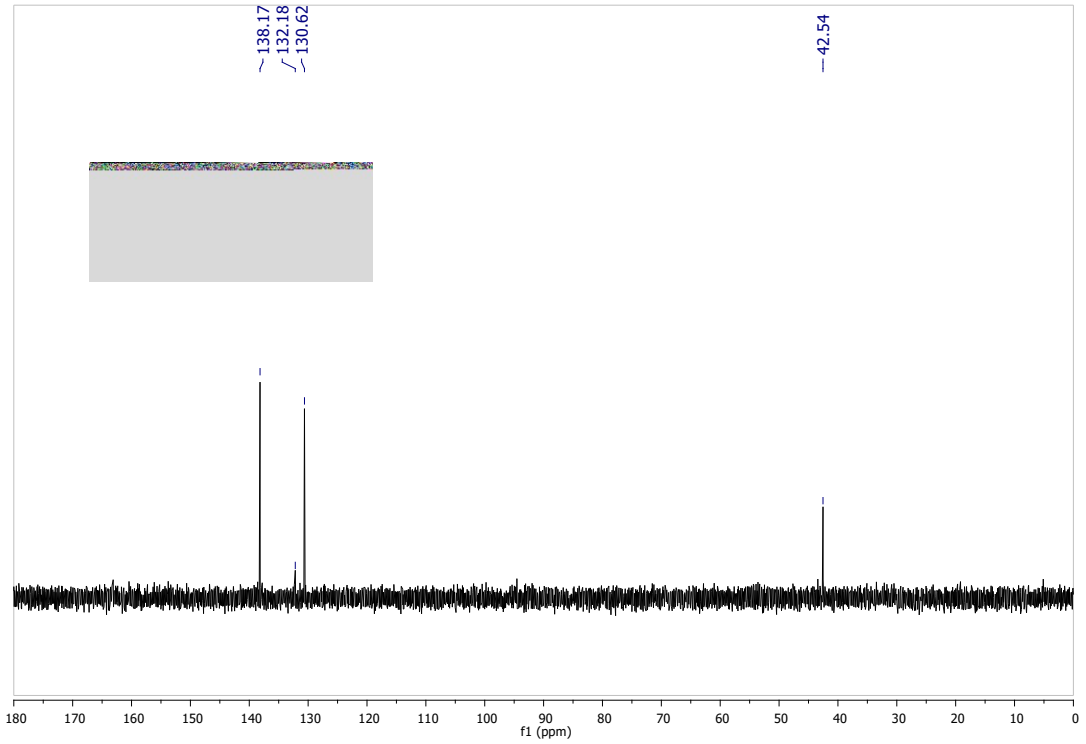

Figure FS 75. ^{13}C{^{1}H} NMR (100 MHz, D_2O, 298 k) spectrum of **7e**.

4. Catalytic hydroboration of esters

4.1 General procedure for the catalytic hydroboration of esters

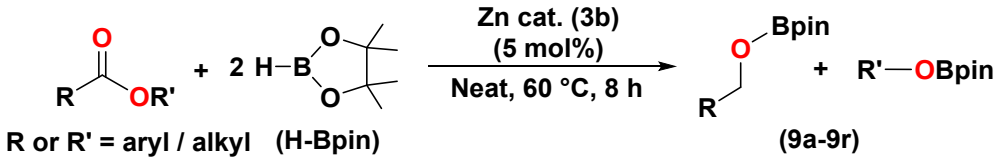

Inside the glove box, the zinc catalyst **3b** (5 mol %) and HBpin (1.1 mmol, 2.2 equiv) were added to a Schlenk tube followed by the addition of ester (0.5 mmol, 1 equiv). The Schlenk tube was taken out from the glove box and the reaction mixture was stirred at 60 °C for 8 hours. Finally, volatiles of the mixture were removed under the reduced pressure to obtain the hydroboration product. The yield was calculated from ^{1}H NMR spectroscopy with the help of 1,3,5-trimethoxy benzene as the internal standard.

4.2 NMR data of boryl ester

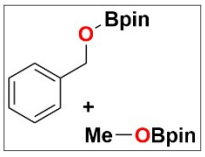

9a and **9b**:[3] Yield (98%): ^{1}H NMR (300 MHz, $CDCl_3$, 298 K): δ_H 7.25 - 7.18 (m, 5H), 4.84 (s, 2H), 3.51 (s, 3H), 1.17 (s, 24H) ppm. $^{13}C\{^{1}H\}$ NMR (75 MHz, $CDCl_3$, 298 K): δ_C 128.3, 127.4, 126.7, 82.9, 82.8, 66.7, 24.6 ppm. $^{11}B\{^{1}H\}$ NMR (96.3 MHz, $CDCl_3$, 298 K): δ_B 22.33 ppm.

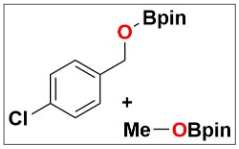

9c and **9b**:[3] Yield (95%): ^{1}H NMR (300 MHz, $CDCl_3$, 298 K): δ_H 7.20 (m, 4H), 4.79 (s, 2H), 3.51 (s, 3H), 1.17 (s, 24H) ppm. $^{13}C\{^{1}H\}$ NMR (75 MHz, $CDCl_3$, 298 K): δ_C 128.4, 128.1, 83.1, 82.8, 65.9, 24.6 ppm. $^{11}B\{^{1}H\}$ NMR (96.3 MHz, $CDCl_3$, 298 K): δ_B 22.30 ppm.

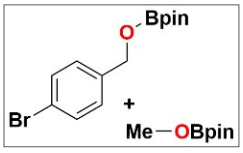

9d and **9b**:[3] Yield (94%): ^{1}H NMR (300 MHz, $CDCl_3$, 298 K): δ_H 7.92 - 7.91 (m, 2H), 7.37 - 7.36 (m, 2H), 4.41 (s, 2H), 3.68 (s, 3H), 1.19 (s, 24H) ppm.

$^{13}C\{^{1}H\}$ NMR (75 MHz, $CDCl_3$, 298 K): δ_C 138.9, 137.4, 128.7, 114.8, 92.8, 83.1, 82.8, 66.0, 24.8, 24.7, 24.6 ppm. $^{11}B\{^{1}H\}$ NMR (96.3 MHz, $CDCl_3$, 298 K): δ_B 22.30 ppm.

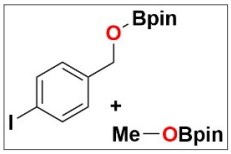

9e and **9b**:[3] Yield (96%): ^{1}H NMR (600 MHz, $CDCl_3$, 298 K): δ_H 7.56 (d, 2H, J = 6 Hz), 7.00 (d, 2H, J = 6 Hz), 4.78 (s, 2H), 3.52 (s, 3H), 1.17 (s, 24H) ppm. $^{13}C\{^{1}H\}$ NMR (150 MHz, $CDCl_3$, 298 K): δ_C 128.2, 128.1, 127.4, 123.7, 82.9, 82.6, 66.6, 60.6, 24.5, 21.3, 17.2 ppm. $^{11}B\{^{1}H\}$ NMR (192.6 MHz, $CDCl_3$, 298 K): δ_B 22.32 ppm.

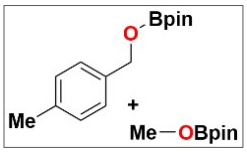

9f and **9b**:[3] Yield (94%): ^{1}H NMR (300 MHz, $CDCl_3$, 298 K): δ_H 7.27 - 7.19 (m, 4H), 4.93 (s, 2H), 3.65 (s, 3H), 1.30 (s, 24H) ppm. $^{13}C\{^{1}H\}$ NMR (75 MHz, $CDCl_3$, 298 K): δ_C 137.0, 136.3, 129.6, 129.2, 129.1, 128.9, 127.2, 126.9, 114.8, 83.1, 82.9, 82.8, 66.6, 52.6, 24.6, 24.5, 21.2 ppm. $^{11}B\{^{1}H\}$ NMR (96.3 MHz, $CDCl_3$, 298 K): δ_B 22.47 ppm.

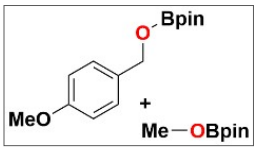

9g and **9b**:[3] Yield (95%): ^{1}H NMR (300 MHz, $CDCl_3$, 298 K): δ_H 7.19 (d, 2H, J = 8 Hz), 6.78 (d, 2H, J = 8 Hz), 4.76 (s, 2H), 3.67 (s, 3H), 3.52 (s, 3H), 1.17 (s, 24H) ppm. $^{13}C\{^{1}H\}$ NMR (75 MHz, $CDCl_3$, 298 K): δ_C 159.1, 131.6, 131.5, 128.6, 113.7, 82.9, 82.8, 66.5, 55.3, 24.7 ppm. $^{11}B\{^{1}H\}$ NMR (96.3 MHz, $CDCl_3$, 298 K): δ_B 22.28 ppm.

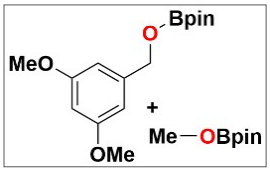

9h and **9b**:[3] Yield (90%): ^{1}H NMR (600 MHz, $CDCl_3$, 298 K): δ_H 6.43 - 6.42 (m, 2H), 6.39 (m, 1H), 4.79 (m, 2H), 3.69 (s, 6H), 3.68 (s, 3H), 1.19 (s, 24H) ppm. $^{13}C\{^{1}H\}$ NMR (150 MHz, $CDCl_3$, 298 K): δ_C 160.8, 116.1, 107.2, 105.8, 104.3, 99.9, 83.0, 66.6, 24.6 ppm. $^{11}B\{^{1}H\}$ NMR (192.6 MHz, $CDCl_3$, 298 K): δ_B 22.27 ppm.

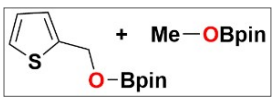

9i and **9b**:[3] Yield (86%): ^{1}H NMR (600 MHz, $CDCl_3$, 298 K): δ_H 7.18 - 7.17 (m, 1H), 6.94 - 6.93 (m, 1H), 6.88 - 6.86 (m, 1H), 4.96 (s, 2H), 3.52 (s, 3H), 1.19 (s, 24H) ppm. $^{13}C\{^{1}H\}$ NMR (150 MHz, $CDCl_3$, 298 K): δ_C 126.6, 125.9, 125.5,

114.8, 83.1, 83.1, 82.8, 61.6, 52.6, 24.6, 24.5 ppm. $^{11}B\{^1H\}$ NMR (192.6 MHz, $CDCl_3$, 298 K): δ_B 22.12 ppm.

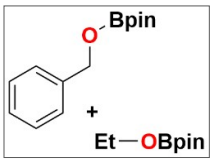

9j and **9k**:[3] Yield (86%): ^1H NMR (600 MHz, $CDCl_3$, 298 K): δ_H 7.26 - 7.22 (m, 4H), 7.18 - 7.15 (m, 1H), 4.84 (s, 2H), 3.81 (q, 2H), 1.17 (s, 24H), 1.13 (t, 3H) ppm. $^{13}C\{^1H\}$ NMR (150 MHz, $CDCl_3$, 298 K): δ_C 139.2, 128.3, 128.3, 127.4, 126.7, 114.8, 82.9, 82.6, 66.7, 60.6, 24.7, 24.6, 24.6, 24.5, 17.2 ppm. $^{11}B\{^1H\}$ NMR (192.6 MHz, $CDCl_3$, 298 K): δ_B 22.15 ppm.

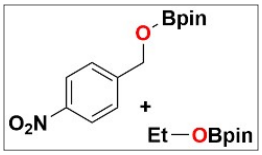

9l and **9k**:[3] Yield (86%): ^1H NMR (600 MHz, $CDCl_3$, 298 K): δ_H 8.09 (d, 2H, J = 12 Hz), 7.41 (d, 2H, J = 6 Hz), 4.93 (s, 2H), 3.79 (m, 2H), 1.18 - 1.15 (m, 24H), 1.12 (t, 3H) ppm. $^{13}C\{^1H\}$ NMR (150 MHz, $CDCl_3$, 298 K): δ_C 130.7, 126.8, 123.6, 123.5, 114.8, 83.4, 83.1, 65.5, 61.9, 24.6, 24.6, 24.5 ppm. $^{11}B\{^1H\}$ NMR (192.6 MHz, $CDCl_3$, 298 K): δ_B 22.05 ppm.

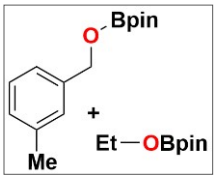

9m and **9k**:[3] Yield (90%): ^1H NMR (600 MHz, $CDCl_3$, 298 K): δ_H 7.12 - 7.11 (m, 1H), 7.09 (m, 1H), 7.05 - 7.03 (m, 1H), 6.98 - 6.97 (m, 1H), 4.80 (m, 2H), 3.82 - 3.79 (q, 2H), 2.24 (s, 3H), 1.17 (s, 24H), 1.14 - 1.12 (t, 3H) ppm. $^{13}C\{^1H\}$ NMR (150 MHz, $CDCl_3$, 298 K): δ_C 128.2, 128.1, 127.4, 123.7, 82.9, 82.6, 66.6, 60.6, 24.5, 21.3, 17.2 ppm. $^{11}B\{^1H\}$ NMR (192.6 MHz, $CDCl_3$, 298 K): δ_B 22.3 ppm.

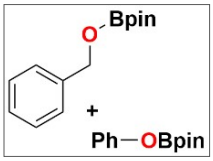

9n and **9o**:[3] Yield (92%): ^1H NMR (600 MHz, $CDCl_3$, 298 K): δ_H 7.26 - 7.09 (m, 7H), 7.01 - 6.94 (m, 2H), 6.79 - 6.75 (m, 1H), 4.84 (s, 2H), 1.22 - 1.17 (m, 24H) ppm. $^{13}C\{^1H\}$ NMR (150 MHz, $CDCl_3$, 298 K): δ_C 153.5, 139.2, 129.5, 129.3, 128.34, 127.4, 126.8, 123.1, 119.6, 115.5, 114.4, 83.6, 83.2, 83.0, 66.7, 24.6, 24.6, 24.6 ppm. $^{11}B\{^1H\}$ NMR (192.6 MHz, $CDCl_3$, 298 K): δ_B 22.14 ppm.

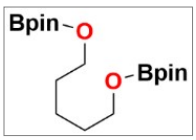

9p:[3] Yield (90%): ^1H NMR (600 MHz, $CDCl_3$, 298 K): δ_H 3.76 - 3.74 (m, 4H), 1.52 – 1.50 (m, 4H), 1.33 – 1.32 (m, 2H), 1.17 (s, 24H) ppm. $^{13}C\{^1H\}$ NMR (150

MHz, $CDCl_3$, 298 K): δ_C 82.5, 64.7, 31.0, 24.5, 21.6 ppm. $^{11}B\{^1H\}$ NMR (192.6 MHz, $CDCl_3$, 298 K): δ_B 22.04 ppm.

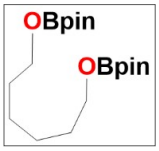

9q:[3] Yield (88%): ^1H NMR (600 MHz, $CDCl_3$, 298 K): δ_H 3.84 - 3.81 (m, 4H), 1.60 - 1.53 (m, 4H), 1.37 - 1.34 (m, 4H), 1.25 (s, 24H) ppm. $^{13}C\{^1H\}$ NMR (150 MHz, $CDCl_3$, 298 K): δ_C 116.0, 82.6, 64.8, 31.4, 25.3, 24.6 ppm. $^{11}B\{^1H\}$ NMR (192.6 MHz, $CDCl_3$, 298 K): δ_B 22.40 ppm.

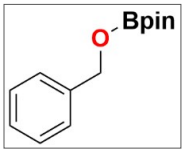

9r:[3] Yield (94%): ^1H NMR (600 MHz, $CDCl_3$, 298 K): δ_H 7.44 - 7.23 (m, 10H), 4.92 (s, 4H), 1.25 (s, 24H) ppm. $^{13}C\{^1H\}$ NMR (150 MHz, $CDCl_3$, 298 K): δ_C 139.3, 128.3, 127.4, 126.8, 83.0, 66.7, 24.7, 24.6 ppm. $^{11}B\{^1H\}$ NMR (192.6 MHz, $CDCl_3$, 298 K): δ_B 22.29 ppm.

4.3 NMR spectra of boryl ester

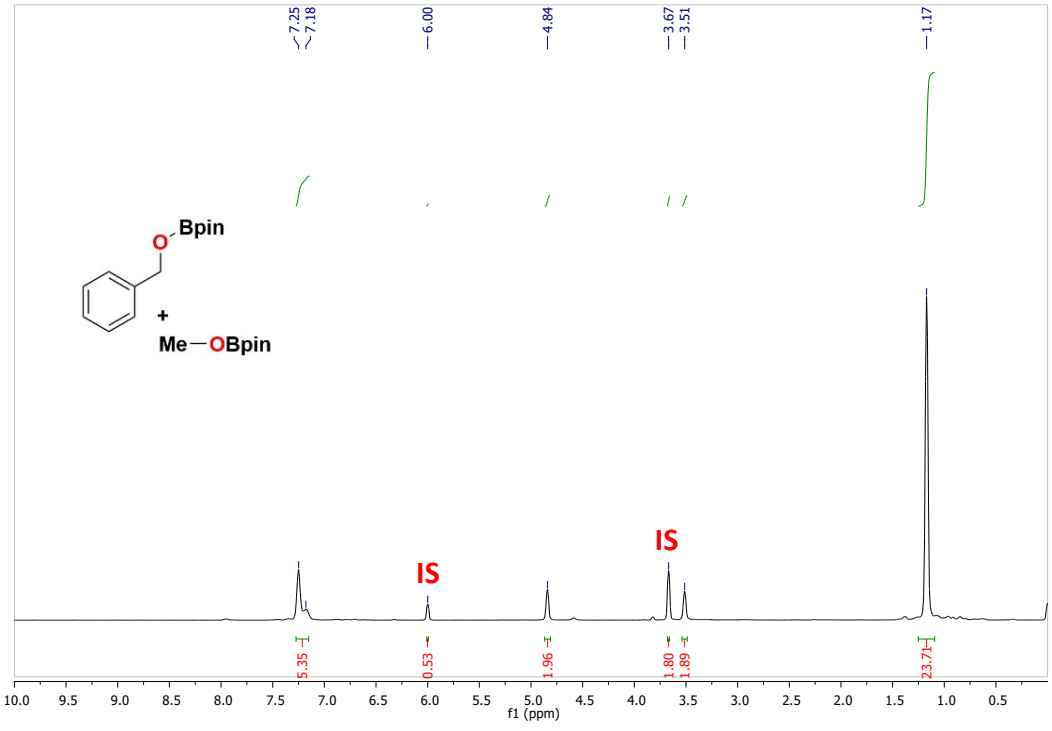

Figure FS 76. ^1H NMR (300 MHz, $CDCl_3$, 298 K) spectrum of **9a** and **9b**.

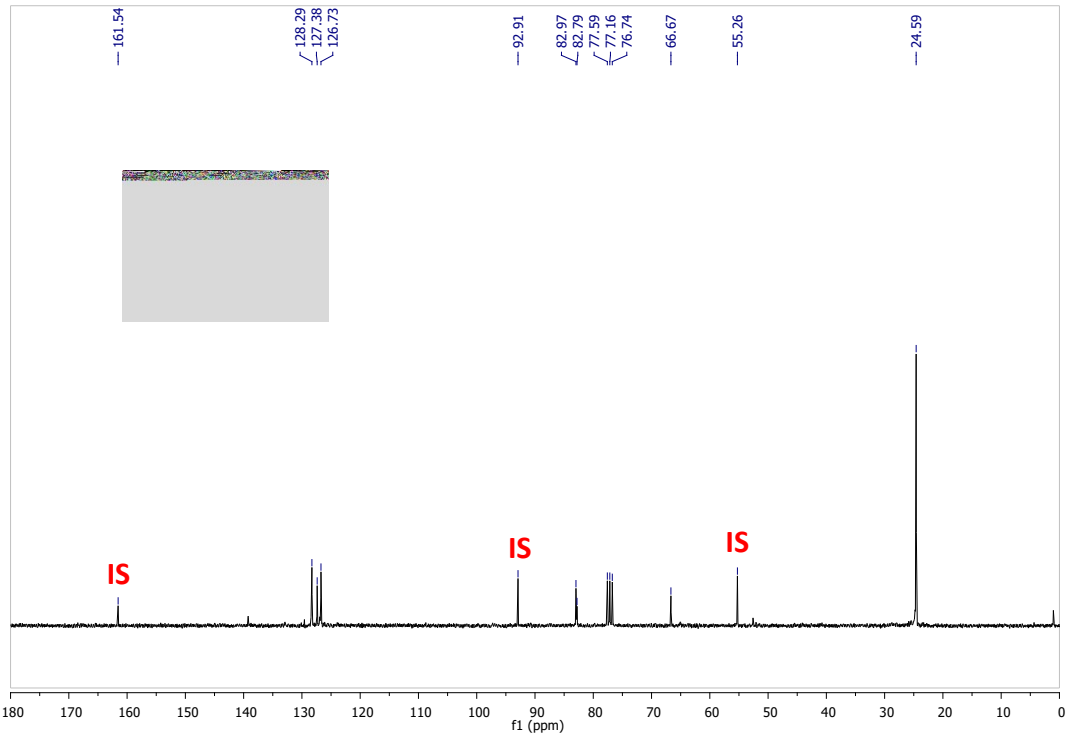

Figure FS 77. $^{13}C\{^{1}H\}$ (75 MHz, $CDCl_3$, 298 K) NMR spectrum of **9a** and **9b**.

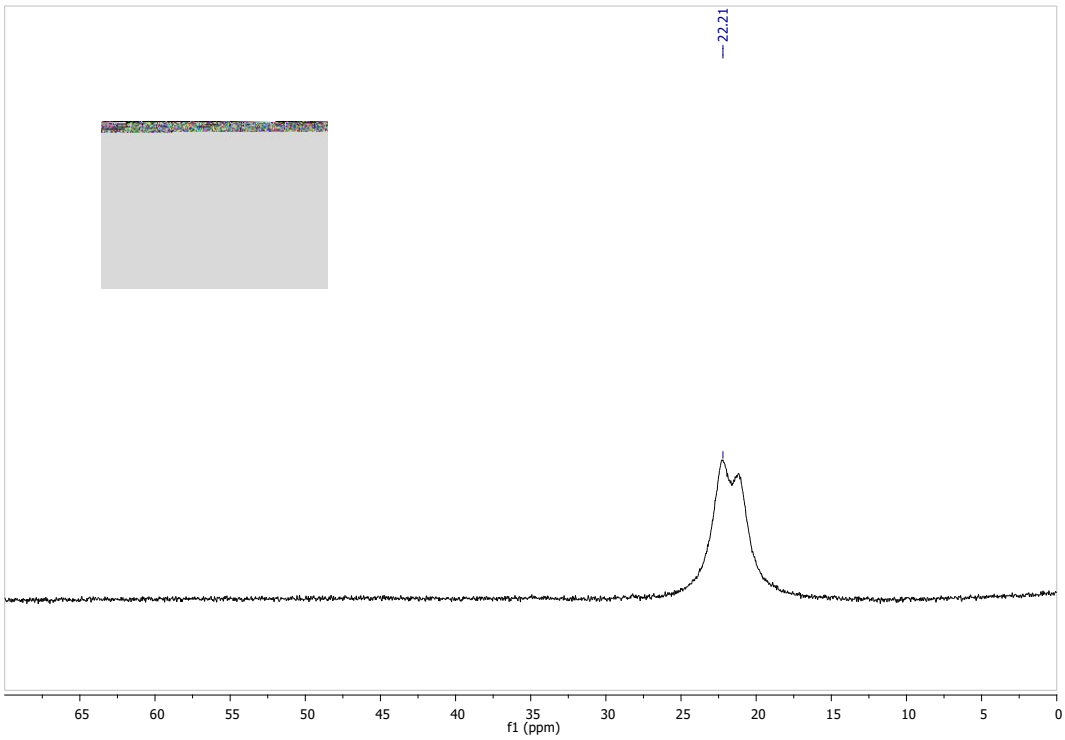

Figure FS 78. $^{11}B\{^{1}H\}$ (96.3 MHz, $CDCl_3$, 298 K) NMR spectrum of **9a** and **9b**.

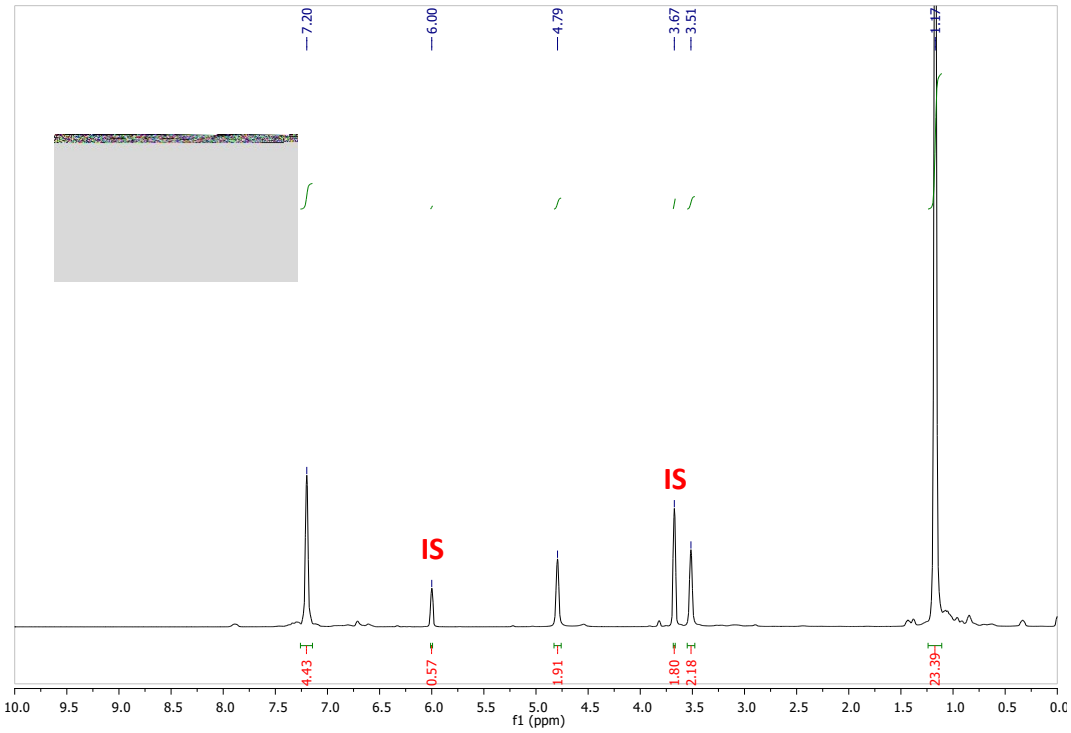

Figure FS 79. ^{1}H NMR (300 MHz, $CDCl_3$, 298 K) spectrum of **9c** and **9b**.

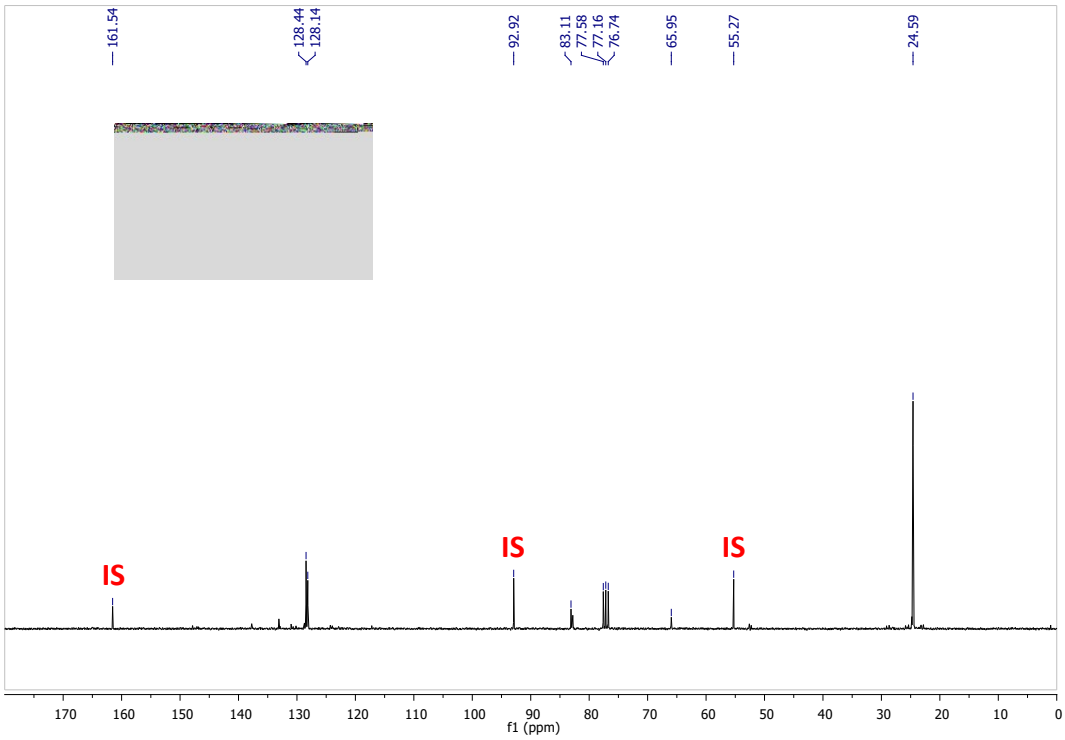

Figure FS 80. $^{13}C\{^{1}H\}$ NMR (75 MHz, $CDCl_3$, 298 K) spectrum of **9c** and **9b**.

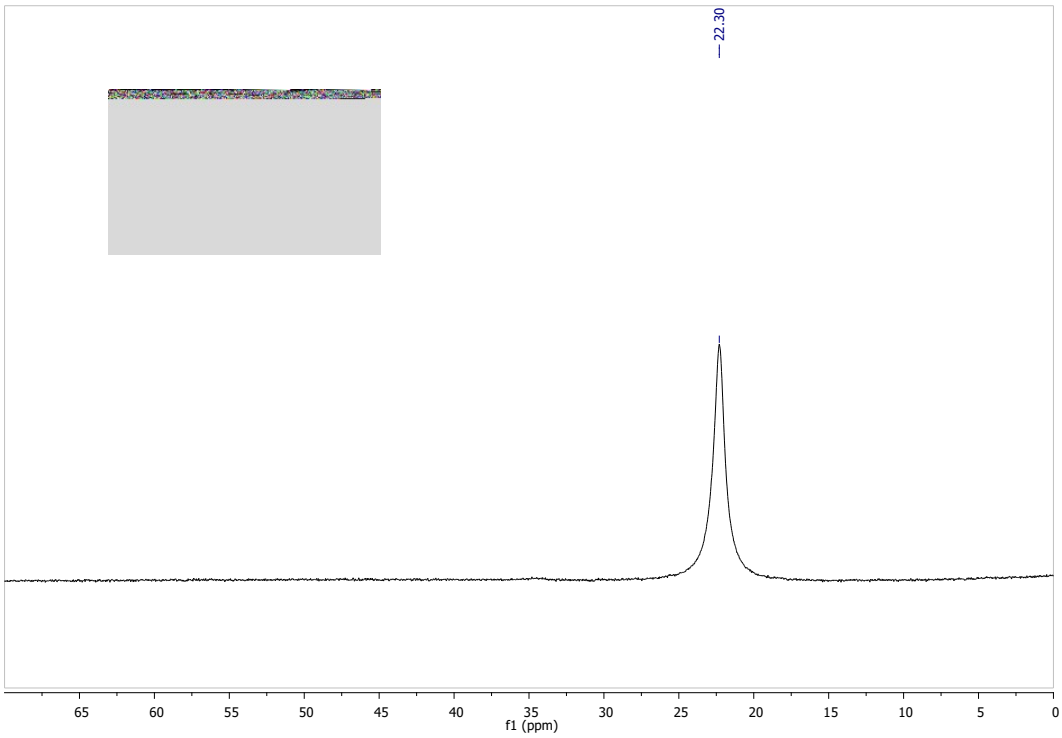

Figure FS 81. $^{11}B\{^{1}H\}$ NMR (96.3 MHz, $CDCl_3$, 298 K) spectrum of **9c** and **9b**.

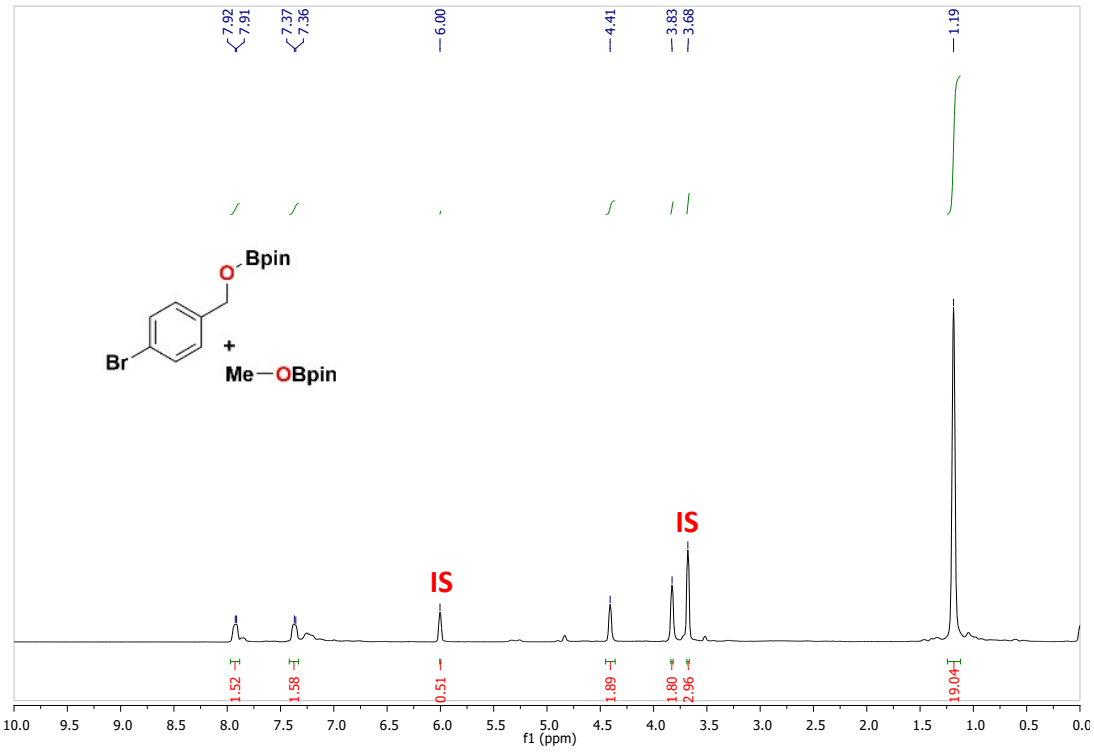

Figure FS 82. ^{1}H NMR (300 MHz, $CDCl_3$, 298 K) spectrum of **9d** and **9b**.

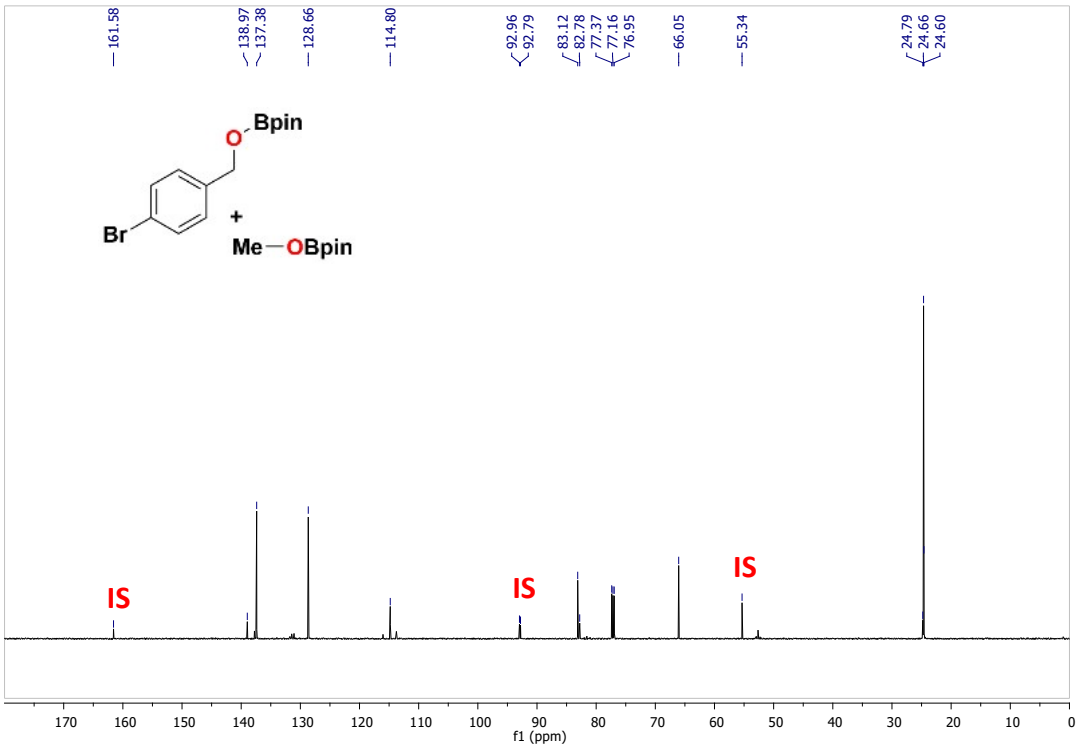

Figure FS 83. $^{13}C\{^{1}H\}$ NMR (75 MHz, $CDCl_3$, 298 K) spectrum of **9d** and **9b**.

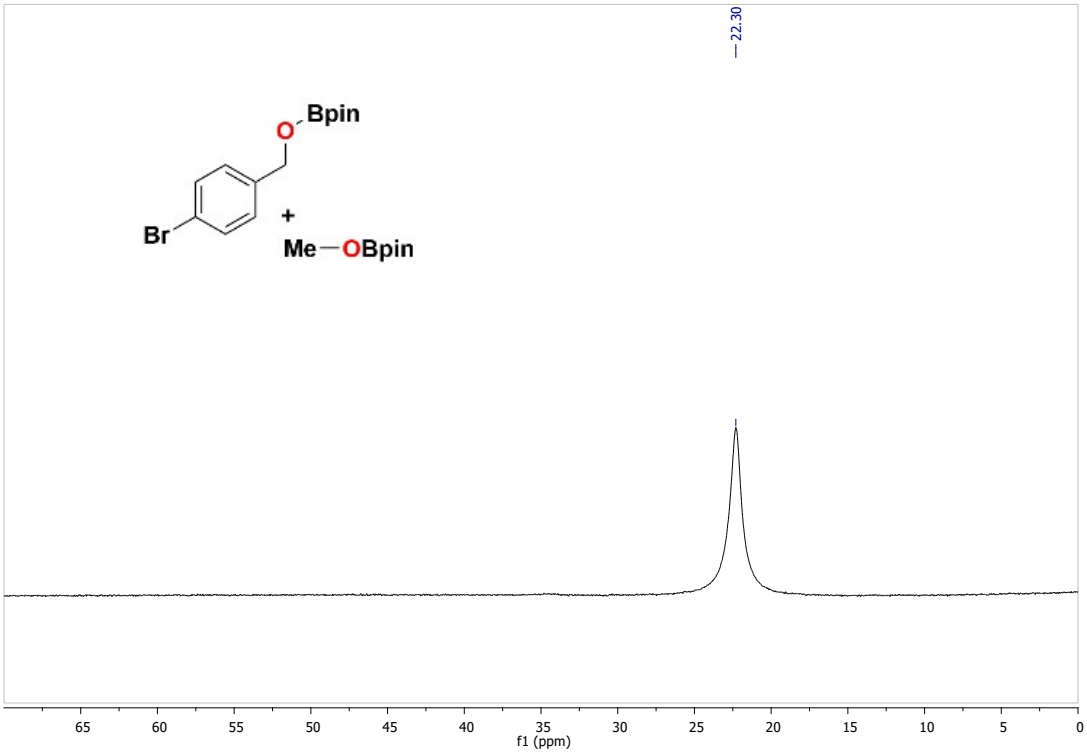

Figure FS 84. $^{11}B\{^{1}H\}$ NMR (96.3 MHz, $CDCl_3$, 298 K) spectrum of **9d** and **9b**.

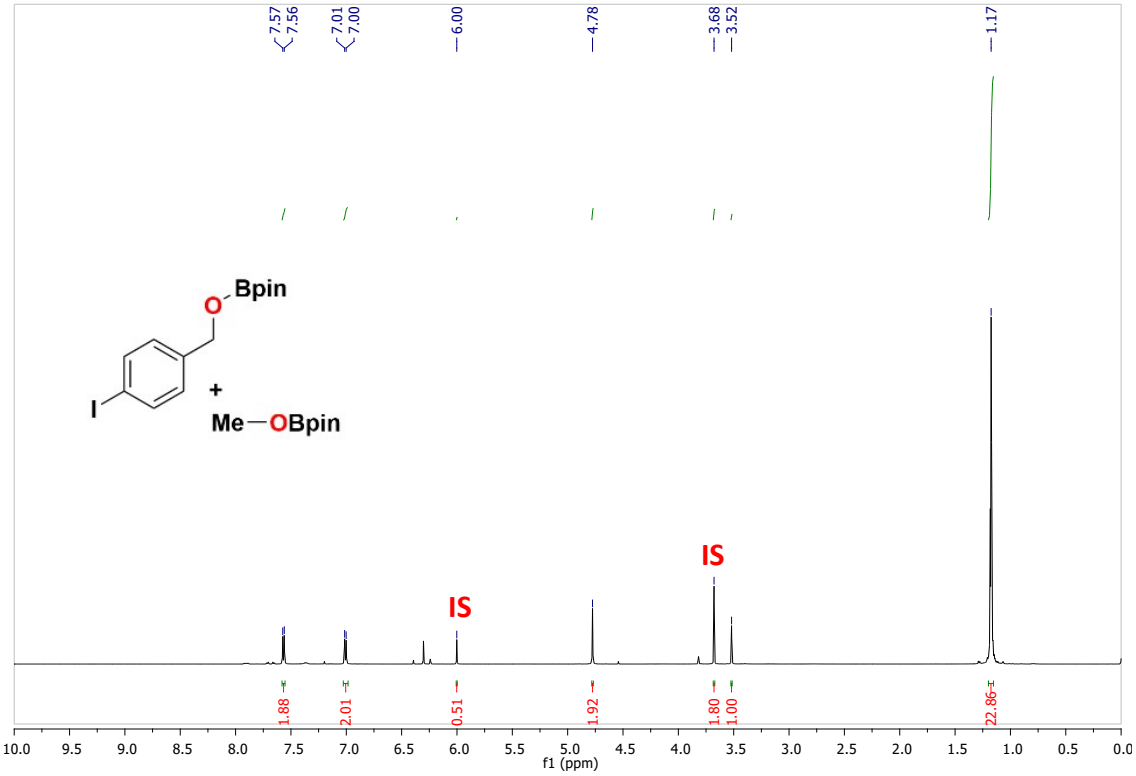

Figure FS 85. ^{1}H NMR (600 MHz, $CDCl_3$, 298 K) spectrum of **9e** and **9b**.

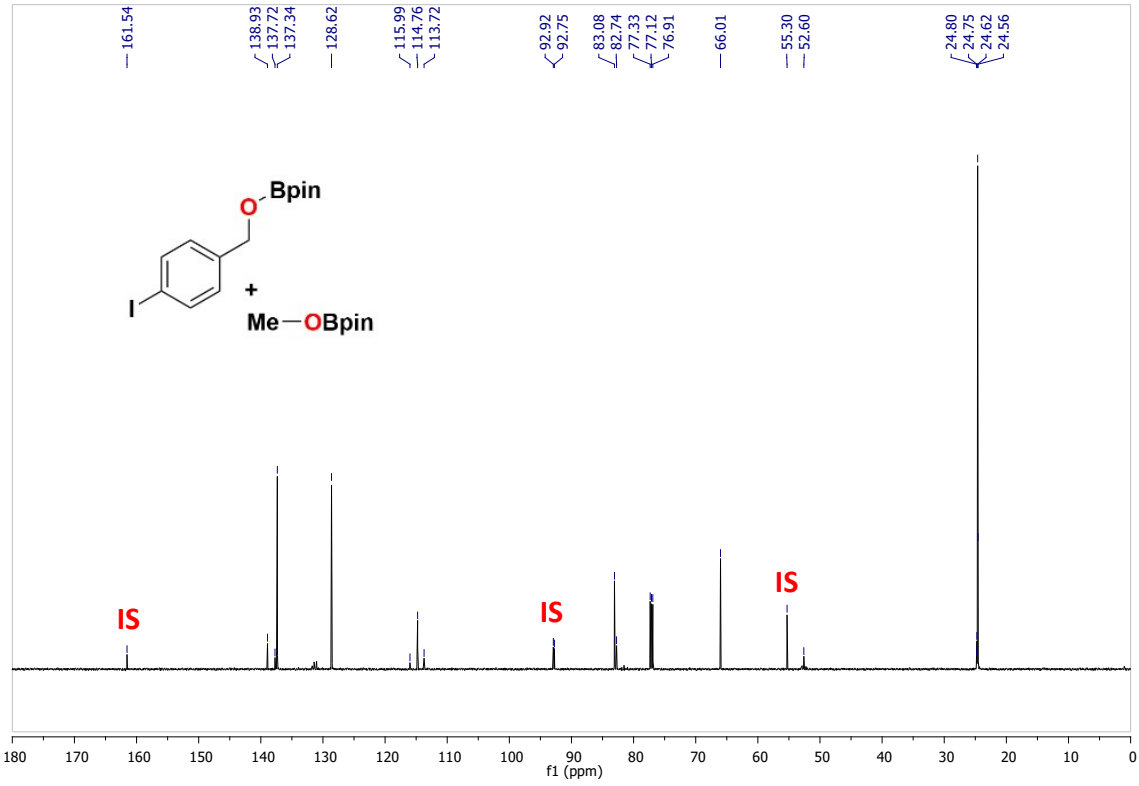

Figure FS 86. $^{13}C\{^{1}H\}$ NMR (150 MHz, $CDCl_3$, 298 K) spectrum of **9e** and **9b**.

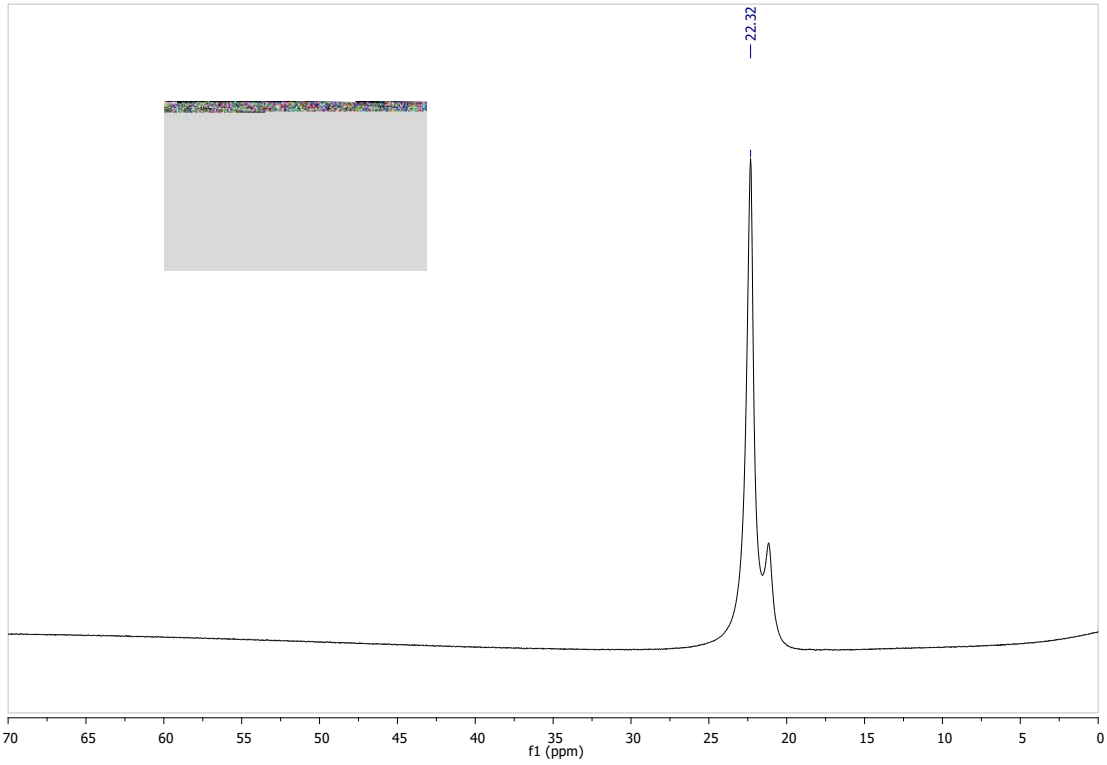

Figure FS 87. $^{11}B\{^{1}H\}$ NMR (192.6 MHz, $CDCl_3$, 298 K) spectrum of **9e** and **9b**.

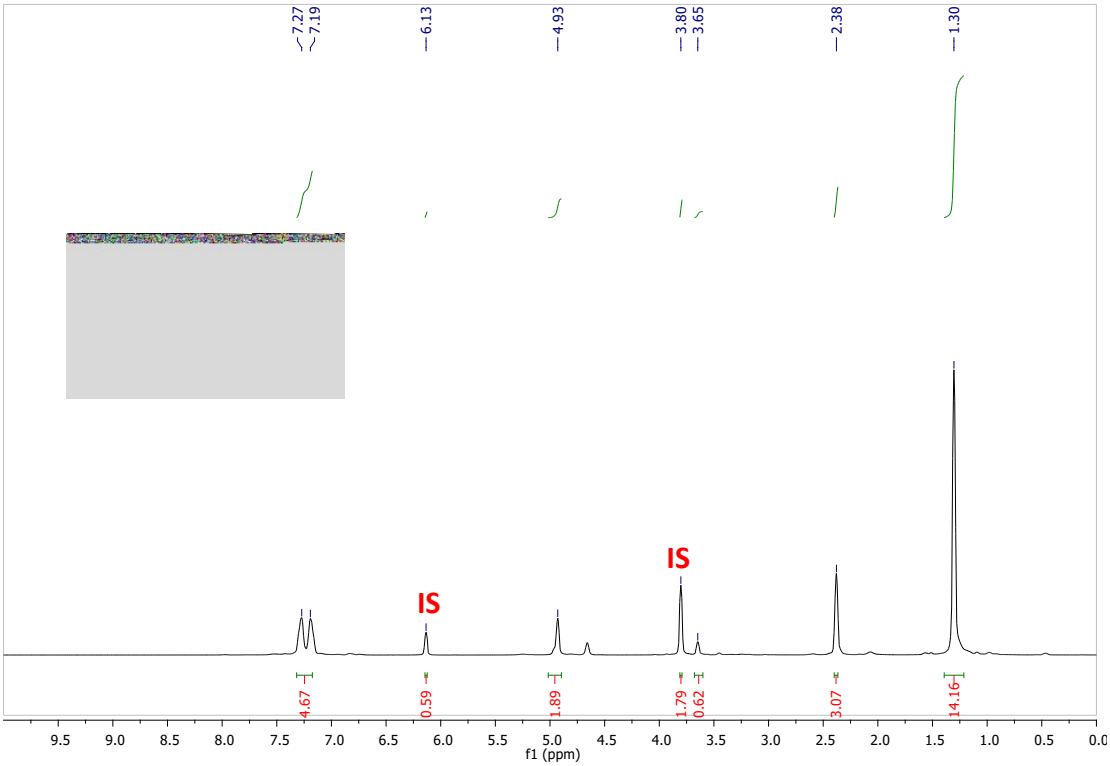

Figure FS 88. ^{1}H NMR (300 MHz, $CDCl_3$, 298 K) spectrum of **9f** and **9b**.

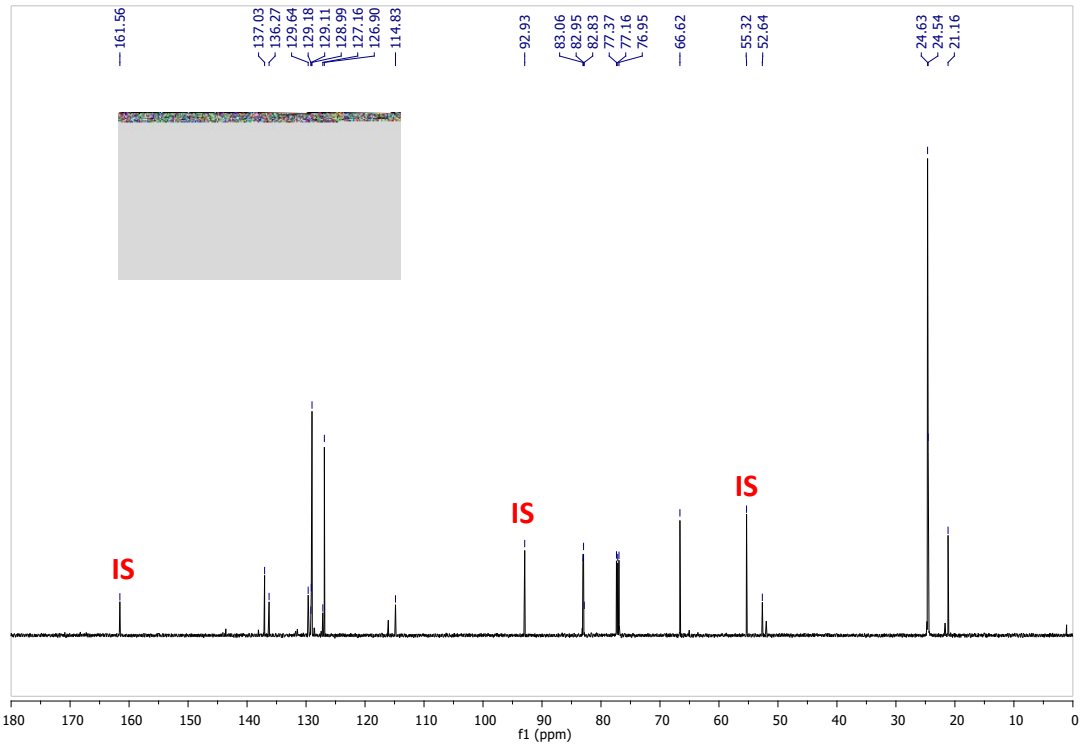

Figure FS 89. $^{13}C\{^{1}H\}$ NMR (75 MHz, $CDCl_3$, 298 K) spectrum of **9f** and **9b**.

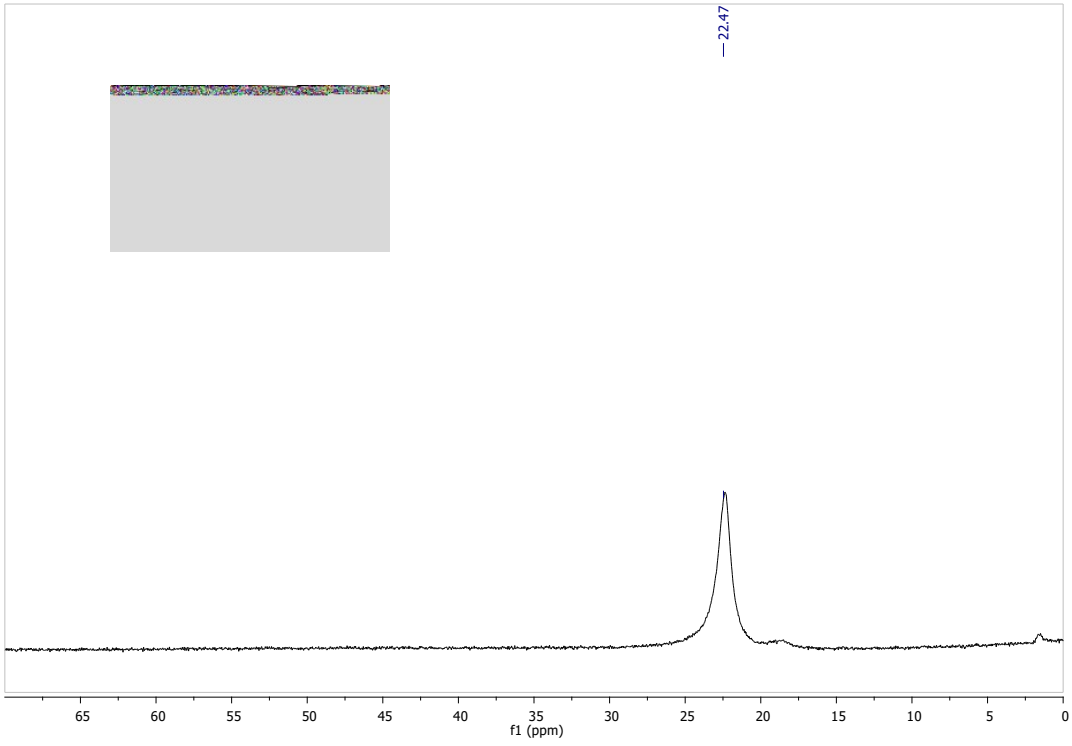

Figure FS 90. $^{11}B\{^{1}H\}$ NMR (96.3 MHz, $CDCl_3$, 298 K) spectrum of **9f** and **9b**.

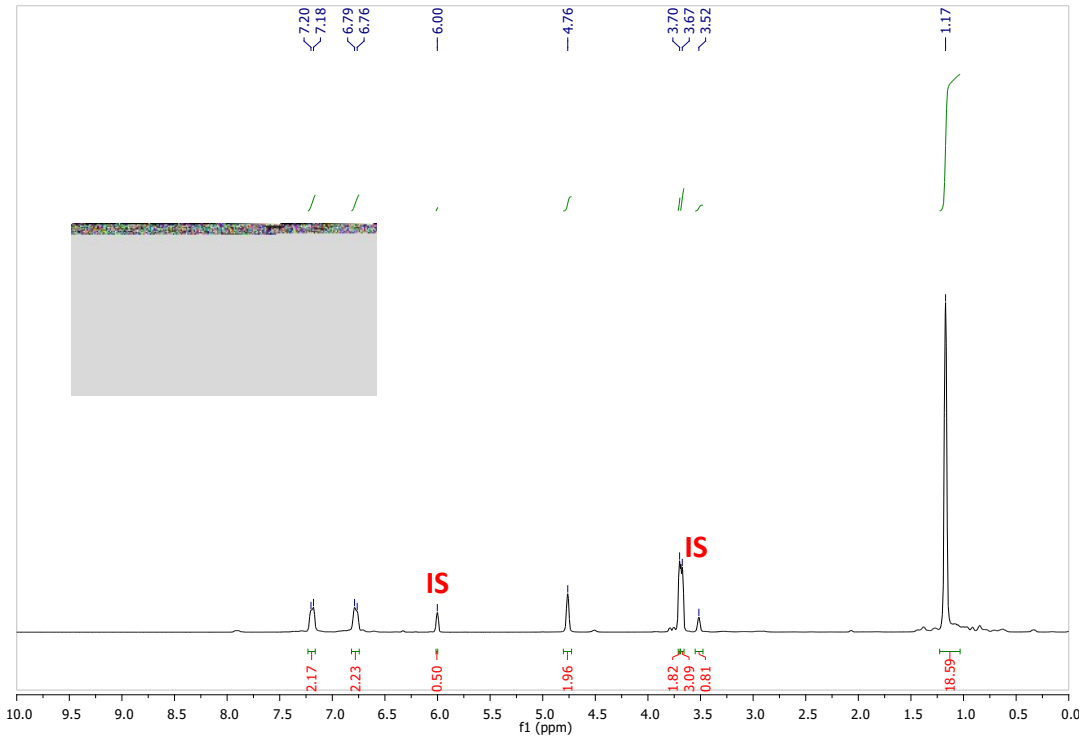

Figure FS 91. ^{1}H NMR (300 MHz, $CDCl_3$, 298 K) spectrum of **9g** and **9b**.

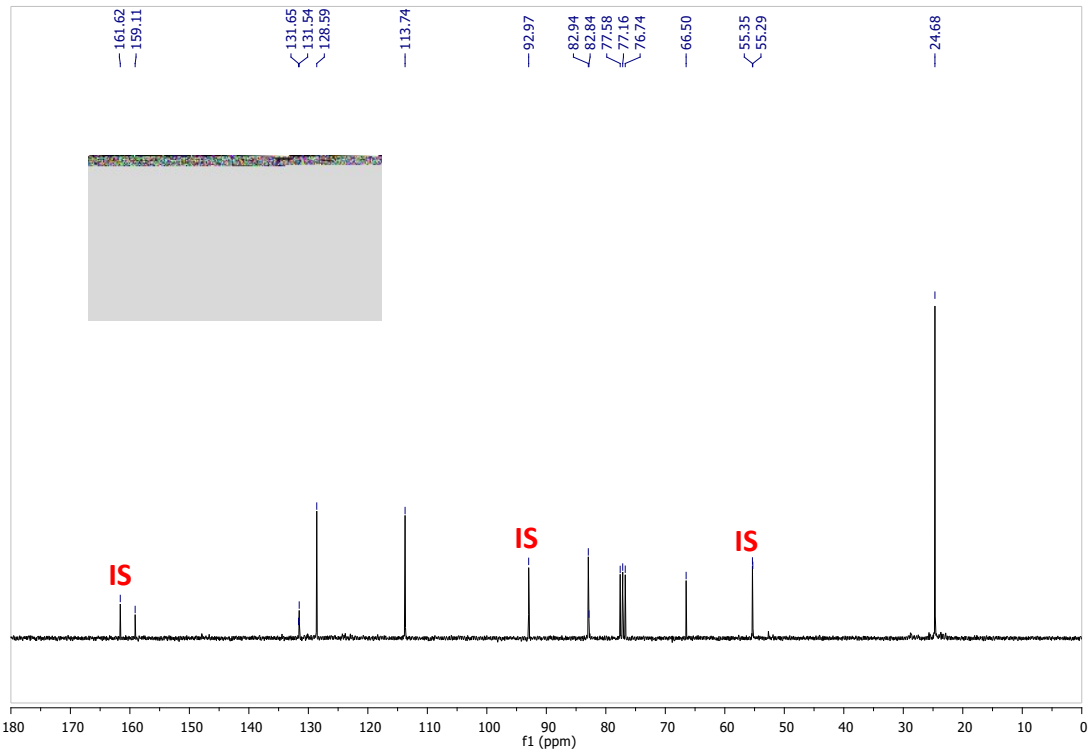

Figure FS 92. ^{13}C{^{1}H} NMR (75 MHz, $CDCl_3$, 298 K) spectrum of **9g** and **9b**.

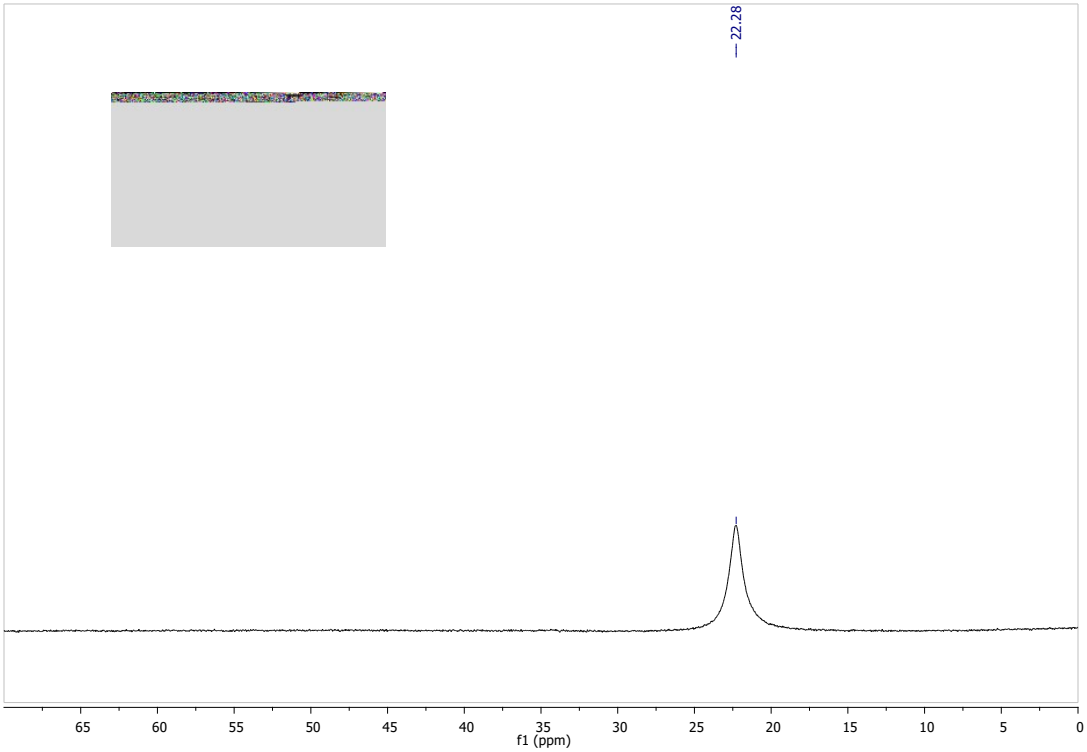

Figure FS 93. $^{11}B\{^{1}H\}$ NMR (96.3 MHz, $CDCl_3$, 298 K) spectrum of **9g** and **9b**.

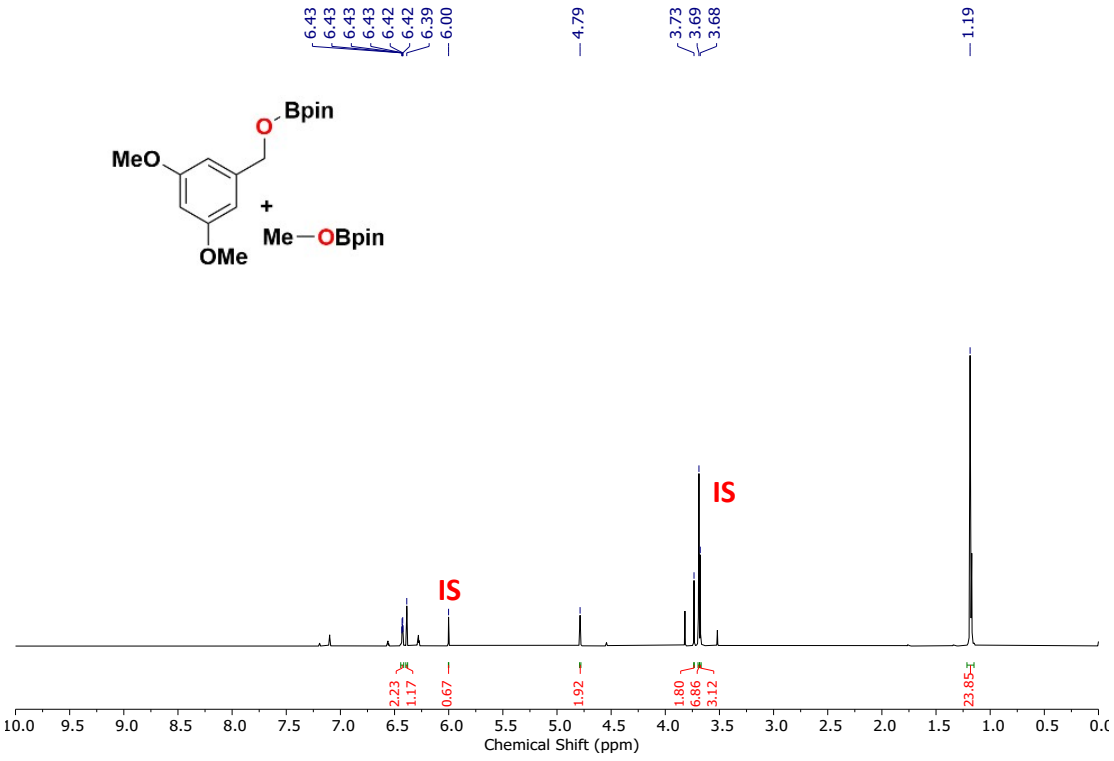

Figure FS 94. ^{1}H NMR (600 MHz, $CDCl_3$, 298 K) spectrum of **9h** and **9b**.

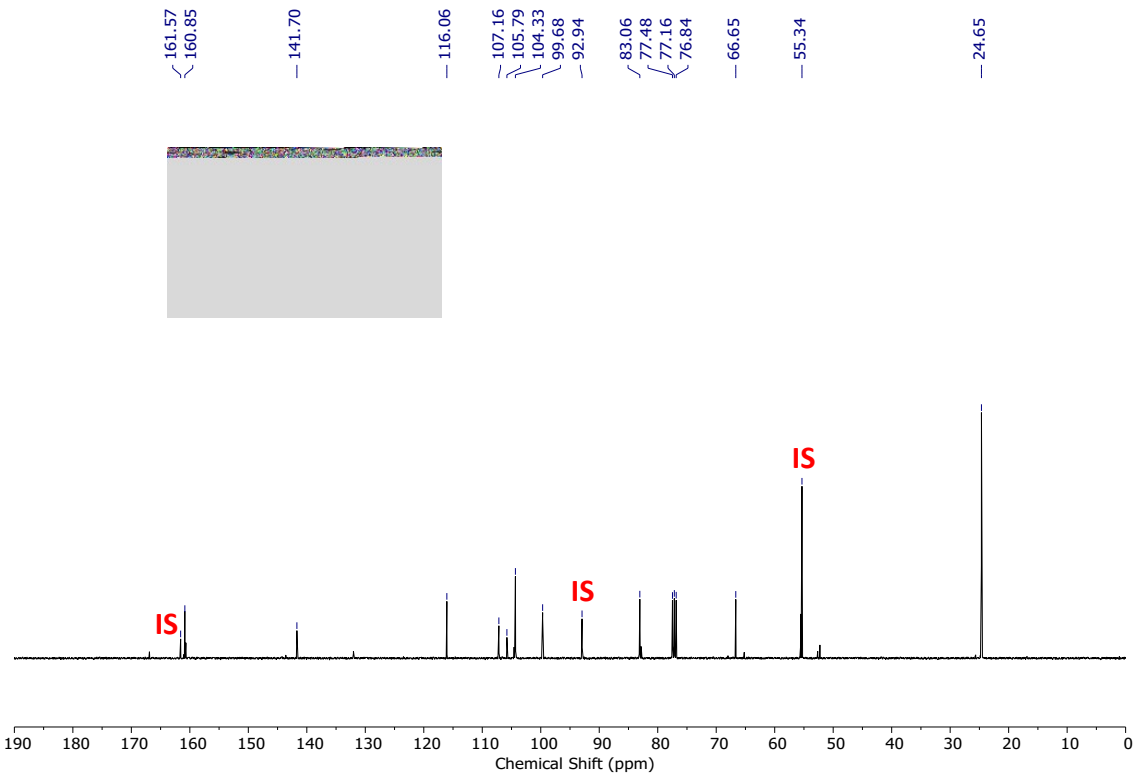

Figure FS 95. $^{13}C\{^{1}H\}$ NMR (150 MHz, $CDCl_3$, 298 K) spectrum of **9h** and **9b**.

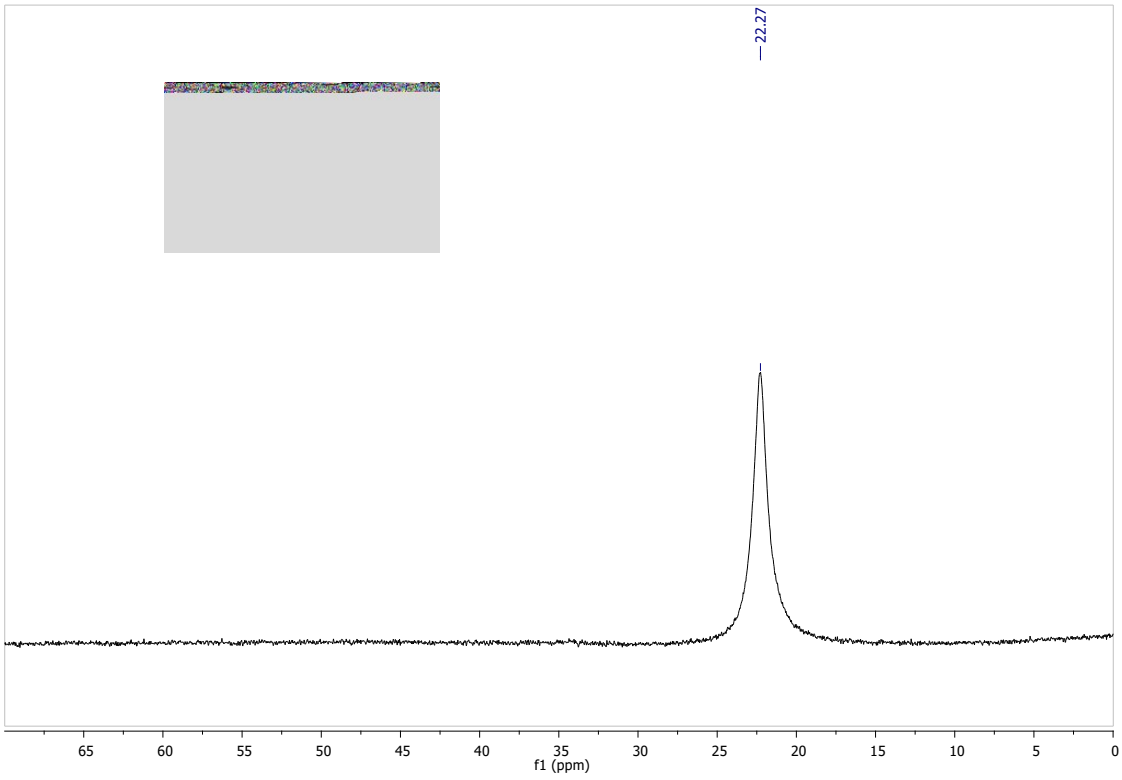

Figure FS 96. $^{11}B\{^{1}H\}$ NMR (192.6 MHz, $CDCl_3$, 298 K) spectrum of **9h** and **9b**.

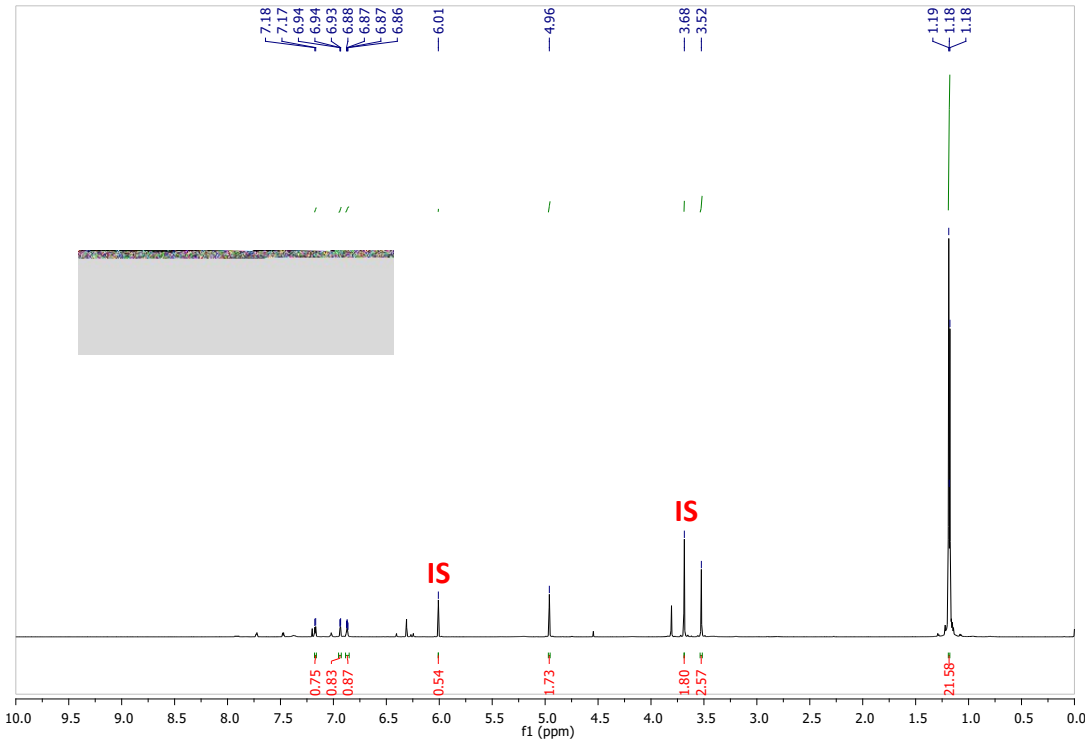

Figure FS 97. ^{1}H NMR (600 MHz, $CDCl_3$, 298 K) spectrum of **9i** and **9b**.

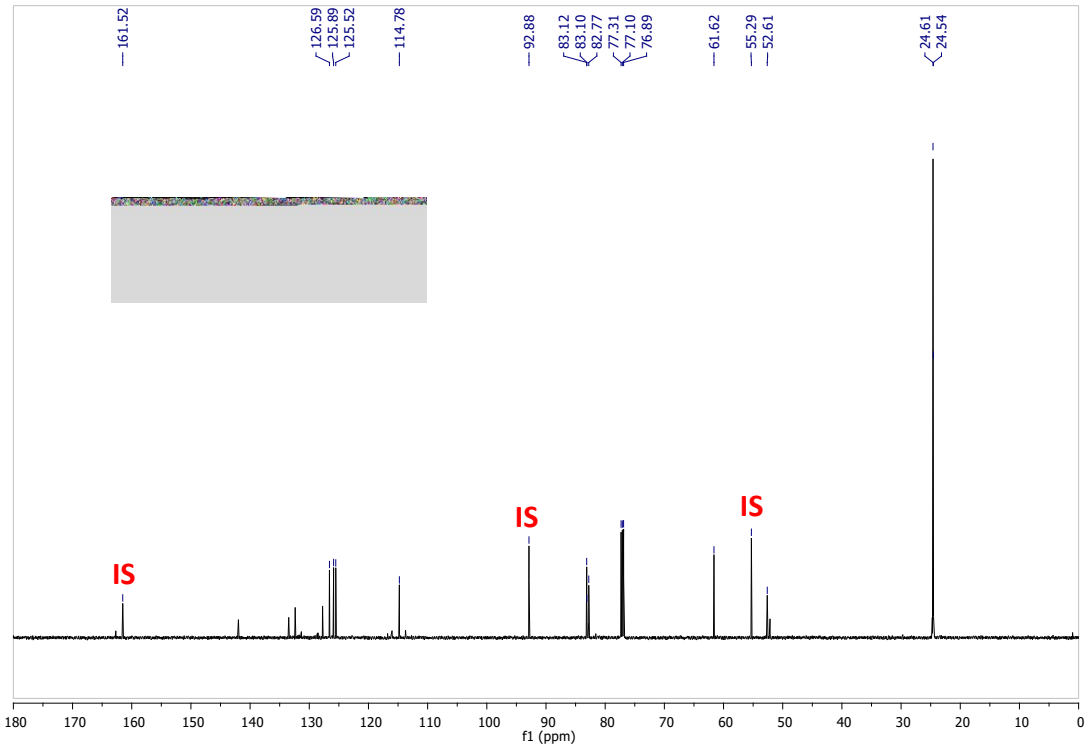

Figure FS 98. ^{13}C{^{1}H} NMR (150 MHz, $CDCl_3$, 298 K) spectrum of **9i** and **9b**.

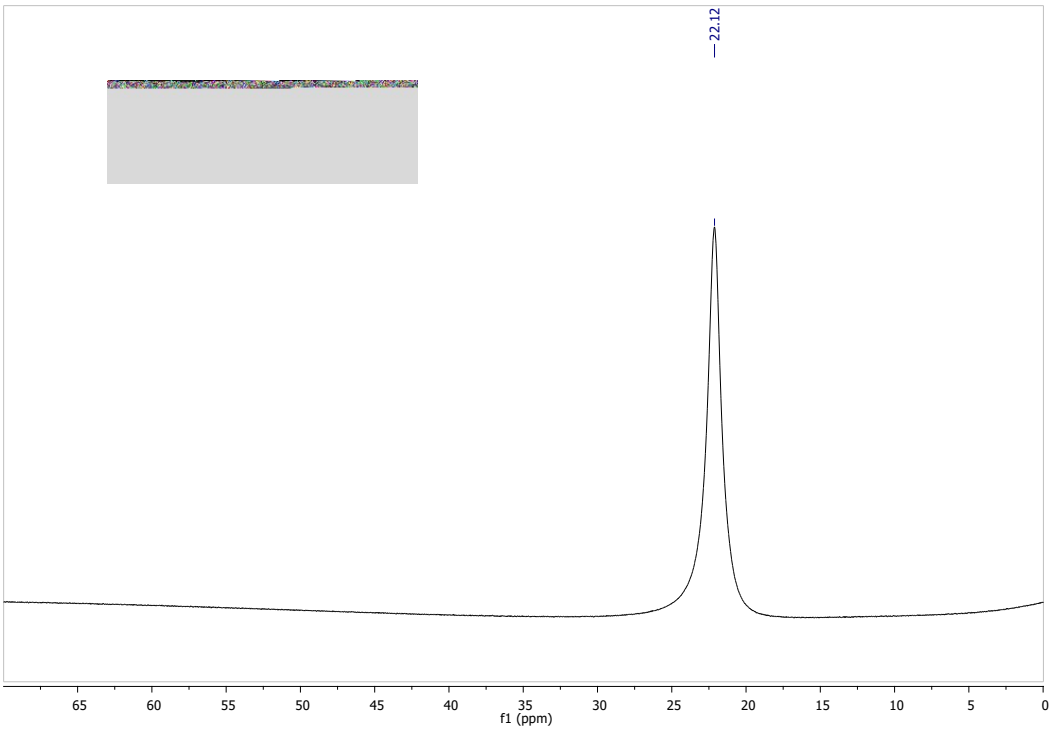

Figure FS 99. $^{11}B\{^{1}H\}$ NMR (192.6 MHz, $CDCl_3$, 298 K) spectrum of **9i** and **9b**.

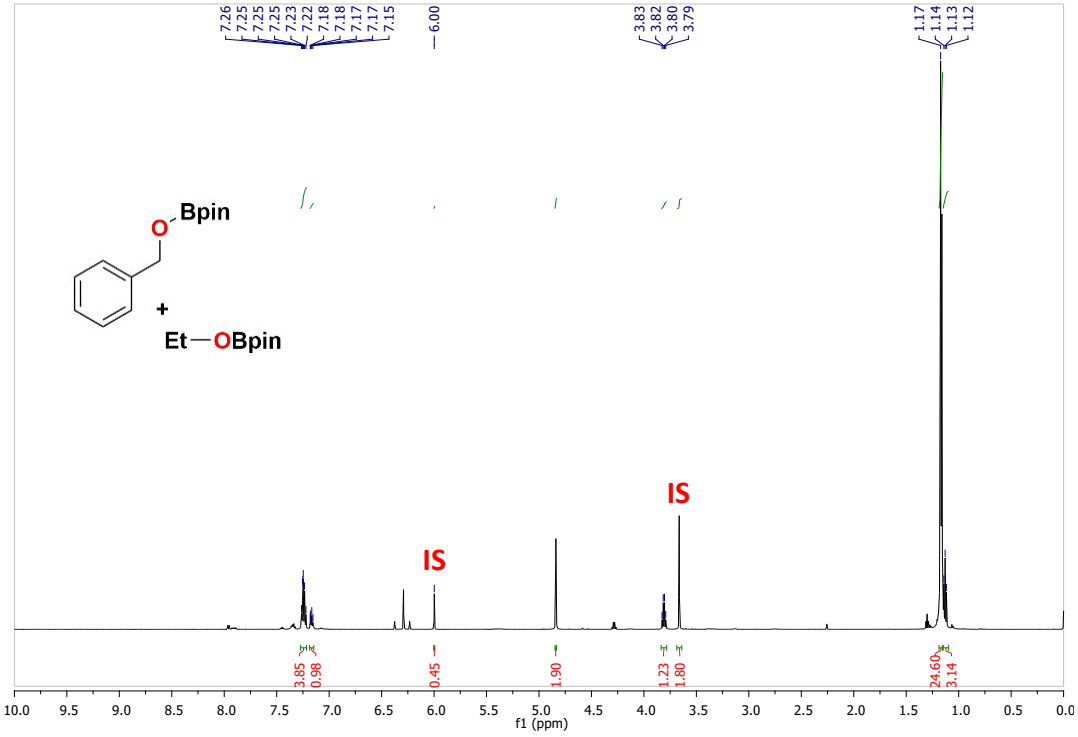

Figure FS 100. ^{1}H NMR (600 MHz, $CDCl_3$, 298 K) spectrum of **9j** and **9k**.

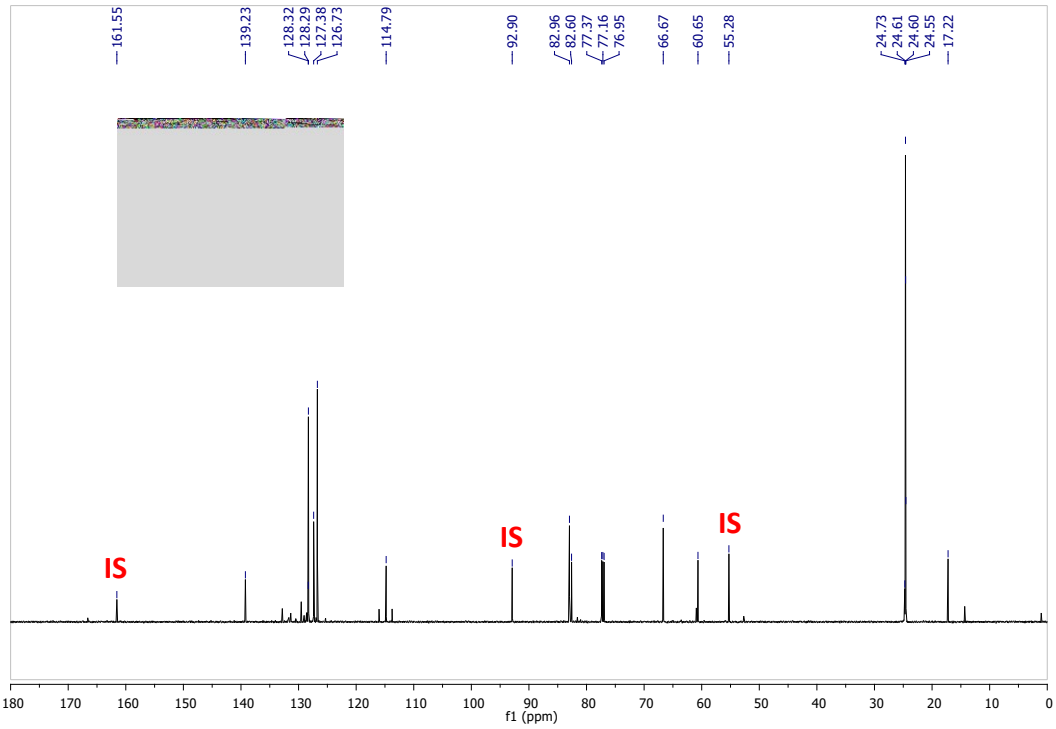

Figure FS 101. $^{13}C\{^{1}H\}$ NMR (150 MHz, $CDCl_3$, 298 K) spectrum of **9j** and **9k**.

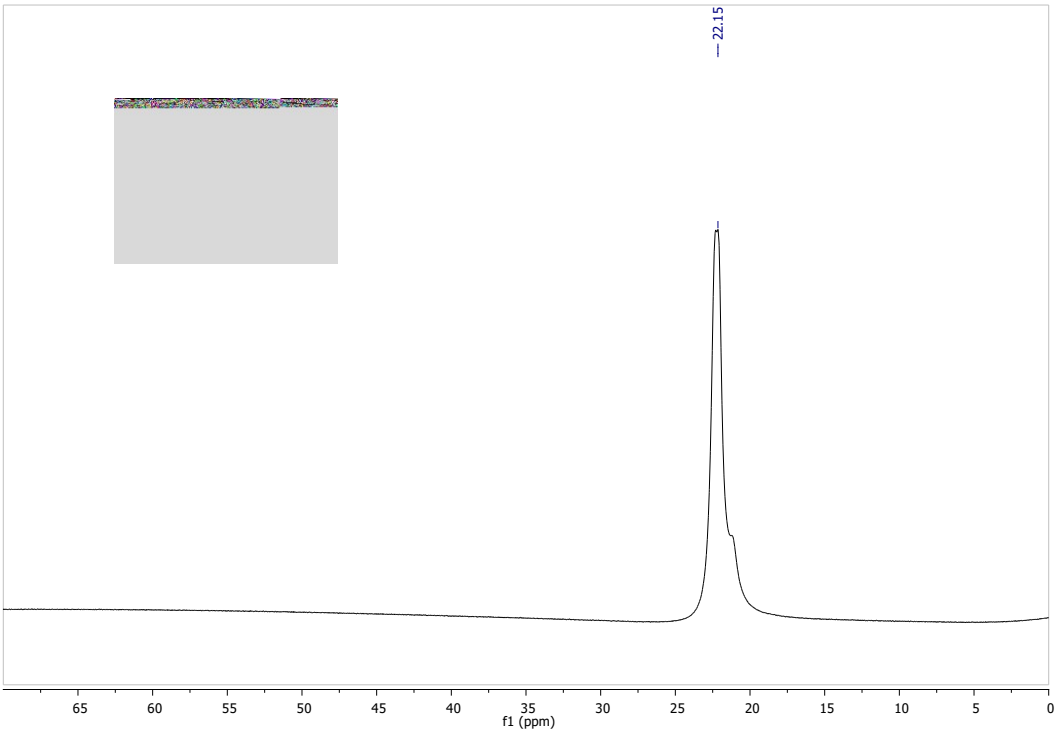

Figure FS 102. $^{11}B\{^{1}H\}$ NMR (192.6 MHz, $CDCl_3$, 298 K) spectrum of **9j** and **9k**.

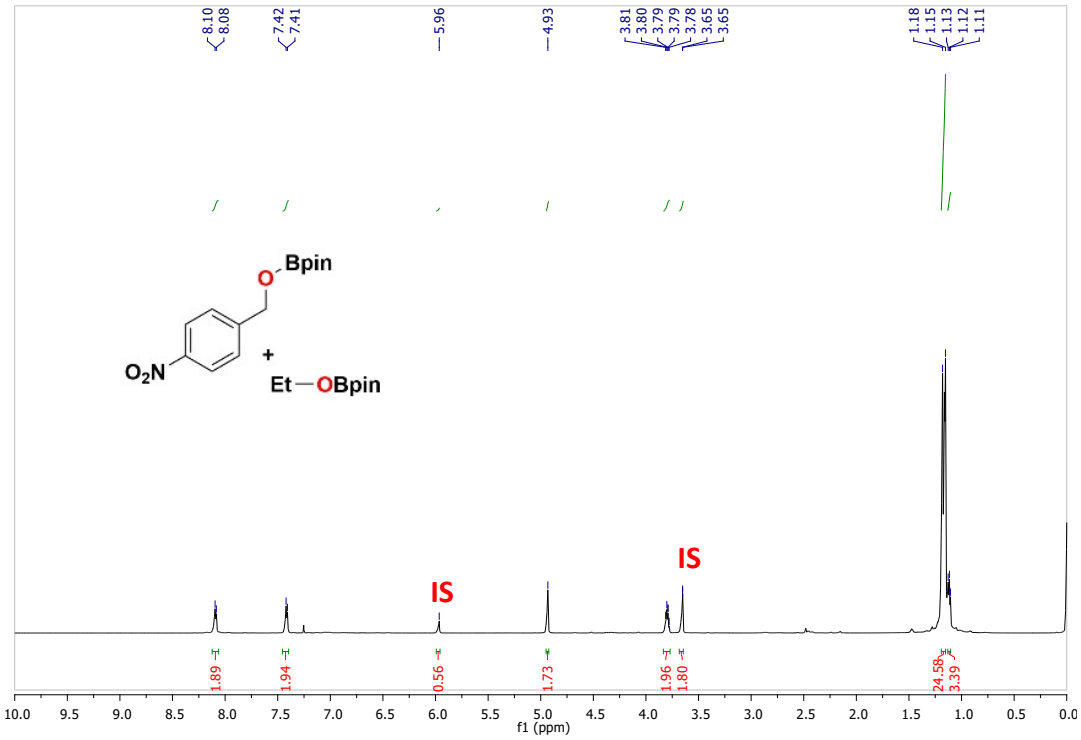

Figure FS 103. ^{1}H NMR (600 MHz, $CDCl_3$, 298 K) spectrum of **9l** and **9k**.

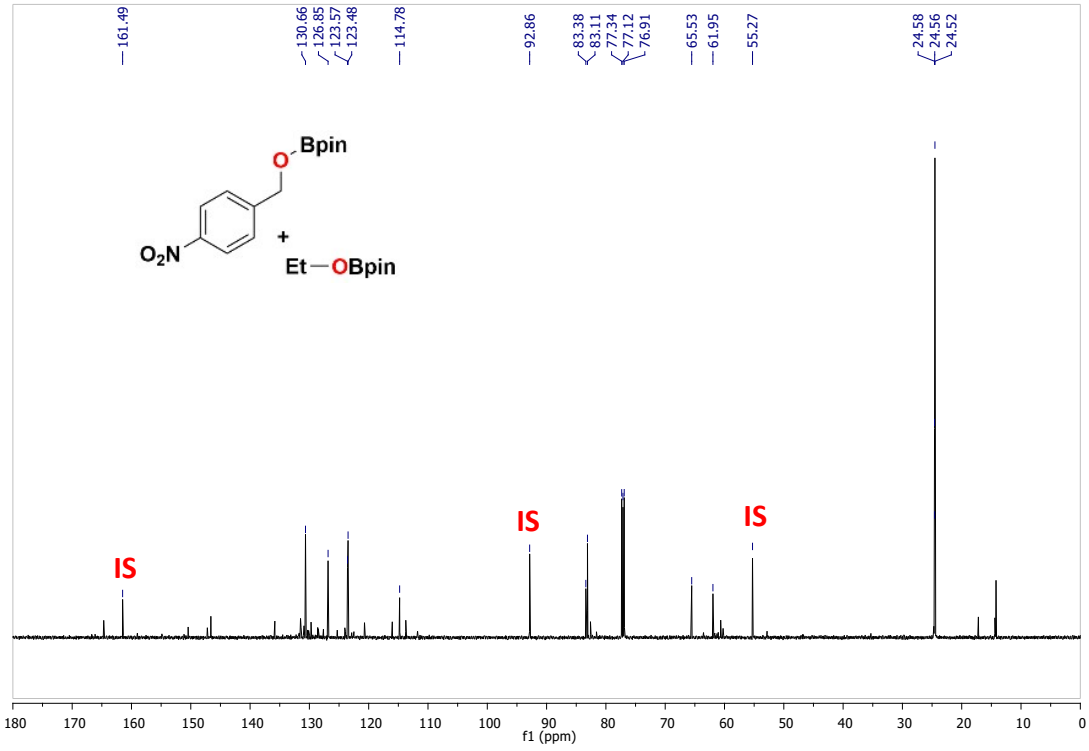

Figure FS 104. $^{13}C\{^{1}H\}$ NMR (150 MHz, $CDCl_3$, 298 K) spectrum of **9l** and **9k**.

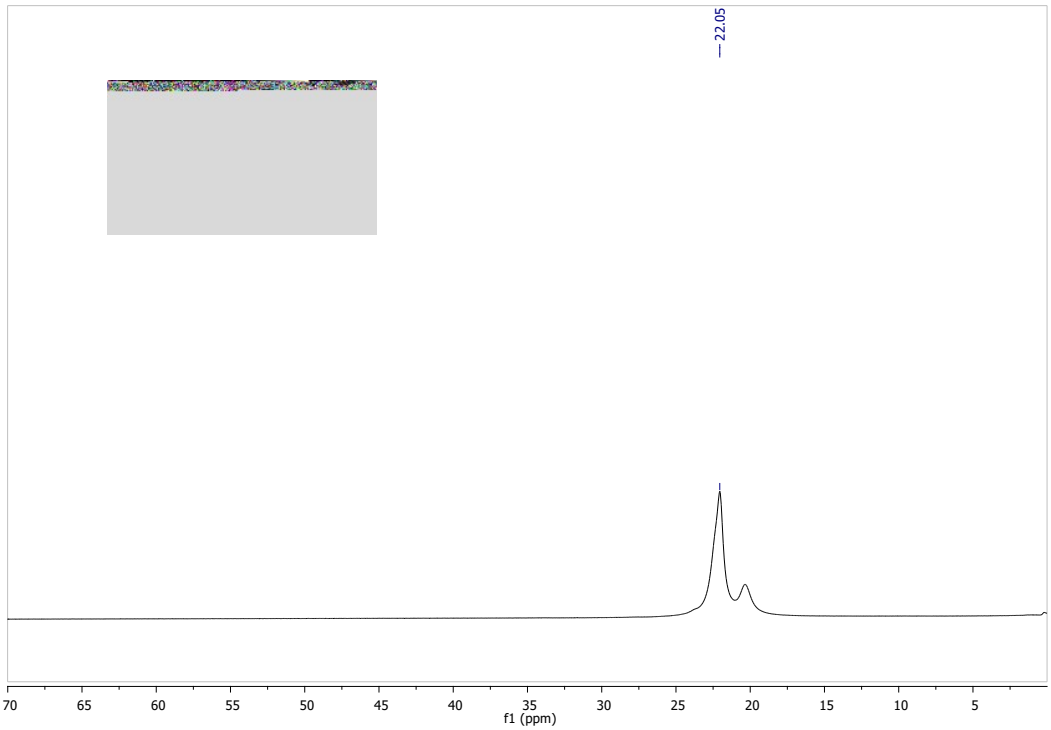

Figure FS 105. $^{11}B\{^{1}H\}$ NMR (192.6 MHz, $CDCl_3$, 298 K) spectrum of **9l** and **9k**.

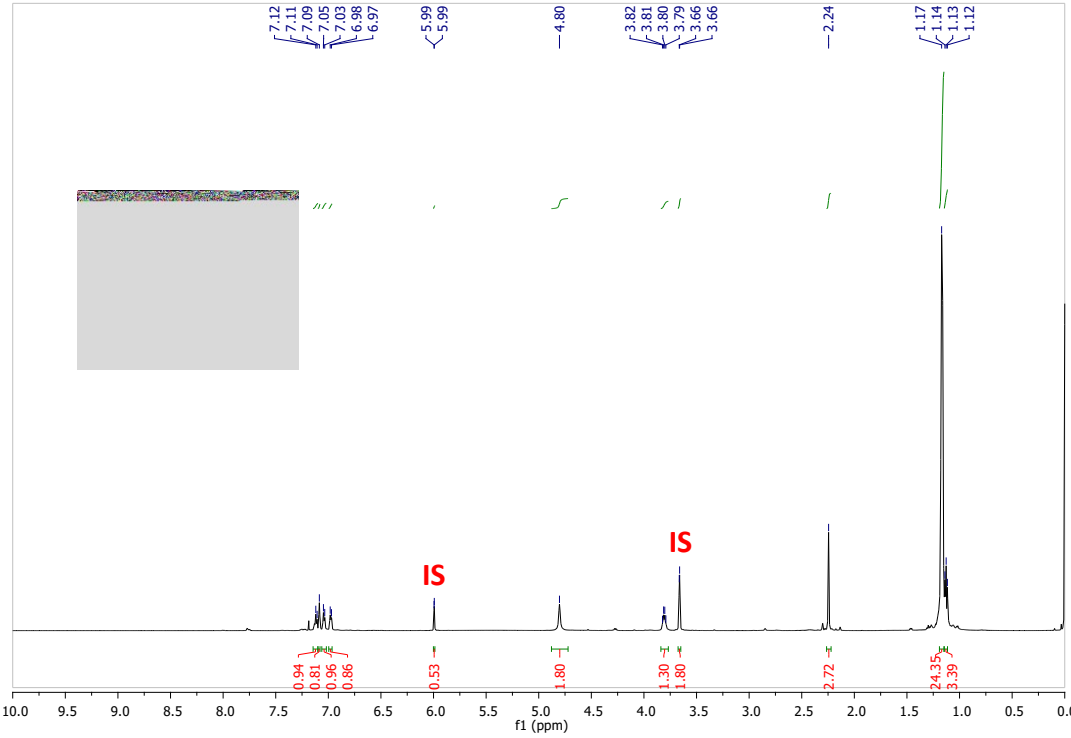

Figure FS 106. ^{1}H NMR (600 MHz, $CDCl_3$, 298 K) spectrum of **9m** and **9k**.

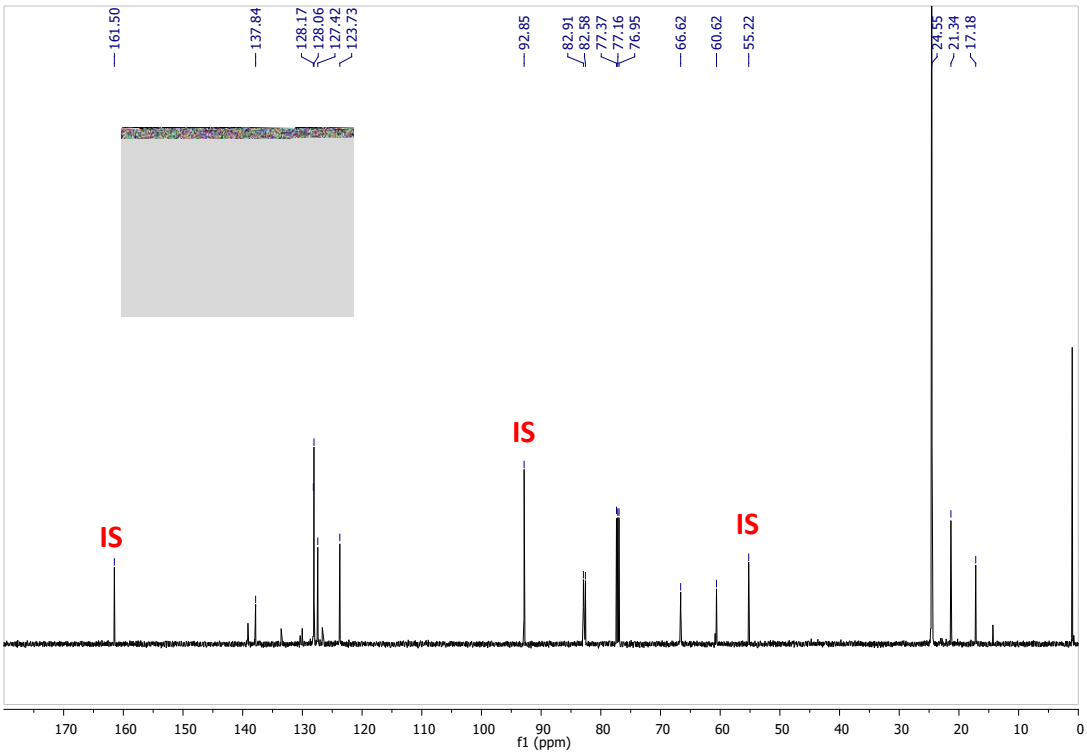

Figure FS 107. $^{13}C\{^{1}H\}$ NMR (150 MHz, $CDCl_3$, 298 K) spectrum of **9m** and **9k**.

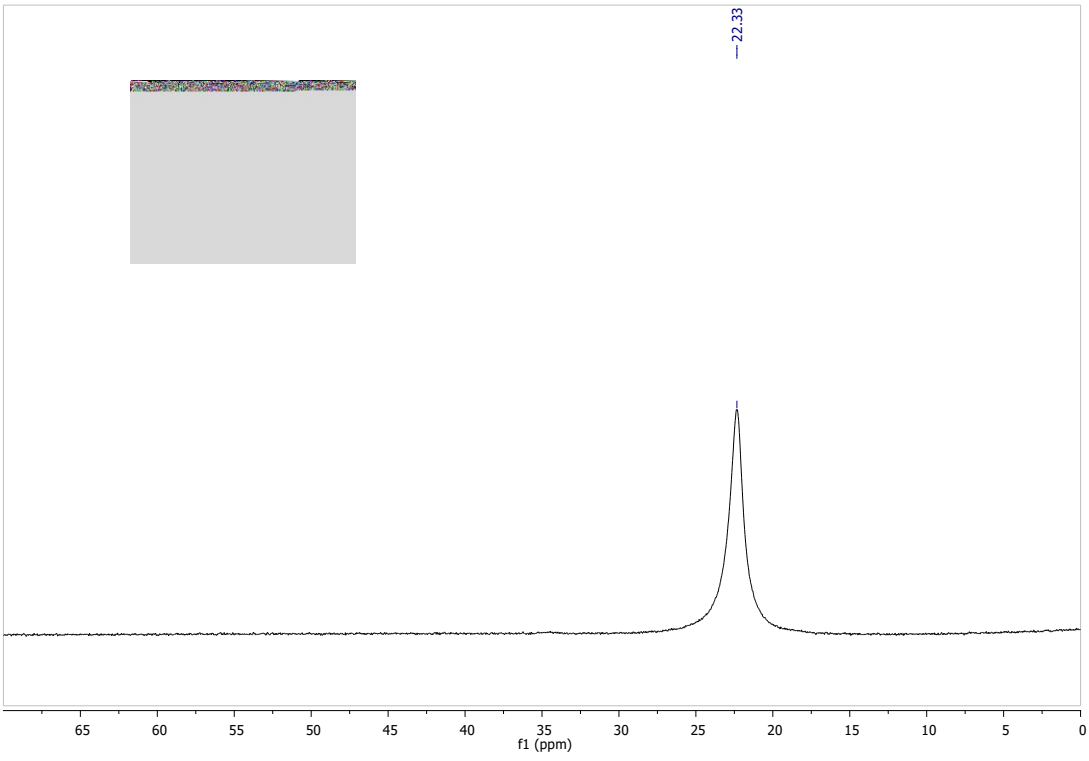

Figure FS 108. $^{11}B\{^{1}H\}$ NMR (192.6 MHz, $CDCl_3$, 298 K) spectrum of **9m** and **9k**.

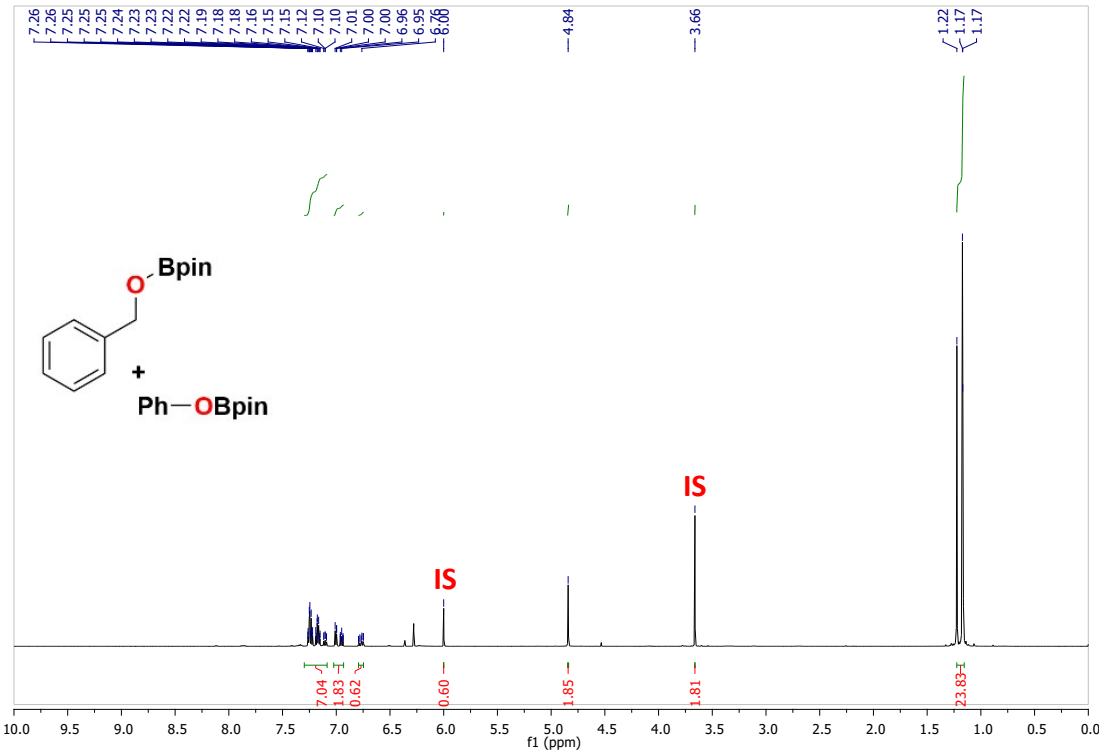

Figure FS 109. ^{1}H NMR (600 MHz, $CDCl_3$, 298 K) spectrum of **9n** and **9o**.

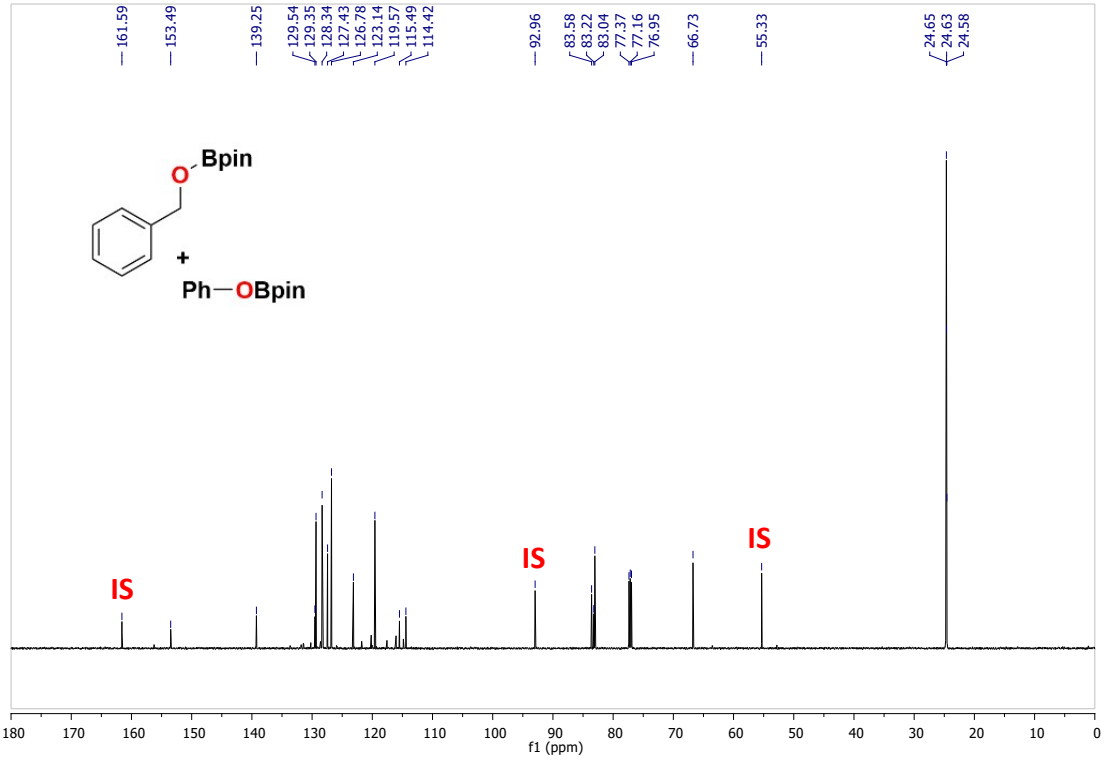

Figure FS 110. $^{13}C\{^{1}H\}$ NMR (150 MHz, $CDCl_3$, 298 K) spectrum of **9n** and **9o**.

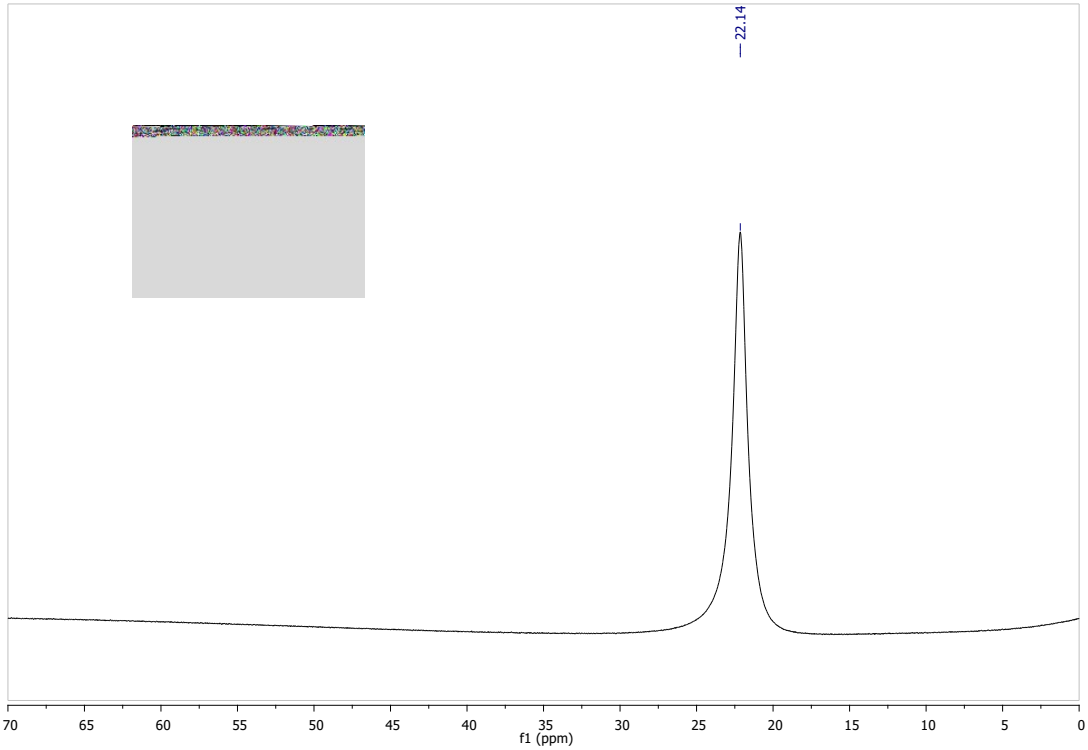

Figure FS 111. $^{11}B\{^{1}H\}$ NMR (192.6 MHz, $CDCl_3$, 298 K) spectrum of **9n** and **9o**.

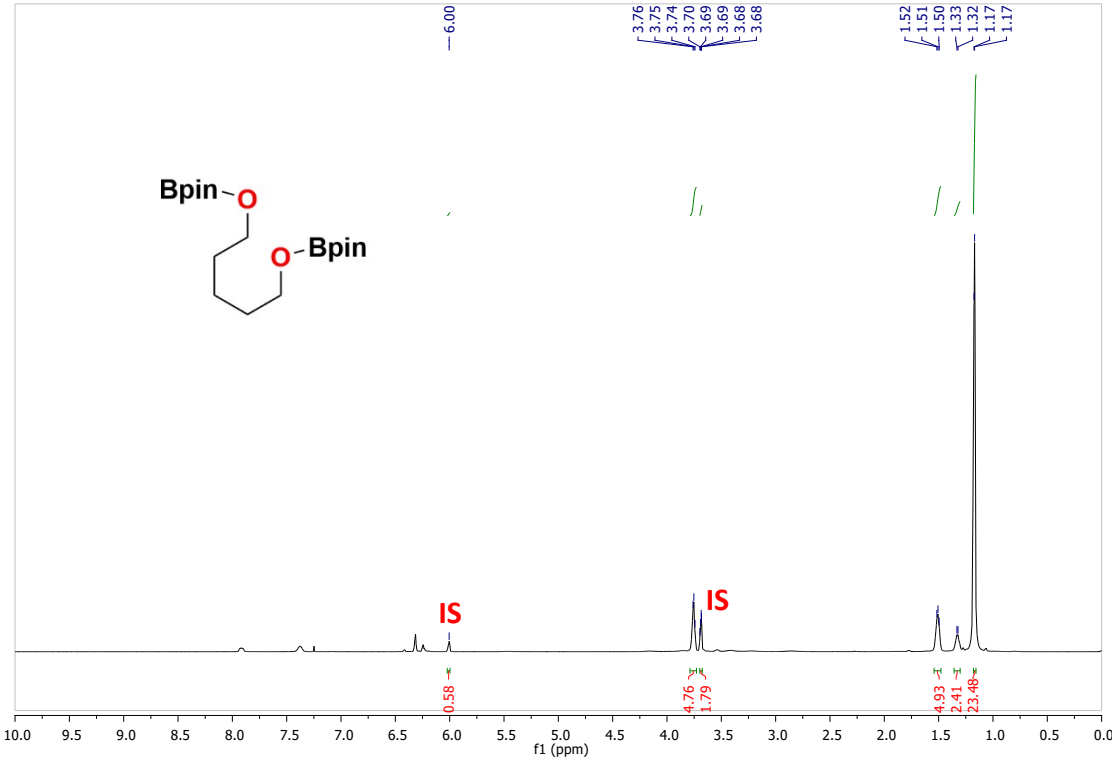

Figure FS 112. ^{1}H NMR (600 MHz, $CDCl_3$, 298 K) spectrum of **9p**.

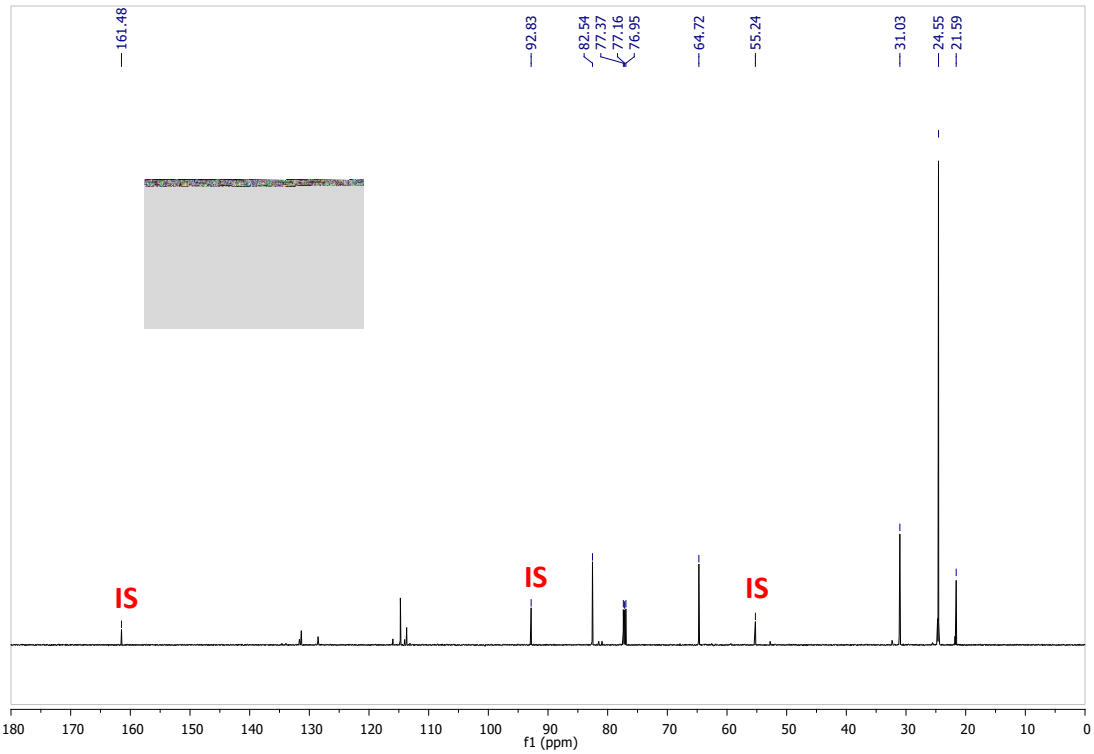

Figure FS 113. $^{13}C\{^{1}H\}$ NMR (150 MHz, $CDCl_3$, 298 K) spectrum of **9p**.

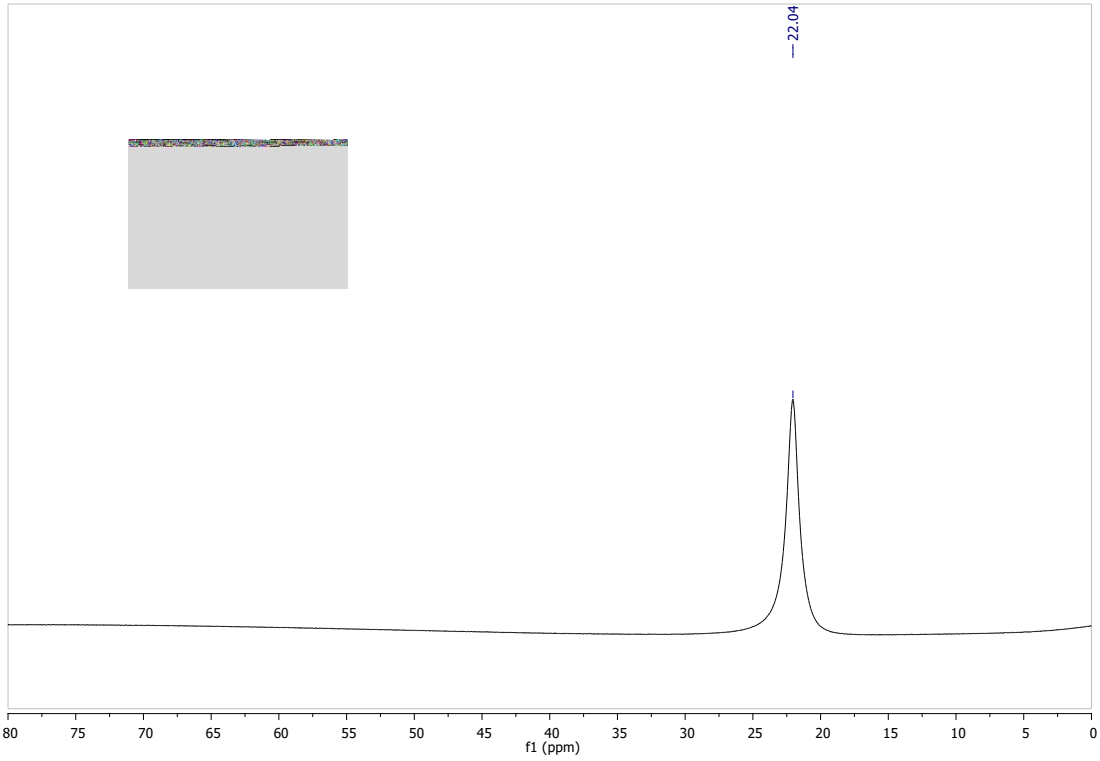

Figure FS 114. $^{11}B\{^{1}H\}$ NMR (192.6 MHz, $CDCl_3$, 298 K) spectrum of **9p**.

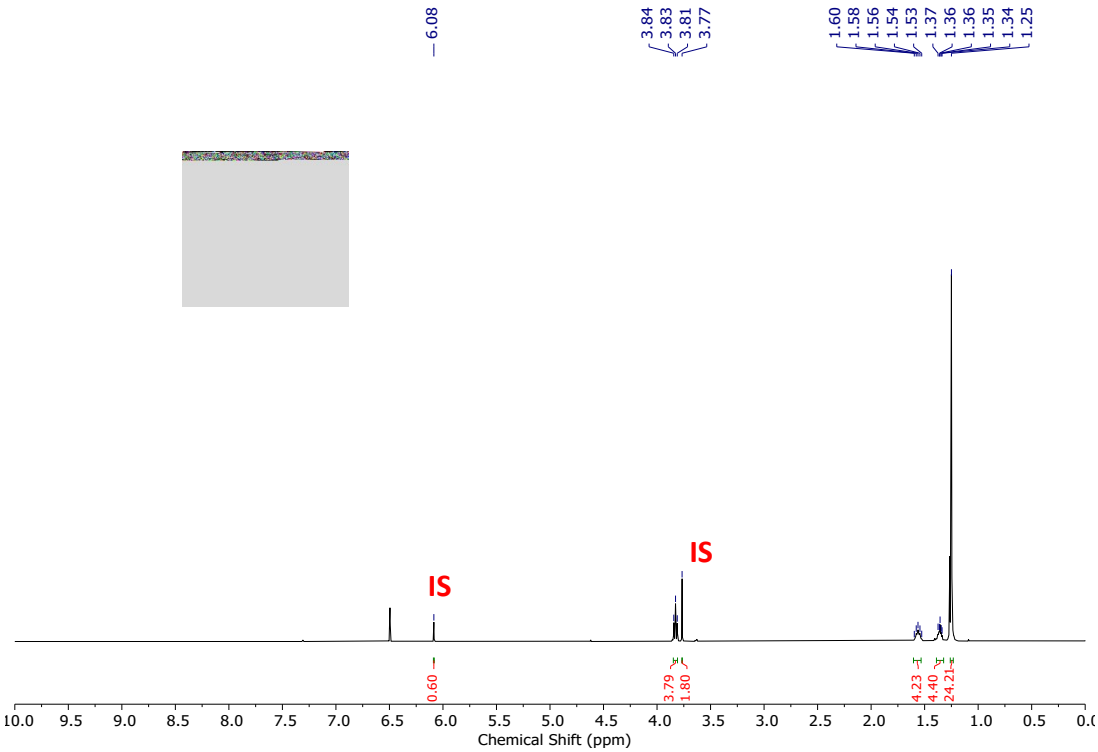

Figure FS 115. ^{1}H NMR (600 MHz, $CDCl_3$, 298 K) spectrum of **9q**.

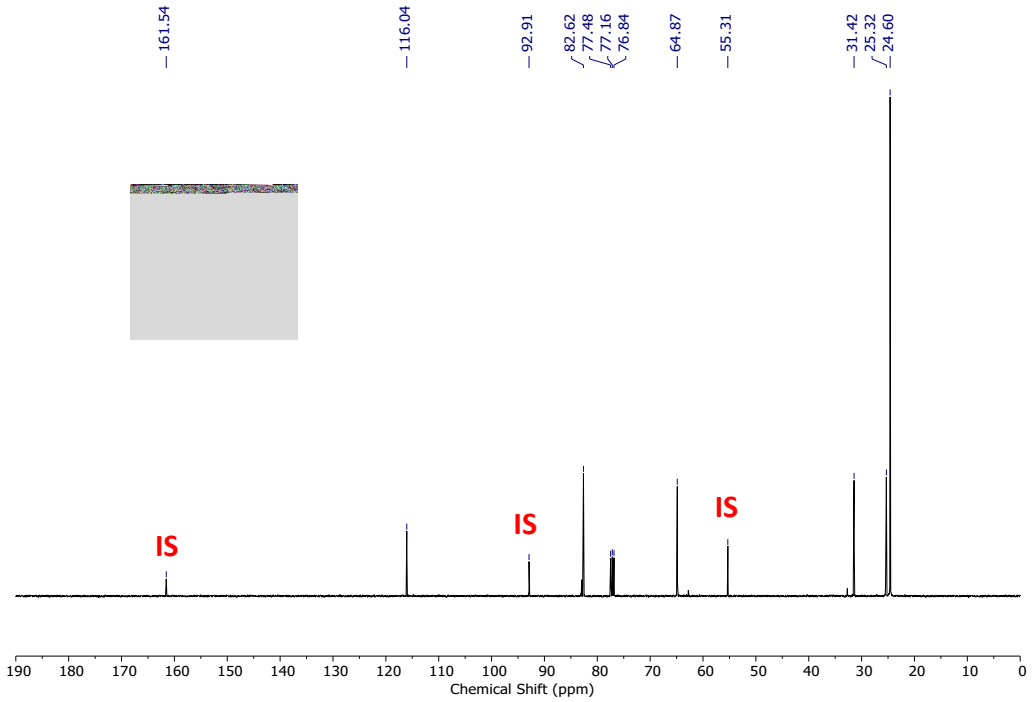

Figure FS 116. $^{13}C\{^{1}H\}$ NMR (150 MHz, $CDCl_3$, 298 K) spectrum of **9q**.

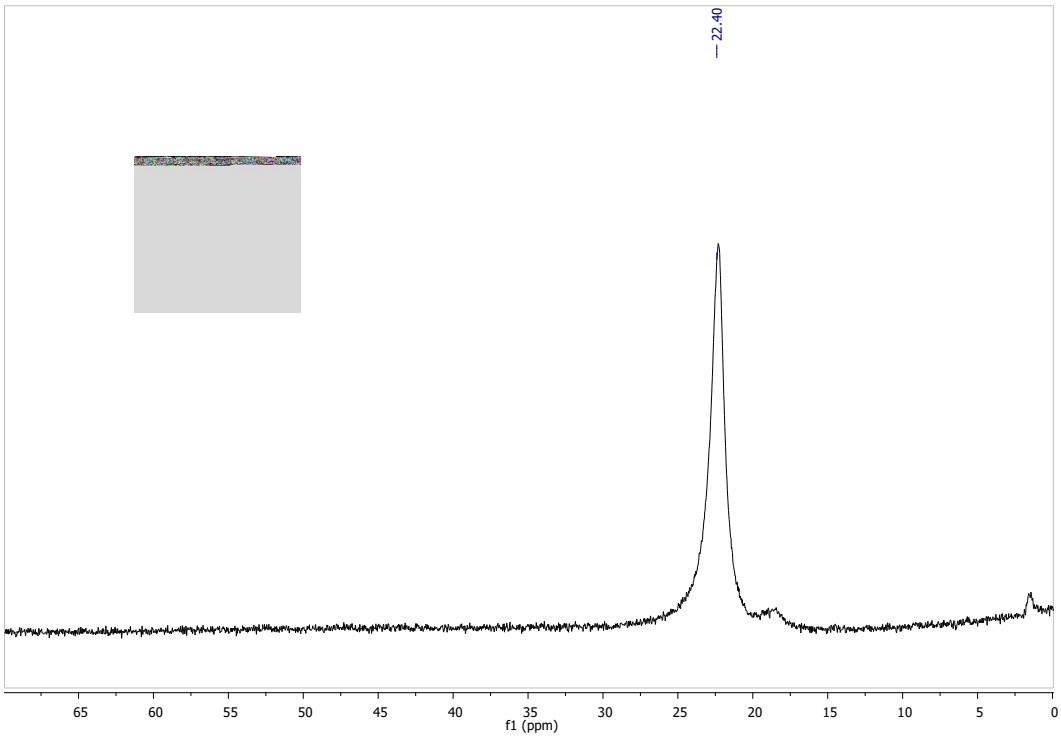

Figure FS 117. $^{11}B\{^{1}H\}$ NMR (192.6 MHz, $CDCl_3$, 298 K) spectrum of **9q**.

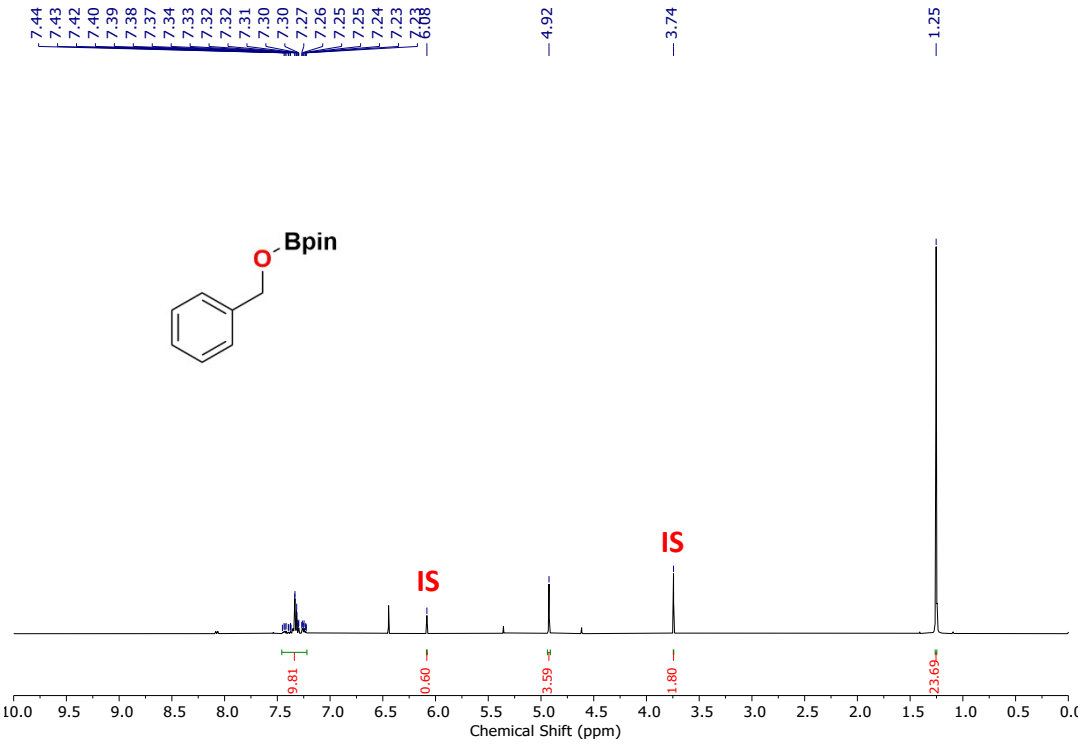

Figure FS 118. ^{1}H NMR (600 MHz, $CDCl_3$, 298 K) spectrum of **9r**.

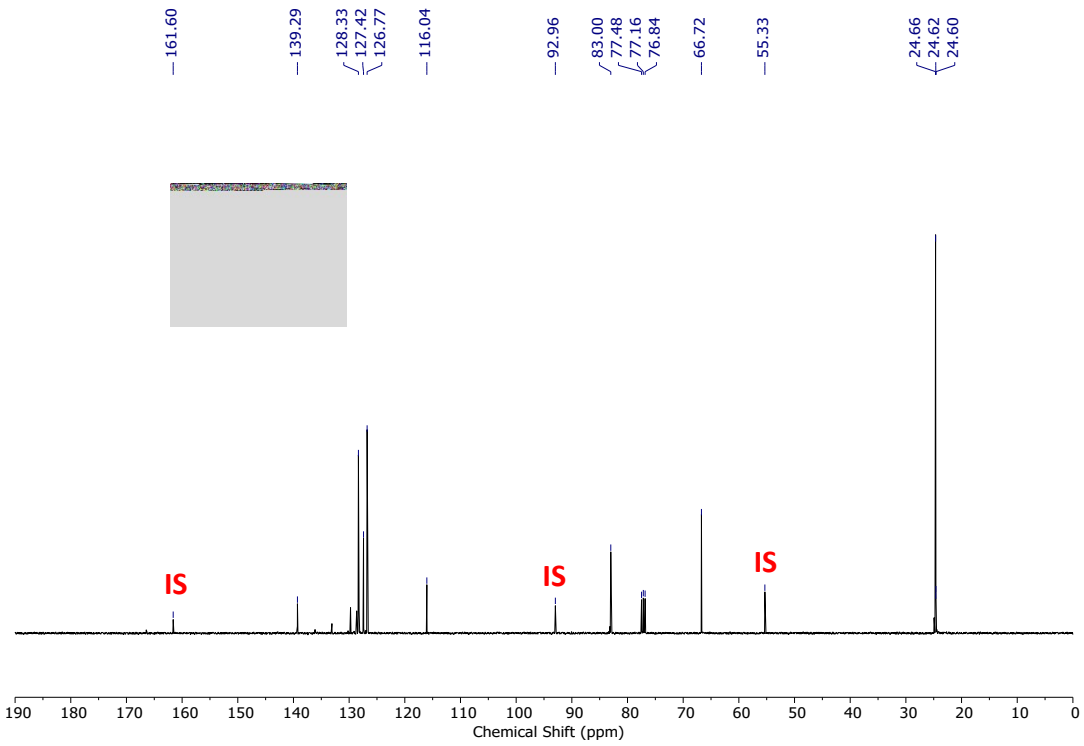

Figure FS 119. $^{13}C\{^{1}H\}$ NMR (150 MHz, $CDCl_3$, 298 K) spectrum of **9r**.

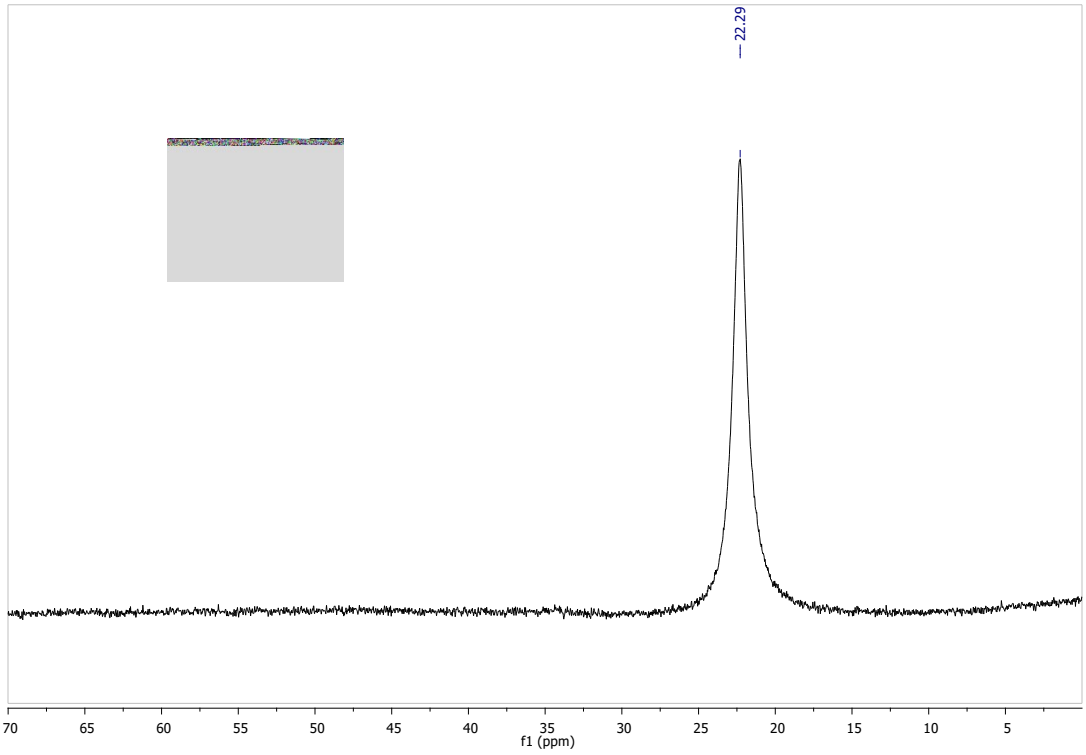

Figure FS 120. $^{11}B\{^{1}H\}$ NMR (192.6 MHz, $CDCl_3$, 298 K) spectrum of **9r**.

4.4 Plausible mechanism of the catalytic hydroboration of esters with pinacolborane

Based on the reported literature,[3] a plausible mechanism of esters hydroboration using zinc alkyl complex as pre-catalyst is depicted in **Figure FS 121**. In the catalytic cycle in situ generated zinc hydride species [**I**] act as active catalyst. In the first step, the Zn-H bond of active catalyst [**I**] is inserted into the C=O bond of ester to produce Zn-hemiacetal species [**II**]. In the next step, Intermediate [**III**] (LZn-OCH_2R) is formed as the C-OR' bond of ester is cleaved by the assistance of an HBpin molecule. In the final step, σ-bond metathesis takes place between intermediate [**III**] and another HBpin molecule to regenerate active catalyst [**I**] along with the production of boryl ester.

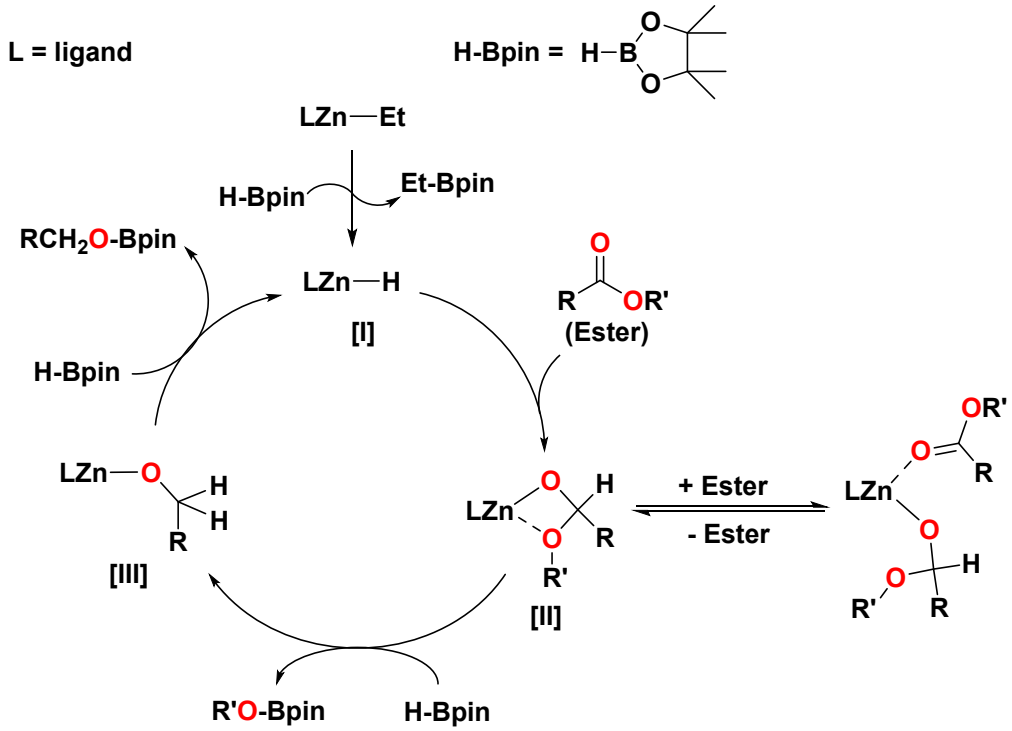

Figure FS 121. A plausible mechanism for catalytic hydroboration of esters using zinc alkyl complex as pre-catalyst.

5. NMR spectra of competitive experiments for chemoselective hydroboration.

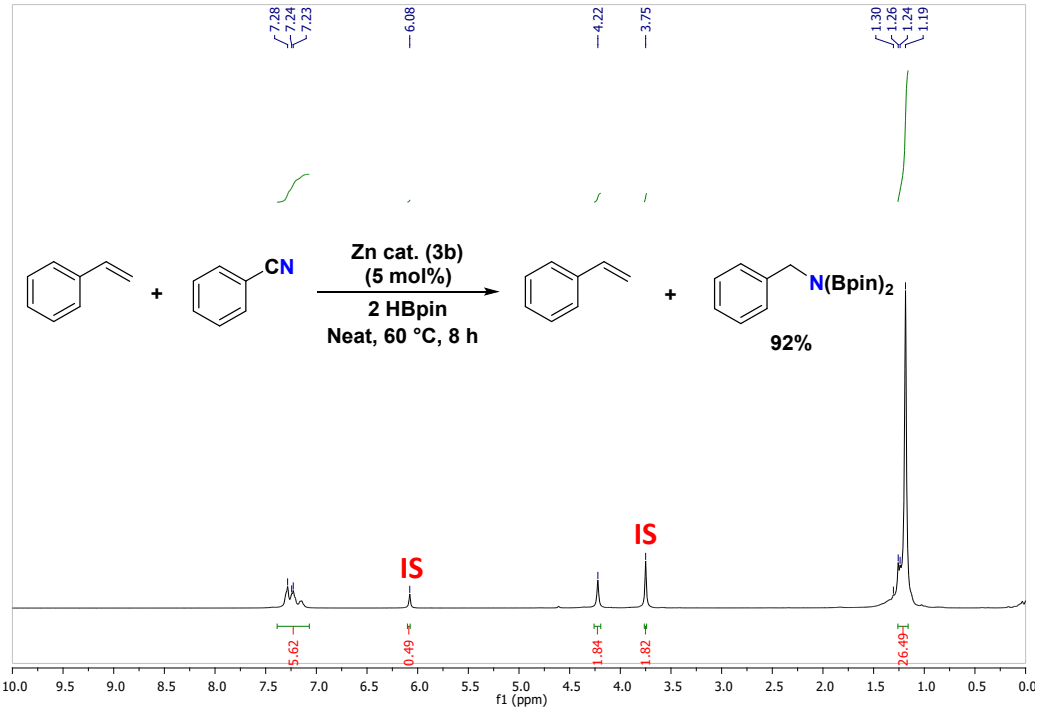

Figure FS 122. ^{1}H NMR (400 MHz, $CDCl_3$, 298 K) spectrum for chemoselectivity test between styrene and benzonitrile.

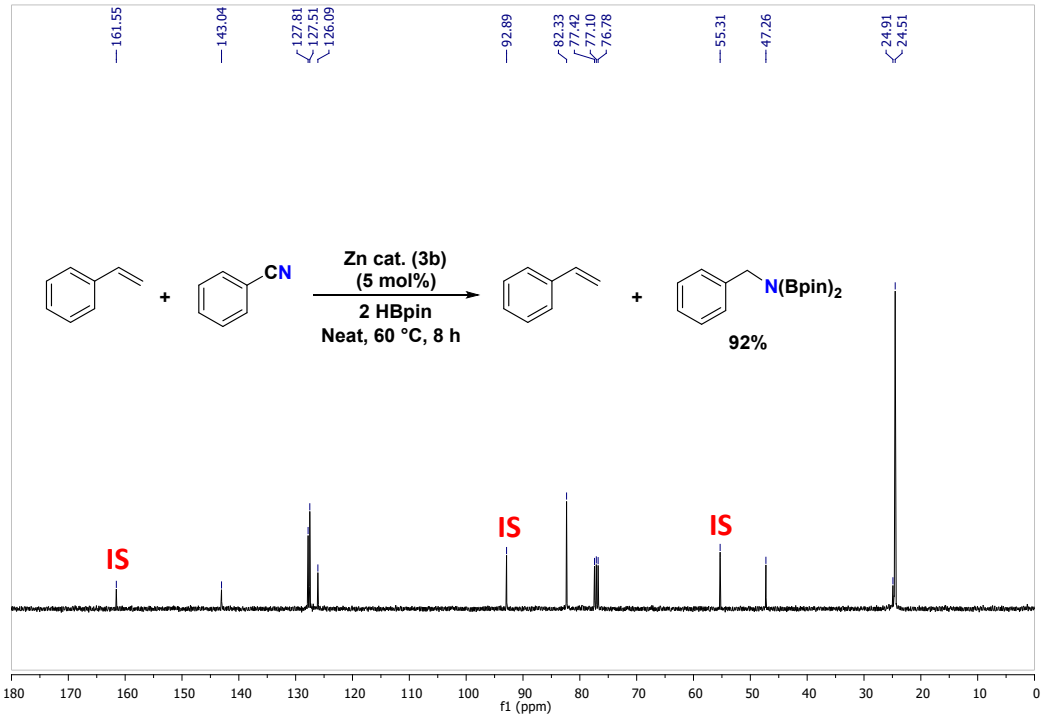

Figure FS 123 $^{13}C\{^{1}H\}$ NMR (100 MHz, $CDCl_3$, 298 K) spectrum for chemoselectivity test between styrene and benzonitrile.

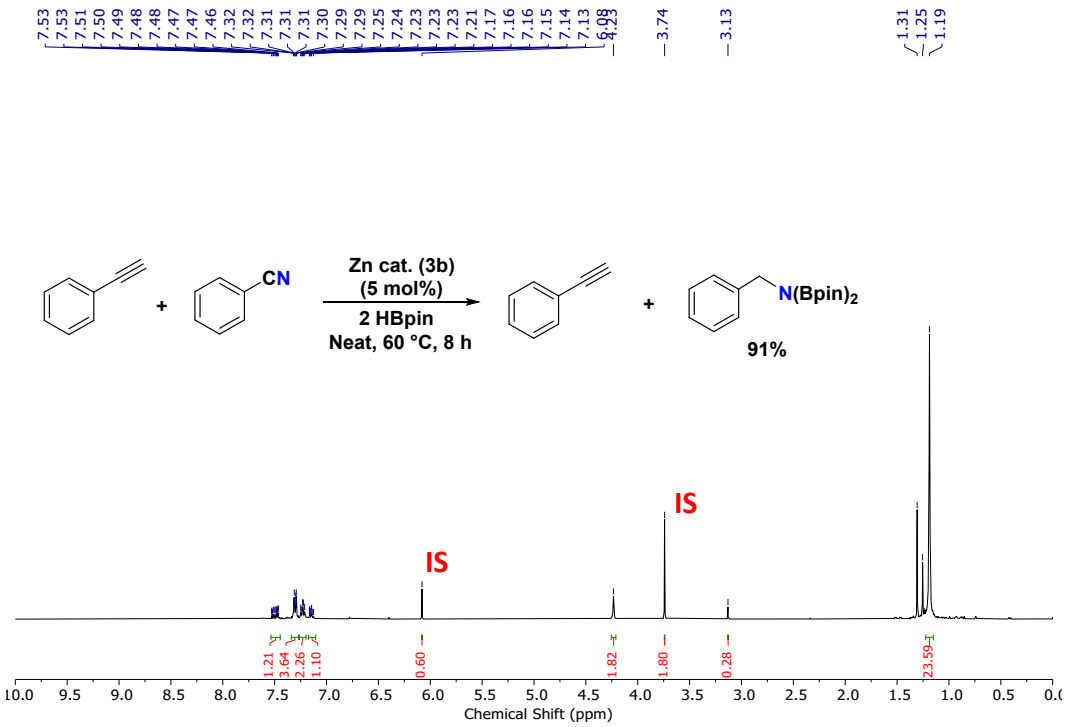

Figure FS 124. ^{1}H NMR (400 MHz, $CDCl_3$, 298 K) spectrum for chemoselectivity test between phenylacetylene and benzonitrile.

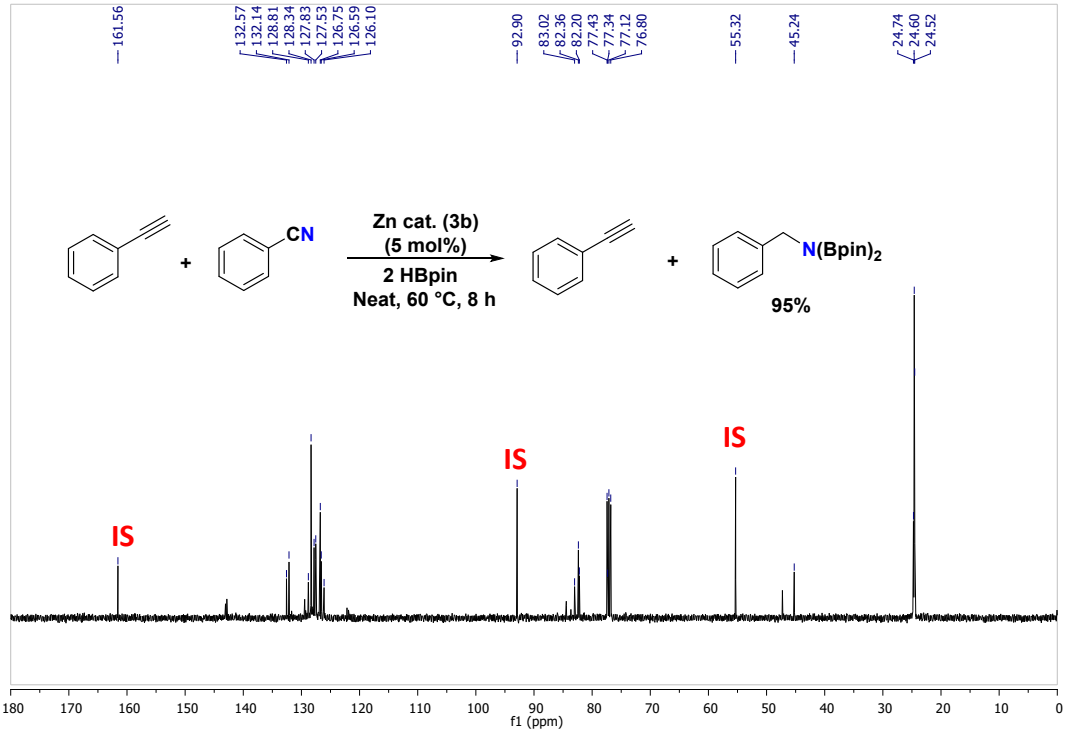

Figure FS 125. $^{13}C\{^{1}H\}$ NMR (100 MHz, $CDCl_3$, 298 K) spectrum for chemoselectivity test between phenylacetylene and benzonitrile.

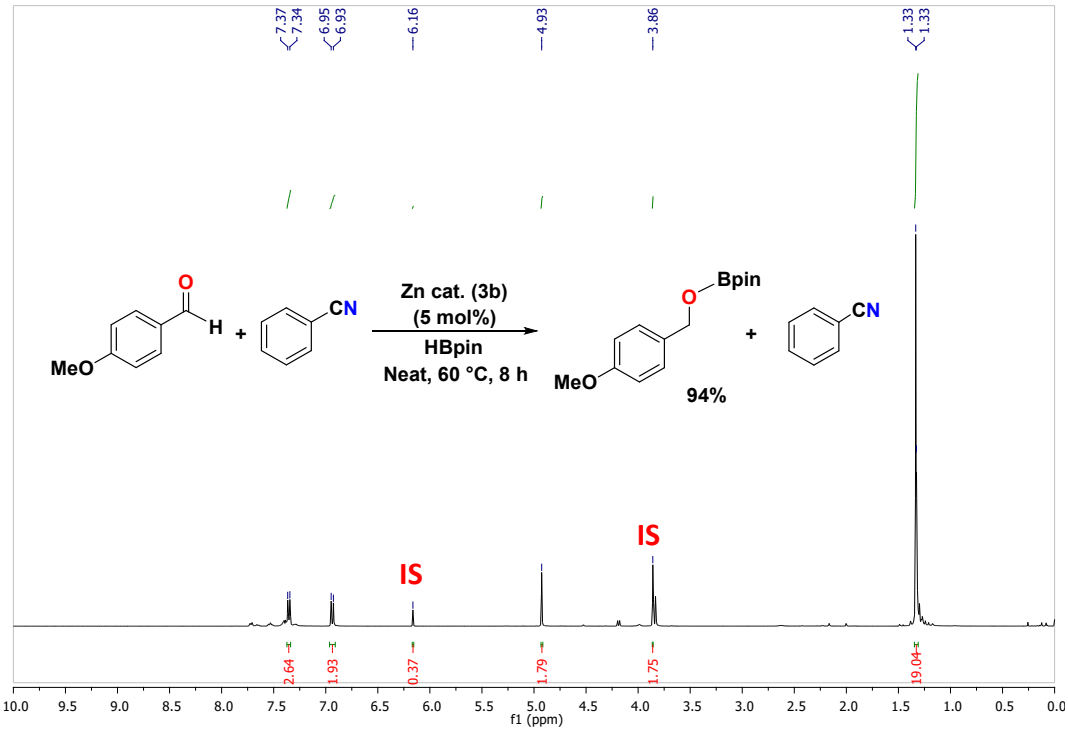

Figure FS 126. ^{1}H NMR (400 MHz, $CDCl_3$, 298 K) spectrum for chemoselectivity test between *p*-methoxybenzaldehyde and benzonitrile.

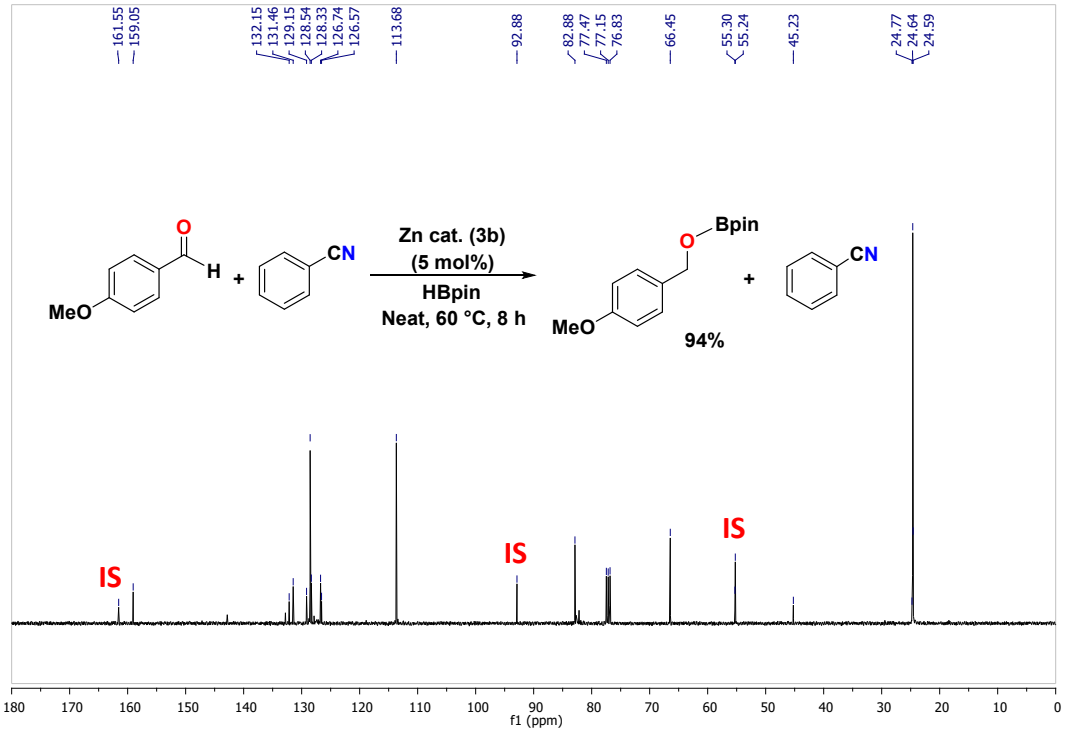

Figure FS 127. $^{13}C\{^{1}H\}$ NMR (100 MHz, $CDCl_3$, 298 K) spectrum for chemoselectivity test between *p*-methoxybenzaldehyde and benzonitrile.

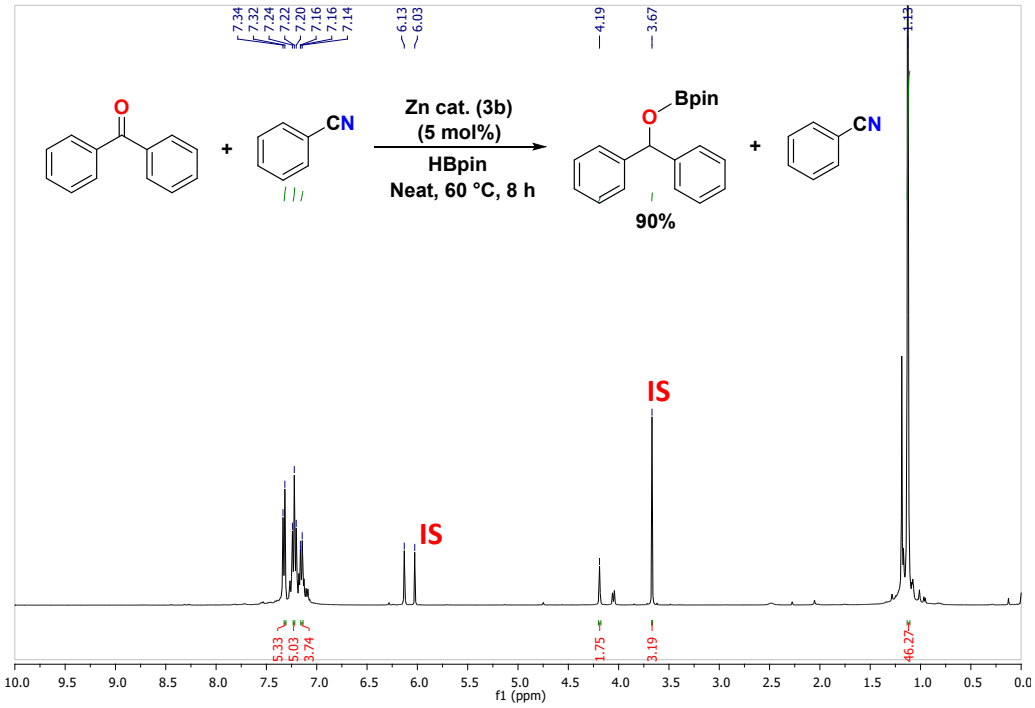

Figure FS 128. ^{1}H NMR (400 MHz, $CDCl_3$, 298 K) spectrum for chemoselectivity test between benzophenone and benzonitrile.

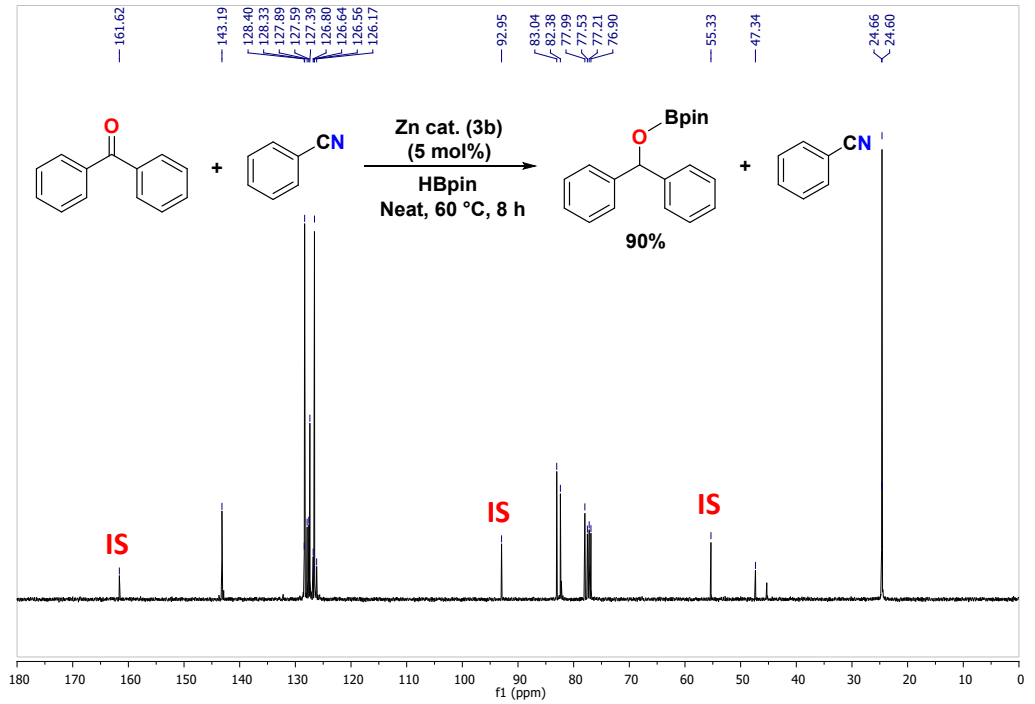

Figure FS 129. $^{13}C\{^{1}H\}$ NMR (100 MHz, $CDCl_3$, 298 K) spectrum for chemoselectivity test between benzophenone and benzonitrile.

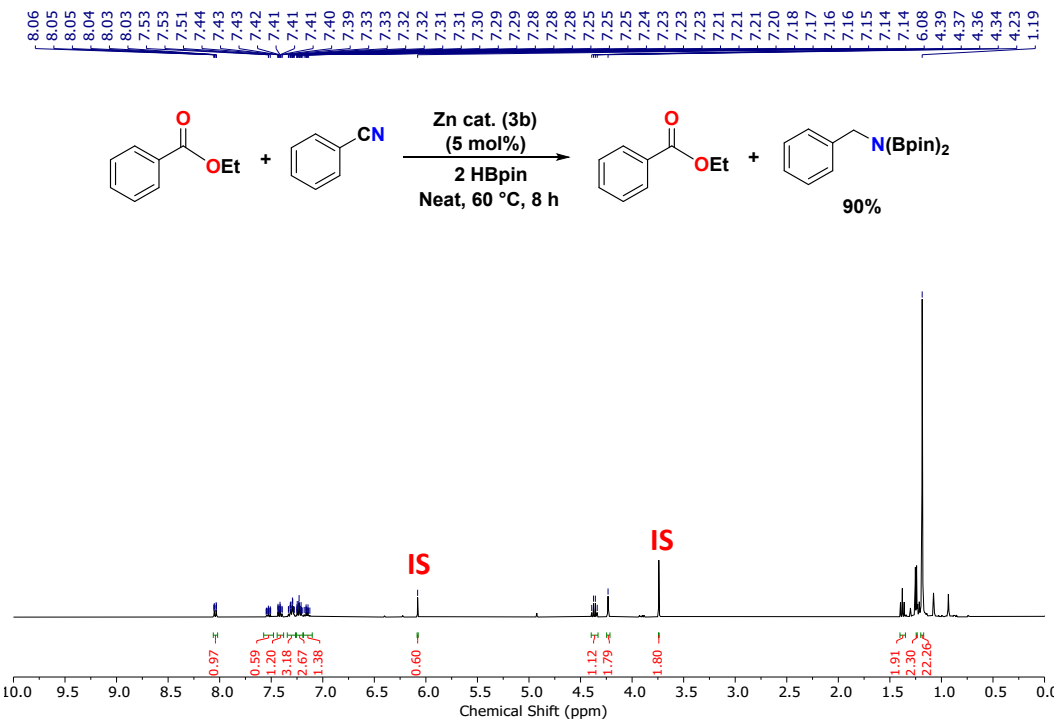

Figure FS 130. ^{1}H NMR (400 MHz, $CDCl_3$, 298 K) spectrum for chemoselectivity test between ethyl benzoate and benzonitrile.

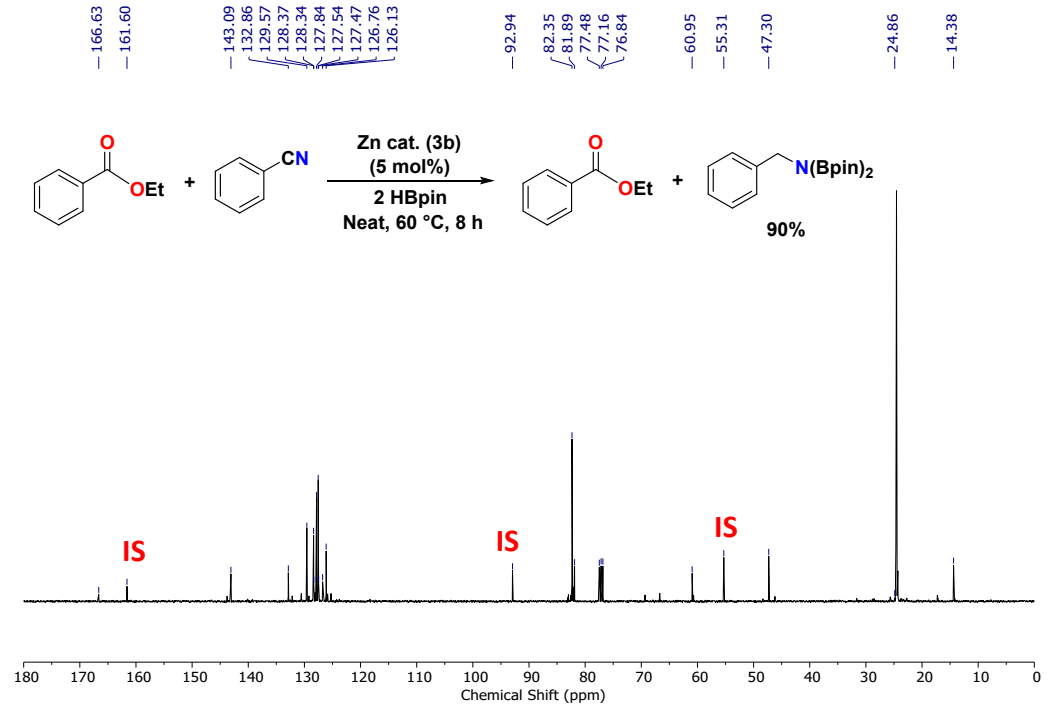

Figure FS 131. $^{13}C\{^{1}H\}$ NMR (100 MHz, $CDCl_3$, 298 K) spectrum for chemoselectivity test between ethyl benzoate and benzonitrile.

6. NMR spectra of controlled reactions:

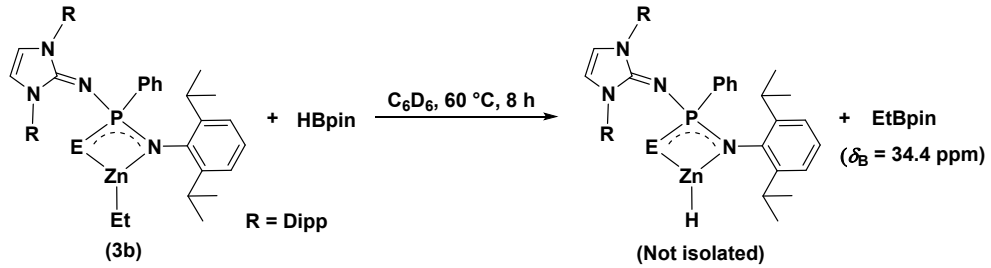

Stoichiometric reaction between complex **3b** and pinacolborane (HBpin) was carried out in benzene-d_6 at 60 °C temperature.

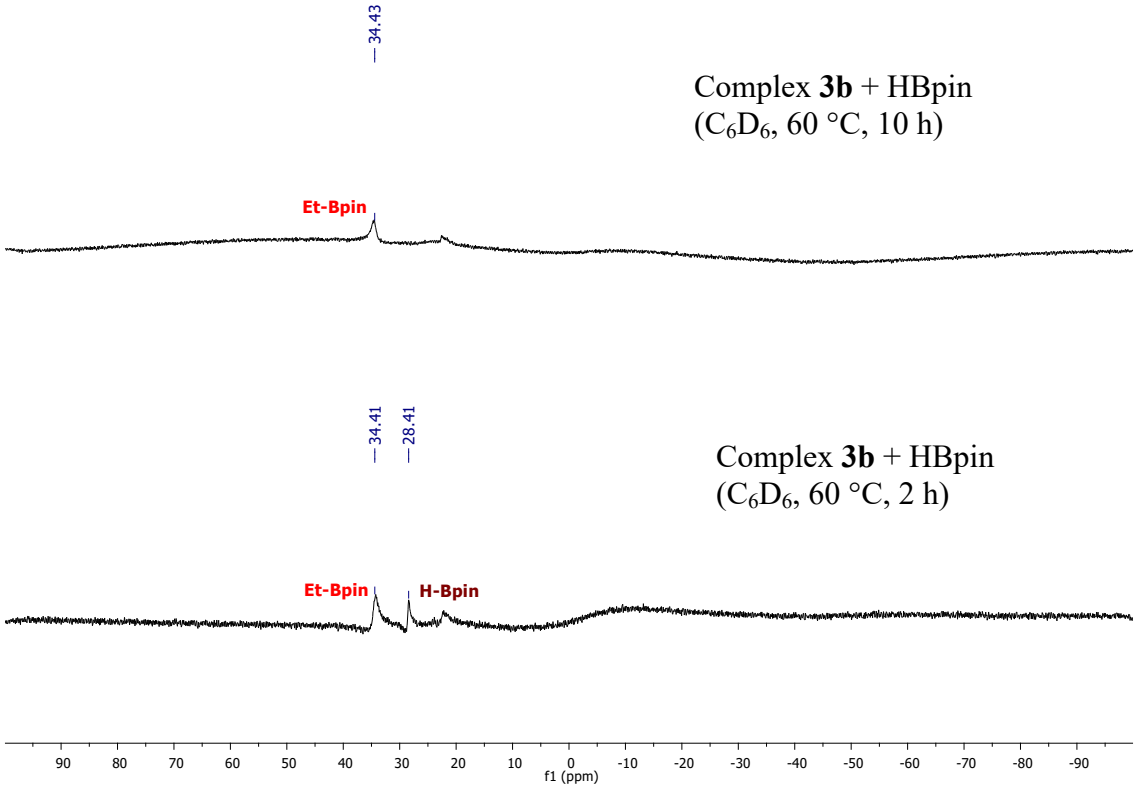

Figure FS 132. $^{11}B\{^1H\}$ NMR (96.3 MHz, C_6D_6, 298 K) spectra of stoichiometric reaction between complex **3b** and HBpin in C_6D_6.

Hydroboration of benzonitrile was carried out under optimized catalytic conditions in the presence and absence of 20 mol% trityl chloride.

Reaction 1: In the absence of trityl chloride, benzonitrile converted into corresponding *N*,*N*-diborylamine (**6a**) smoothly.

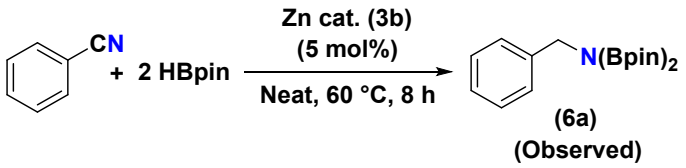

Reaction 2: In the presence of trityl chloride, formation of *N*,*N*-diborylamine (**6a**) was not observed.

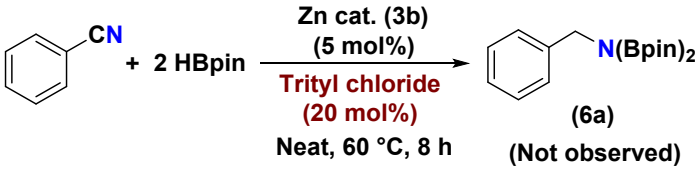

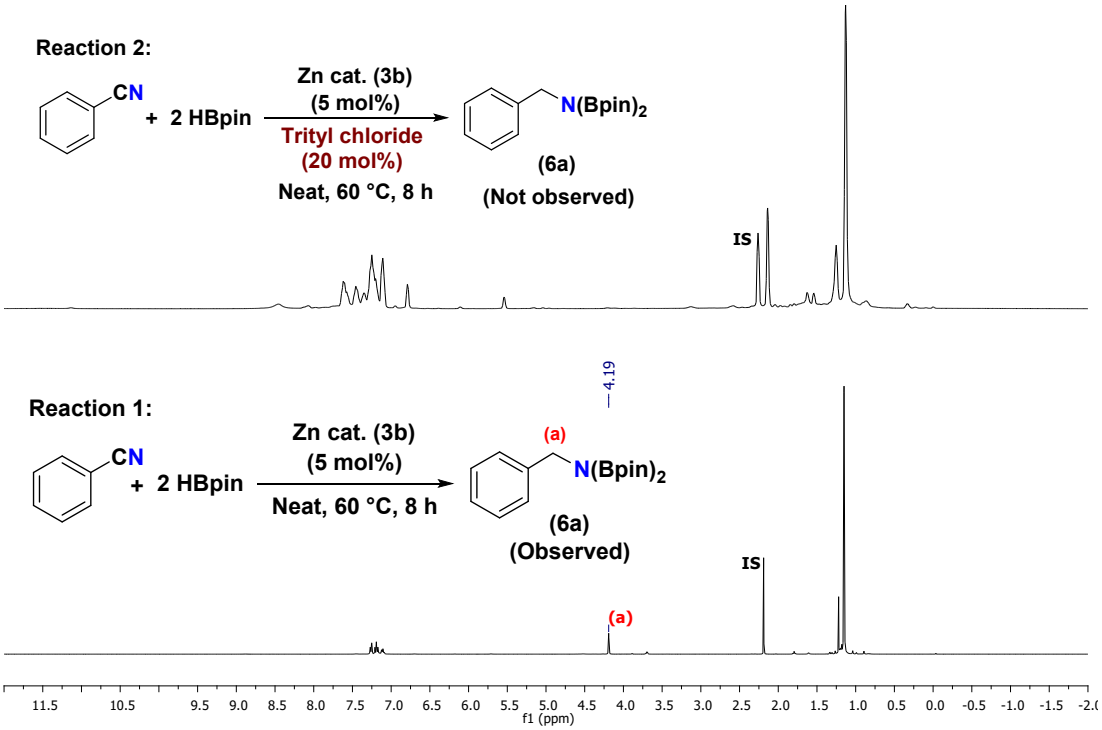

Figure FS 133. ^{1}H NMR (400 MHz, C_6D_6, 298 K) spectra for hydroboration of benzonitrile under optimized catalytic conditions in the presence and absence of 20 mol% trityl chloride. [Internal standard (IS) = mesitylene]

Hydroboration of ethyl benzoate was carried out under optimized catalytic conditions in the presence and absence of 20 mol% trityl chloride.

Reaction 1: In the absence of trityl chloride, ethyl benzoate converted into corresponding boronate esters (**9j** and **9k**).

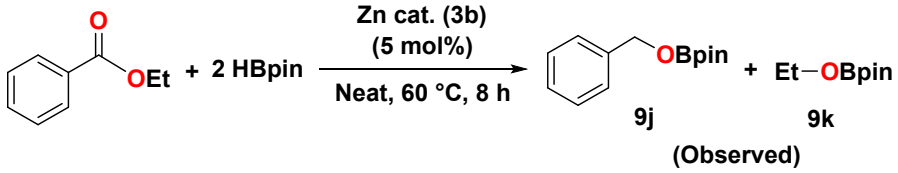

Reaction 2: In the presence of trityl chloride, formation of boronate esters (**9j** and **9k**) was not observed.

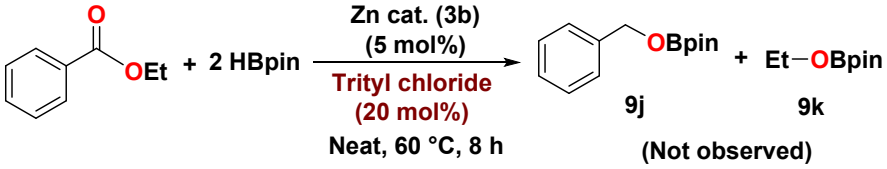

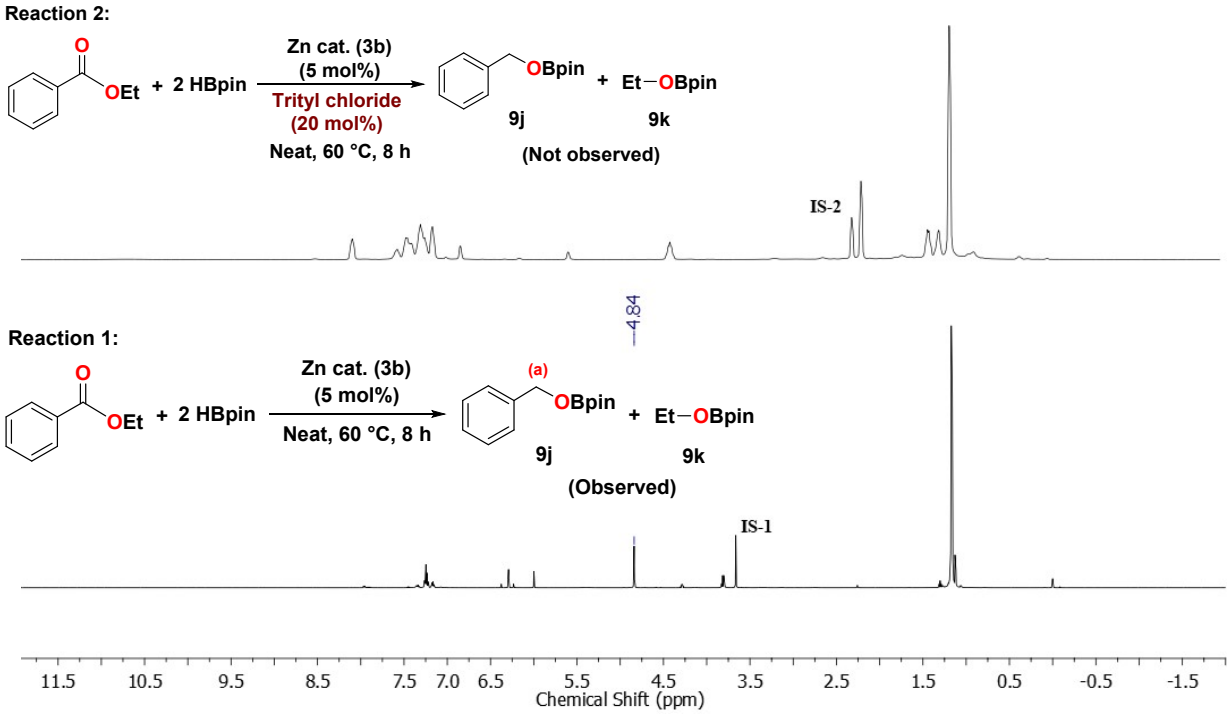

Figure FS 134. ^{1}H NMR (400 MHz, C_6D_6, 298 K) spectra for hydroboration of ethyl benzoate under optimized catalytic conditions in the presence and absence of 20 mol% trityl chloride. [IS-1 = 1,3,5-trimethoxybenzene, IS-2 = mesitylene]

6. References:

1. (a) G. M. Sheldrick, *Acta Crystallogr*, 2008, **A64**, 112-122. (b) L. J. Farrugia, *J. Appl. Cryst*., 2012, **45**, 849-854.
2. (a) Y. Ding, X. Ma, Y. Liu, W. Liu, Z. Yang and H. W. Roesky, *Organometallics*, 2019, **38**, 3092-3097. (b) W. Liu, Y. Ding, D. Jin, Q. Shen, B. Yan, X. Ma and Z. Yang, *Green Chem.*, 2019, **21**, 3812-3815. (c) A. Harinath, J. Bhattacharjee and T. K. Panda, *Adv. Synth. Catal.*, 2019, **361**, 850-857. (d) S. Das, J. Bhattacharjee and T. K. Panda, *New J. Chem.*, 2019, **43**, 16812-16818. (e) C. Weetman, M. D. Anker, M. Arrowsmith, M. S. Hill, G. Kociok-Köhn, D. J. Liptrot and M. F. Mahon, *Chem. Sci.*, 2016, **7**, 628-641. (f) N. Sarkar, S. Bera and S. Nembenna. *J. Org. Chem.*, 2020, **85**, 4999-5009.
3. (a) K. Makarov, A. Kaushansky and M. S. Eisen, *ACS Catal*., 2022, **12**, 273-284. (b) C. J. Barger, A. Motta, V. L. Weidner, T. L. Lohr and T. J. Marks, *ACS Catal*., 2019, **9**, 9015−9024. (c) M. K. Barman, A. Baishya and S. Nembenna, *Dalton Trans*., 2017, **46**, 4152-4156. (d) C. Ni, H. Yu, L. Liu, B. Yan, B. Zhang, X. Ma, X. Zhang and Z. Yang, *New J. Chem*., 2022, **46**, 14635-14641. (e) D. Mukherjee, A. Ellern and A. D. Sadow, *Chem. Sci*., 2014, **5**, 959-964. (f) (g) J. Bhattacharjee, P. Rawal, S. Das, A. Harinath, P. Gupta and T. K. Panda, *Dalton Trans.*, 2022, **51**, 5859-5867. (h) G. S. Kumar, R. Kumar, A. Sau, V. Chandrasekhar and T. K. Panda, *J. Org. Chem.*, 2023, **88**, 12613-12622.